PHOTOCHEMICAL STRATEGIES FOR MACROMOLECULAR SYNTHESES IN NEAR INFRARED REGION

Dissertation

to obtain the academic degree of
Doctor of Natural Sciences
- Dr. rer. nat. -

by

Ceren Kütahya

born in Istanbul, Turkey

Faculty of Chemistry
University of Duisburg Essen

Essen, 2020

DOI: 10.17185/duepublico/72664
URN: urn:nbn:de:hbz:464-20200831-101452-4

The present work was carried out in the period from January 2017 to February 2020 under the supervision of Prof. Dr. Jochen Gutmann at the Institute of Physical Chemistry at the University of Duisburg-Essen in cooperation with the Niederrhein University of Applied Sciences in the working group of Prof. Dr. Bernd Strehmel at the Institute for Coatings and Surface Chemistry.

Date of Defense: 17.08.2020

Thesis Advisor: **Prof. Dr. Jochen Stefan Gutmann**
University of Duisburg-Essen

Prof. Dr. Bernd Strehmel
Niederrhein University of Applied Sciences

Prof. Dr. Cyrille Andre Boyer
The University of New South Wales

Chair: **Prof. Dr. Gebhard Haberhauer**
University of Duisburg-Essen

Explanation

I hereby confirm that I am entitled the present work with the title

“PHOTOCHEMICAL STRATEGIES FOR MACROMOLECULAR SYNTHESES IN NEAR INFRARED REGION”

independently written and have not used other than the sources and resources indicated, and this work submitted in this or similar form has never been done at any other university.

Ceren Kütahya

Foreword

First and foremost, I would like to thank to my supervisor Prof. Dr. Bernd Strehmel for his patience, motivation, effort, and great knowledge during my PhD study and research. I feel the honor to be PhD student working with him. His invaluable support helped me a lot in during my PhD study. Without his guidance, this work would have not been possible for me to finish. I know he is going to be the support for the rest of my academic struggling and I need to thank him for every idea inspire me.

I would like to thank also Prof. Dr. Jochen Gutmann for his guidance, encouragement and his valuable suggestions to my research. His immense knowledge helped me to extend my knowledge.

I am really grateful to have Prof. Cyrille Boyer in my PhD committee. His inspiring publications leaded me a lot during my research.

I would like to express my thanks to all the members of “Strehmel’s Group” for their friendship and the nice atmosphere they made in the lab. In particular, Dennis Oprych, Dr. Christian Schmitz, Serbest Sheikhmous, Yulian Pang, Paul Hermes, Qunying Wang, Nicolai Meckbach, Taner Poplata, Katrin Mathea, Berit Schuster, Micheal Schläpfer and Dr. Thomas Brömme, it has really been a great pleasure working with you.

I need to thank Prof. Dr. Veronika Strehmel for her support and inspiring ideas. It was always a pleasure for me to discuss with her about my research. Furthermore, I would like to thank to her group members, Berran Sanay, Markus Heinz and Dr. Micheal Schmitt, for their help and friendship.

I also would like to thank Prof. Dr. Yusuf Yagci who always hopes the best for my academic development. It has been always privileged being his student. I need to thank for the collaboration during my PhD studies.

Finally, I would like to express my deep gratitudes to my parents. They always do their very best for my education. Their love, understanding and encouragement are indispensable for me.

Table of Contents

Abbreviations

NIR	Near-infrared
ATRP	Atom Transfer Radical Polymerization
CuAAC	Copper Catalzyed Azide-Alkyne Click Reaction
UV	Ultraviolet
UCNP	Up-conversion nanoparticle
ITX	2-isopropyl thioxanthane
Sens	Sensitizer
LED	Light emitting diodes
CDs	Carbon nanodots
CtP	Computer-to-plate
3D	Three dimensional
Vis	Visible
CRP	Controlled radical polymerization
RAFT	Reversible Addition/Fragmentation Chain Transfer Polymerization
NMRP	Nitroxide-mediated Radical Polymerization
photo-ATRP	Photoinduced ATRP
Đ	Dispersity
RDRP	Reversible-deactivation radical polymerization
CRDP	Controlled reversible-deactivation radical polymerization
IUPAC	Union of Pure and Applied Chemistry
TEMPO	2,2,6,6-tetramethyl-1-piperidinyloxy
K	Activation-deactivation equilibrium constant
ATRA	Atom transfer radical addition
Mt^mX/L	Low-oxidation state transition metal complex
L	Ligand
Mt^m	Metal catalyst in its lower oxidation state
Mt^{m+1}	Metal complex in its higher oxidation state
k_p	Rate constant of propagation
k_t	Rate constant of termination
k_{act}	Activation rate constant
k_{deact}	Deactivation rate constant

I	Initiator
SR&NI	Simultaneous reverse and normal initiation
AGET	Activator generated by electron transfer
ARGET	Activator regenerated by electron transfer
SARA	Supplemental activator and reducing agent
e-ATRP	Electrochemically mediated ATRP
ICAR	Initiators for continuous activator regeneration
ppm	Parts per million
CFLs	Compact fluorescent lamps
$Ir(ppy)_3$	Tris[2-phenylpyridinato-C2,N]iridium(III)
CQ	Camphorquinone
Irgacure 819	(2,4,6-trimethylbenzoyl)-phenylphosineoxide
TPMA	Tris(2-pyridylmethyl)amine
TPMA*	Tris((4-methoxy-3,5-dimethylpyridin-2-yl)amine)
PTZ	10-phenylphenothiazine
PS	Photosensitizer
$Mn_2(CO)_{10}$)	Dimanganese decacarbonyl
DMPA	2,2-dimethoxy-2-phenylacetophenone
$[Fe(dtc)_3]$	Ferric tri(N,N-diethyldithiocarbamate)
MMA	Methyl methacrylate
DA	Diels-Alder Cycloaddition
PSt	Polystyrene
PMMA	poly(methylmethacrylate)
PEO	Poly(ethylene oxide)
PSt-*b*-PCL	polystyrene-b-(ε-caprolactone)
PSt-*g*-PEO	polystyrene-g-poly(ethylene oxide)
PSt-*g*-PMMA	polystyrene-g-poly(methylmethacrylate)
DMSO	Dimethylsulfoxide
DMF	N, N'-dimethylformamide
Et_2O	Diethyl ether
CH_2Cl_2	Dichloromethane
MeOH	Methanol
n-Hex	n-hexane
EtOAc	Ethyl acetate

EBiP	Ethyl α-bromo-2-methylpropionate
EBPA	Ethyl α-bromophenylacetate
EBP	Ethyl α- bromopropionate
S	Styrene
TPGDA	Tri(propylene glycol) diacrylate
$CuBr_2$	Copper(II)bromide
Me-PEG	Poly(ethylene glycol) methyl ether
DCC	N,N′-dicyclohexylcarbodiimide
DMAP	4-(dimethylamino)pyridine
$NaNO_2$	Sodium nitrite
$MgSO_4$	Magnesium sulfate
$NaHCO_3$	Sodium bicarbonate
NMR	Nuclear Magnetic Resonance
FTIR	Fourier-transform Infrared
GPC	Gel permeation chromatography
Photo-DSC	Photo Differential Scanning Calorimeter
PEG-N_3	Poly(ethylene glycol)
PS-N_3	ω-azido terminated polystyrene
Alkyne-PCL	Acetylene terminated poly(ε-caprolactone)

List of Schemes

List of Figures

List of Charts

List of Tables

Abstract

Different photoinitiating systems were carried out for the design of well-defined macromolecular structures using near-infrared (NIR) light via Atom Transfer Radical Polymerization (ATRP) and Copper-Catalyzed Azide-Alkyne Click Reactions (CuAAC). Lower-oxidation state copper salts are required for both processes, however; this brings some limitations into the reactions. In order to mitigate these limitations, the use of light energy has been utilized by starting with higher-oxidation state copper salts and reducing them via photoinduced electron transfer reactions (PET).

In addition, there have been huge affords to conduct these reactions in metal-free conditions. For the first time, the use of NIR irradiation for the controlled radical polymerization system via ATRP process in the absence of inorganic catalyst was demonstrated in this thesis. In order to do that, the emitting ultraviolet (UV) light from up-conversion nanoparticles (**UCNP**s) after NIR laser irradiation was used to excite UV photoinitiator which is 2-isopropyl thioxanthone (ITX). The initiation mechanism involves PET from the electron donor amine to the excited state of ITX in order to form radical anion of ITX. The generated radical anion of ITX reduces the alkyl initiator to generate initiating radicals which allow the addition of the monomers and the polymerization to be proceeded.

Additionally, the use of NIR sensitizers (**Sens**) for both reactions (ATRP and CuAAC), for the first time, were successfully investigated in this thesis. The initiation mechanism involves a photoinduced electron transfer reaction between the exited state of a heptamethine cyanine absorber and Cu^{II}/Ligand complex. The oxidation potential of the **Sens** resulted in a negative free enthalpy in combination with the Cu^{II}/Ligand complex considering successful electron transfer reactions after excitation by near-infrared light emitting diodes (NIR LEDs). After the photochemical reaction, the back electron transfer was presented which allows the system to be a catalytic cycle. The characterization of the polymers obtained were analyzed by spectroscopic and chromatographic methods. Controlled molecular weight characteristics were observed and block copolymer synthesis was achieved in both ATRP and CuACC reactions via NIR exposure.

As an alternative, similar photocatalytic system using carbon nanodots (**CD**s) which were prepared from seaweeds was shown to be able to catalyze free radical and controlled radical polymerization processes using blue light emitting diodes. The use of these materials was included in this work because they can be an alternative as biocompatible

and green photocatalyst. They showed no toxicity and good efficiency for the synthesis of tailor-made materials.

Kurzfassung

Verschiedene Photoinitiatorsysteme zur Synthese von klar definierten makromolekularen Strukturen wurden unter Verwendung von Licht im nahen Infrarot (NIR) mittels radikalischer Atomtransferpolymerisation (ATRP) und Kupfer-katalysierter Azid-Alkin-Klick-Reaktion (CuAAC) durchgeführt. Beide Reaktionen erfordern, dass das Kupfersalz in der niedrigeren Oxidationsstufe vorliegen muss, was einige Einschränkungen für diese Reaktionen mit sich bringt. Es wurden daher neue Verfahren entwickelt, welche basierend auf der Basis der Absorption von Licht diese Nachteile überwinden, indem Kupfersalze mit einer höheren Oxidationsstufe eingesetzt werden und diese durch photoinduzierten Elektronentransfer reduziert werden.

Darüber hinaus gab es Bestrebungen, diese Reaktionen unter metallfreien Bedingungen durchzuführen. In dieser Arbeit wurde erstmals unter Verwendung von NIR-Strahlung das Ablaufen die kontrollierte radikalische Polymerisation mittels ATRP in Abwesenheit eines anorganischen Katalysators gezeigt. Zu diesem Zweck wurde das von aufwärtskonvertierenden Nanopartikeln (**UCNP**s) emittierende ultraviolette (UV) Licht, welches mittels NIR-Laserbestrahlung generiert wurde eingesetzt, um den UV-Photoinitiator 2-Isopropylthioxanthon (ITX) anzuregen. Der Initiierungsmechanismus basiert auf einem photoinduzierten Elektronentransfer zwischen dem angeregten Zustand des ITX und einem Amin welches als Elektronendonator fungiert. Das gebildete Radikalanion des ITX reduziert das Alkylhalogenid, wobei Bromid und Alkylradikale gebildet werden. Diese initiieren die radikalische Polymerisation bei Zugabe von Monomer.

Weiterhin wurden NIR Sensibilisatoren (**Sens**) für beide Reaktionen (ATRP and CuAAC) zum erstem ersten Mal erfolgreich eingesetzt in dieser Arbeit. Der Initiierungsmechanismus basiert auf einem photoinduzierten Elektronentransfer zwischen dem angeregten Zustand eines Absorbers, welcher voneinem Cyanine aus der Gruppe der Heptamethine ausgewählt wurde, und dem Cu^{II}/Ligand Komplex. Das Oxidationspotenzial von **Sens** führt dabei zu einer negativen freien Enthalpy in Kombination mit dem Cu^{II}/Ligand Komplex als Reaktionspartner, wobei der Elektronentransfer erfolgreich abläuft unter Verwendung von NIR LEDs. Nach dem Elektronentransfer wird der Elektronenrücktransfer in einem katalytischen Zyklus erkennbar. Die erhaltenen Polymere wurden mit spektroskopischen and chromatographischen Methoden analysiert. Das ermittelte Molekulargewicht und die entsprechende Charakteristik bestätigen das Ablaufen eines kontrollierten Mechanismus der Polymerbildung, was durch Blockcopolymer Synthese in

beiden Fällen bestätigt werden konnte. Das bezieht sich auf die ATRP und CuACC Reaktion, wobei NIR Licht zur Anregung eingesetzt worden ist.

Alternativ wurde gezeigt, dass Kohlenstoffnanopunkte (**CD**s), welche aus Meeresalgen hergestellt wurden, einen ähnlichen photokatalytischen Mechanismus unter Verwendung von blauen Leuchtdioden (LEDs) aufweisen. Die Verwendung dieser Materialien wurde in diese Arbeit einbezogen, da sie eine Alternative als biokompatible und grüne Photokatalysatoren darstellen können. Sie zeigten keine Toxizität und gute Wirksamkeit für die Synthese von maßgeschneiderten Materialien.

1. Introduction

1.1. General Aspects

After the introduction of macromolecules to chemistry 100 years ago [1, 2], these materials have been introduced not only in daily life but they also play an important role in natural sciences. Many fields in chemistry, physics, biology, material sciences, and engineering have benefit from chemical and physical properties of these molecules based on molecular weight, chemical composition, and linking of different units with various properties for their use in distinct applications [3]. Certain thermal and mechanical properties of these materials possess vital effect on the performance and application. Although syntheses of macromolecules have been extensively investigated, there still exist in both academic and industrial fields a need to develop more environmentally friendly, energy saving alternatives, and comparable synthetic procedures in particular for the preparation of macromolecules with well-defined architectures.

By the inspiration from the naturally occurring reactions in nature, chemists have utilized photochemical strategies on various chemical syntheses. Therefore, light has been the smallest reagent that is used in the field of chemistry in numerous technological processes. Photochemistry is an interdisciplinary science that deals with the interaction of light with light sensitive compounds in chemistry, biology, physics and materials science. In principle, it is therefore possible to deal with practical questions relating to surface and coating technology using photochemical methods as this interdisciplinary field integrates with the aspects of photochemistry [4, 5, 6]. Photochemical syntheses hold several advantages in contrast to the conventional methods such as spatiotemporal control and low-energy requirement [7]. The possibility of sustainable and low-energy demanding processes demonstrate the power of light initiated processes for technologies needed in daily life. Thus, it has been approved as a misbelieve that chemical reactions, in general, would be mostly connected to thermal-based processes while light might receive a nice-to-have option.

Photochemical reactions are initiated by the excitation of a molecule by light energy. In addition to the visible range of electromagnetic radiation, the energy in the UV and NIR range are also summarized under the term of light energy. After the absorption of light energy, photochemical reactions takes place from the excited state of the molecule to form reactive species which then initiate the several chemical processes. Several methods have been developed in order to investigate reactive species such as laser flash photolysis and electron paramagnetic resonance techniques.

Photopolymerization has been the most of the research on the utilization of photoinduced procedures in polymer science. In this well-known process, polymer formation occurs by a light source. Photopolymerization processes have been widely explored in numerous conventional applications in the coating industry, in adhesives, in the printing and ink industries, and in optoelectronics and microelectronics [8]. In addition, this process has been commonly used in the application of laser video discs, dental fillings, fabrication of 3D objects, and in bioapplications including implants for bones, drug delivery, and tissue engineering [8, 9, 10]. These systems facilitate also the access to technical processes such as lithography or chemical solidification of coating materials in radiation-curing systems [11, 12, 13]. Although applications of photochemistry to the synthetic polymer science recently gains higher priority, it dates back to more than fifty years since its benefits in comparison with traditional syntheses have been noticed from day to day [14, 15]. Applications benefiting from photochemistry can be also found in digital imaging with focus on computer-to-plate (CtP) technology [12, 13], three-dimensional (3D) printing used in medicine and mechanical engineering to construct prototypes on demand [16], and for chemical drying of coatings as alternative to energy wasting oven techniques - just to count a few examples [17].

By initiation with a light-sensitive initiator, photopolymerization leads to the molecular enlargement of liquid or viscous monomers, resins or prepolymers, which are thereby chemically solidified. The building blocks are linked via a chain reaction for compounds with several functional groups to form polymer networks. As a rule, polymer networks are used in the application as a material or coating to achieve improved mechanical properties, such as high hardness and shock resistance, or less solubility or reduced capability for swelling compared to organic solvents or other media, depending on the network density. Investigation of various photoinitiating systems in a wide range of absorption spectrum exhibited several advantages. These photoinitiator systems have been reported as rapid reactions, easy to perform at ambient temperature, and to be moderated easily in order to generate reactive species at the desired position of the molecules [18].

Photopolymerization is a modern method for polymer synthesis, which is widely used in coating technology as an alternative to furnace processes for the chemical solidification of monomers and prepolymers by means of cross-linking reactions in numerous applications [19]. Network formation is understood to mean the build-up of three-dimensional structures, which requires the use of monomers comprising at least a functionality of three reacting centers. These materials are insoluble in organic solvents, which makes it clear

why these materials, in particular, are in demand to protect various substrates from chemical and/or mechanical wear. Furthermore, the cross-linking density enables the control of the required properties of the coating for the desired application. These include the mechanical properties which should generally exhibit a high level of hardness and therefore tensile strength. On the other hand, this may also result in a high degree of brittleness. The latter should be avoided, which typically leads to break and loss of the adhesive strength. To date, initiators that absorb in the UV range have predominantly been used in the industrial practice of coating technology [11, 18]. The photolytic cleavage of these compounds according to a *Norrish type 1* protocol [20] yields initiating radicals and/or cations which initiate the polymerization and may serve the cross-linking of the monomer. In the past 30 years, UV technology has established itself in many branches to refine different substrates with selected shadings. UV printing, automotive industry, and the furniture industry represent selected industrial applications for photopolymerization by UV initiation [11].

Excitation with UV radiation, however; has disadvantages in some applications. Numerous organic compounds that are incorporated into the coatings absorb UV radiation. Therefore, these compounds prevent photopolymerization of high layer thicknesses since these materials act as an internal filter. In practice, a multi-stage process for layer build-up is often required for this reason. In addition, mercury lamps commonly used for photopolymerization are harmful to the operator due to the emitted UV radiation and ozone formation, and this is why additional precautionary measures must be taken in the operational processes. Due to the wide emission spectrum of the mercury lamps, a large part of the radiation generated is not absorbed by the initiator leading the energy to be useless in photochemical reactions. This reduces the efficiency of this radiation method. There have been several approaches to deal withs these problems. One solution is provided by LEDs with an emission range in the UV range. This leads to higher efficiency and radiation in UV-A (315 nm - 380 nm) providing lower safety risk for the operator since no ozone is formed in this range. In addition, new regulations of the EU prohibit the use of mercury lamps in future technologies [17]. Another alternative is to shift the absorption into the visible range (Vis) of electromagnetic spectrum. This can be done by spectral sensitization. A two-component initiator system is often used in which the absorber/ sensitizer is excited with light however the energy of the absorbed light is not sufficient to break bonds directly [21]. This initiates a photochemical reaction with another component, which results in the formation of the initiating species. In practice, photopolymers that have been initiated with visible light have been used for several years and their initiation rate is

lower than that of UV systems, which enables processing under moderate ambient light [22, 23].

Researchers have been able to use the light in polymerization reactions following different mechanism including radical, cationic, anionic and step-growth polymerization routes. Conventional radical or ionic (anionic and/or cationic) polymerization techniques are useful to synthesize polymeric structures in which their molecular weights are high and molecular weight distributions are broad. Even though these techniques have been widely used for conventional processes, there also exist some applications which need to be synthesized according to a controlled polymerization reaction scheme. Controlled polymer synthesis enables to synthesize well-defined polymeric structures with precise molecular weight characteristics (molecular weight and molecular weight distribution) and different functionalities. Molecular weight and monomer conversion increases linearly by time while the classical termination between two polymer radicals is restricted. Controlled radical polymerization (CRP) techniques are applicable to with a wide range of monomers for several applications such as surface modification, block copolymer synthesis for bio-applications including drug delivery and hydrogel applications [24]. In recent years, light induced processes are successfully employed also in CRP techniques and click reactions for the preparation of complex macromolecular structures. Several types of conventional monomers such as (meth)acrylates, styrenes, vinyl acetates are effectively polymerized under ambient temperatures. CRP has divided into three fundamental techniques which are called as Atom Transfer Radical Polymerization (ATRP) [25, 26], Reversible Addition/ Fragmentation Chain Transfer Polymerization (RAFT) [27, 28], and Nitroxide-mediated Radical Polymerization (NMRP) [29, 30]. ATRP has been the frequently used method due to the high availability of suitable monomers with different structures and an increasing number of initiators for the syntheses of well-defined polymeric materials. Photoinitiated reactions have become an important field in ATRP due to the easy reaction control. Polymerization can be initiated by light and the propagating chains can be paused or re-initiated just by switching light on and/or off [31].

1.2 Motivation of the Thesis

Even though NIR initiator systems are already used in industrial applications such as CtP technology [23, 32], the basics of this system have not been extensively investigated compared to UV initiating systems. These systems can be seen in its infancy. Although basic knowledge and detailed mechanistic studies on photosensitized radical and cation formation with diaryliodonium compounds and triazine derivatives as electron acceptors

with dyes that absorb in the visible light range are available, partial studies on photopolymerization with heptamethine cyanines as NIR absorbers or sensitizers have still not been well investigated in detailed. As well known, the relaxation of the excited NIR absorbers into a ground state takes place to an excessive extent via internal conversion [17, 23] by converting the light into heat. This explains why NIR initiator systems may be seen as a niche in industrial processes. Additionally, heat release on demand by internal conversion may become of interest for applications requiring thermal triggering of physical or chemical processes. Form this point of view, photopolymerization technology in NIR region can serve an additional benefit by heat release as a secondary requirement [17]. For a further increase in the efficiency of the industrial application, the use of light sources with a high overlap of the emission with the absorption of LED arrays or diode lasers is also relevant. The tailor-made synthesis of NIR absorbers facilitates optimal spectral overlap with the LED source. Another advantage of the absorption in the NIR is that it does not overlap with the absorption of other components such as functional additives absorbing in the UV in which UV filter materials or yellow pigments depict as examples. Furthermore, the introduction of colored micro- and nanoparticles can be seen as less problematic in contrast to UV initiation systems. This can also include the photopolymerization of monomers comprising UV absorbing moieties such as benzophenone.

The utilization of the light-induced processes into the synthetic polymer chemistry have been recently adapted in Atom Transfer Radical Polymerization (ATRP) and Copper-catalyzed Azide-Alkyne Click (CuAAC) processes. The requirement of Cu^{I} catalyst in both processes brings some limitations regarding the experimental conditions and some applications. Therefore, in-situ generation of Cu^{I} species from the Cu^{II} salts by photochemical reactions has become a very popular approach which makes the reaction handled under much more simple conditions due to the better chemical stability of Cu^{II} under air. There have been many approaches proposed to reduce Cu^{II} in the reaction media for example the addition of reducing agents or the use of electronic current [33, 34]. Additionally, the use of light induced processes have been also successfully shown as a powerful strategy for the in-situ formation of Cu^{I} catalyst in the reaction. This approach can be performed either direct or indirect photochemical reduction procedures. Direct photochemical reduction of copper(II) ions was shown in the UV range in the absence of photoinitiators, however; this process needs longer irradiation times. In the presence of a photoinitiator, the formed reactive species (radicals or cations) upon irradiation reduce Cu^{II} in order to form the Cu^{I} species.

The motivation of the thesis is to investigate the examination of PET reactions for the synthesis of a variety of polymeric structures with an initiating system, which generates radicals via a sensitized photoreaction by absorption of radiation in the NIR range between 750 nm and 1000 nm. The selection of the NIR spectral range enables the incorporation of functional materials that absorb in the UV and Vis range. Initiator systems with heptamethine cyanines as sensitizer are already used in the production of lithographic printing plates using radical photopolymerization [13, 35]. The aim of the work is a comprehensive investigation of several sensitizers used for the photopolymerization of commonly used monomers to understand their interactions with the NIR initiator system, which requires a variation of the initiator component. Different photoinitiating systems for controlled-radical polymerization were developed in this thesis through ATRP process. In addition, another photoinitiated strategy for CuAAC reaction with several clickable compounds are presented to connect polymers with small dispersity derived from polar and non-polar polymers. During the thesis, chromatographic, spectroscopic and thermographic analyses were performed for the characterization of polymers obtained.

This thesis represents an efficient photoinitialting system for metal-free ATRP of methyl methacrylate under laser irradiation at 974 nm by **UCNP**s. In this approach, **UCNP**s converts the NIR light to UV light that can initiate the system comprising 2-isopropylthioxanthone (ITX) as photoinitiator. Polymers obtained via this process exhibited controlled properties and successful chain-end fidelity. Chain-end fidelity was proven by chain extension experiment.

Additionally, it also demonstrates a novel photoinitiating system for contolled radical polymerization using NIR sensitizers in the presence of ppm scale of copper catalysts. This new photoinitiating system showed, for the first time, the use of NIR light for the synthesis of polymers with well-defined structures, narrow molecular weight distrubutions and good photostability. It was also demonstrated that this system is applicable for the syntheses block copolymers which demonstrated the chain-end functionality.

Alternatively, it is also showed the similar photochemical strategy using carbon dots (**CD**s) as green photosensitizer in photoinduced ATRP (photo-ATRP) protocol. The use of these cheap and green materials for photopolymerization is successfully studied in this thesis. These preliminary studies were pursued with blue light LEDs while correct research in the lab extends their exploration with red and NIR light as well.

Finally, this thesis also discusses the use of NIR sensitizers for the photoinduced reduction of Cu^{II} salts to Cu^{I} species to catalyze the CuAAC reactions. The applicability of this reaction both small molecules and macromolecules were tested.

These aforementioned approaches depict parts of this thesis while most of the results appeared already in the following publications. Results were also presented at international conferences. General ideas for controlled macromoleculer synthesis were also contributed in two reviews [23, 36].

Publications as First Author or shared First Authorship:

1. C. Kütahya, P. Wang, S. Liu, J. Li, Z. Chen, B. Strehmel, "Carbon Dots as Promising Green Photocatalyst for Free Radical and ATRP-Based Radical Photopolymerization with Blue LEDs", *Angew. Chem. Int. Ed.*, **2020**, in press, https://doi.org/10.1002/anie.201912343. "Kohlenstoff−Nanopunkte als Photokatalysatoren für die freie radikalische und ATRP−basierte radikalische Photopolymerisation mit blauen LEDs.", *Angew. Chem.*, **2020**, in press, https://doi.org/10.1002/ange.201912343. Selected as Hot Paper from the Editor based on the reviews.
2. A. Kocaarslan, C. Kütahya, D. Keil, Y. Yagci, B. Strehmel, NIR and UV-LED Sensitized Photopolymerization with Onium Salts Comprising Anions of Different Nucleophilicity. ChemPhotoChem, 2019, *3*, 1127 – 1132. (shared First Authorship)
3. C. Kütahya, Y. Yagci, B. Strehmel, "Near−Infrared Photoinduced Copper−Catalyzed Azide−Alkyne Click Chemistry with a Cyanine Comprising a Barbiturate Group." *ChemPhotoChem*, **2019**, *3*, 1180-1186.
4. C. Kütahya, C. Schmitz, V. Strehmel, Y. Yagci, B. Strehmel, Near−Infrared Sensitized Photoinduced ATRP with ppm of Cu(II) Catalyst. *Angew. Chem. Int. Ed.*, **2018**, *57*, 7898-7902, *Angew. Chem.*, **2018**, *130*, 7898-7902. "Nahinfrarot−sensibilisierte photoinduzierte ATRP mit einer Kupfer(II)−Katalysatorkonzentration im ppm−Bereich", *Angew. Chem.*, **2018**, *130*, 8025-8030. Selected as Hot Paper from the Editor based on the reviews.
5. C. Kütahya, N. Meckbach, V. Strehmel, J. S. Gutmann, B. Strehmel, "NIR Light-induced ATRP of Block Copolymers comprising UV-Absorbing Moieties", *Chemistry – A European Journal*, **2020**, 26, 1-9.

Publications as Co-author:

6. B. Strehmel, C. Schmitz, C. Kütahya, Y. Pang, A. Drewitz, H. Mustroph, "Photophysics and photochemistry of NIR absorbers derived from cyanines: key to new technologies based on chemistry 4.0", *Beilstein Journal of Organic Chemistry*, **2020**, accepted for publication by the editorial office. Review. Contributed with controlled polymerization.

7. Z. Chen, D. Oprych, C. Xie, C. Kutahya, S. Wu, B. Strehmel , "Upconversion Nanoparticle Assisted Radical Polymerization at 974 nm and Generation of Acidic Cations", *ChemPhotoChem* **2017**, *1*, 499-503. Contributed with controlled polymerization.

Book Chapter (review):

8. Photopolymerization Initiating Systems. C. Schmitz, D. Oprych, C. Kutahya, B. Strehmel, "NIR Light for Initiation of Photopolymerization", (Editors: J. Lalevée, J.-P. Fouassier), Royal Society of Chemistry, **2018**, Chapter 14, pages 431-478. Contributed with controlled polymerization.

Conference Contributions as Oral Presentation:

1. Controlled Polymer Synthesis with light in Near-Infrared Region, C. Kütahya, B. Strehmel, 83. Lacktagung, Erfurt, Germany, September 11-13. 2019.
2. NIR Sensitizers as Photocatalysts with Cu(II) in the ppm Range: Tailor Made Synthesis of Polymers by photo-ATRP and Click Reactions, C. Kütahya, Y. Yagci, B. Strehmel, 26. Lecture Conference on Photochemistry, September 10 - 12, Garching/Munich, 2018.
3. Visible and NIR Light Photoinduced Metal-Free Atom Transfer Radical Polymerization, C. Kütahya, C. Schmitz, Y. Yagci, V. Strehmel, B. Strehmel, 256th ACS Meeting, Boston, USA, August 19-23, 2018. Conference travel was sponsored by the GDCh after application to a scholarship in a competitive selection procedure ("GDCh Studienreise").
4. Photocatalysis with NIR Sensitizers and Cu(II) at ppm scale: photo-ATRP and Azide-Alkyne Cycloaddition Click Reactions, C. Kütahya, Y. Yagci, B. Strehmel, 27th Photo IUPAC, Dublin, Ireland, July 8-13, 2018.
5. Visible and NIR Light Photoinduced Metal-Free Atom Transfer Radical Polymerization,C. Kütahya, C. Schmitz, Y. Yagci, V. Strehmel, B. Strehmel, 255th ACS Meeting, New Orleans, USA, March 18-22, 2018. Excellence in Polymer Graduate Research Symposium 2018. Selection as oral presentations according to computational procedure.

Conference Contributions as Poster Presentation:

1. Macromolecular Synthesis with Light in Near-Infrared Region., C. Kütahya, N. Meckbach, B. Strehmel, GDCh-Wissenschaftsforum Chemie 2019 (WIFO 2019), Aachen, Germany, September 14-18, 2019.
2. NIR Sensitizers for Tailor-Made Polymer Synthesis Based on photo-ATRP and Click Chemistry, C. Kütahya, Y. Yagci, K. Licha, B. Strehmel, European Symposium of Photopolymer Science (ESPS), Mulhouse, France, September 3-6, 2018. (3rd Poster Prize winner).
3. Metal Free Photo-ATRP with NIR-Sensitizers, C. Kütahya, Y. Yagci, J. S. Gutmann, V. Strehmel, B. Strehmel, GDCh-Wissenschaftsforum Chemie 2017 (WIFO 2017), Berlin, Germany, September 10-14, 2017.
4. Metal-Free ATRP with Light as the Smallest Activator: Visible and NIR Light for Synthesis of Tailor-Made Polymers, C. Kütahya, Y. Yagci, J. S. Gutmann, B. Strehmel Advanced Polymers via Macromolecular Engineering (APME 2017), Ghent, Belgium,May 21-25, 2017.

2. Fundamentals and State of the Art

2.1 Reversible-Deactivation Radical Polymerization (RDRP)

Conventional radical polymerization has been one of the most widely used reactions of low molecular weight compounds comprising unsaturated carbon-carbon double bonds; that is vinyl monomers to transform them into polymers. Mild reaction conditions based on low-cost technique, and compatibility with a range of monomers make this method important in the industry for the preparation of various polymeric materials. However, there still exist some limitations with classical radical polymerization systems considering the polymers obtained. These include the inadequate design in preparation of pre-determined polymer architectures with the controlled molecular weight and living characteristics. Traditional free radical polymerization techniques mostly result in the polymers showing broad molecular weight distributions (high dispersity, *Đ*) due of the poor control of the process. Such preparation is often difficult or sometimes even impossible using this method.

The limitations of the classical radical polymerization regarding the molecular weight characteristics and architectural design of the polymers synthesized promote scientists to develop new approaches for synthesis of macromolecular materials that are well defined regarding their structure, architecture and composition [37]. These approaches called as either controlled radical polymerization (CRP) or reversible-deactivation radical polymerization (RDRP) International Union of Pure and Applied Chemistry (IUPAC) to describe the procedures [38].

It was first established by Otsu et al. to introduce the idea of chain-end functionalized polymers to free radical systems in which the termination step can be removed providing the degree of livingness [39]. With the utilization of CRP concept to synthetic polymer chemistry, the preparation of macromolecular architectures with well-defined structures, narrow molecular weight distributions (narrow dispersity, *Đ*), and excellent living characteristics have become possible. One of the biggest advantage of CRP is that polymers obtained by these methods show low dispersity (typically between 1.1 to 1.5). Additionally, molecular weight increases linearly with respect to time and monomer conversion. Due to the their properties being able to applicable to various monomers, these techniques have been commonly used in synthetic polymer chemistry [40]. Polymerization of conventional monomers such as methyl metharcylate, styrene or acrylamide can be performed using a variety of iniferters. Indeed, these techniques provide the combination of the advances of conventional free radical polymerization with

those of living ionic polymerization by controlling the polymerization and allowing the preparation of living polymers which can be used for post-polymerization processes [40].
The application of this method has expanded many areas of research [41]. In particular, it gives access to well defined amphiphilic block copolymers comprising hydrophilic and hydrophobic polymeric chains on the structural pattern. The various morphologies which can be obtained using this method provides them unique properties. They can be used for many applications in fields as biomedical, cosmetics or coatings. Since the beginning of 1980s, various controlled radical polymerization techniques have developed in homogeneous medium with numerous studies on polymerization mechanism and polymer architecture [40]. Additionally, applicability of these techniques in aqueous dispersed medium possesses many advantages over bulk or solution processes. Indeed, the absence of organic solvent, the dissipation of the heat of the reactions through the aqueous phase, the high polymerization rates and the reduction of the viscosity are characteristics appreciated by researchers focussing to environmental constraints requiring processes considered as always more or less “clean”.
The most common methods of CRP are namely the Atom Transfer Radical Polymerization (ATRP) [42, 43, 44, 45], Reversible Addition/Fragmentation Chain Transfer Polymerization (RAFT) [46, 47, 48, 49] and Nitroxide-mediated Radical Polymerization (NMRP) [50, 51]. Among them, ATRP has been the most widely explored method because of its tunable properties to a number of monomers and initiators [43]. The applications of these systems can be found in many areas. For example, polymers mostly obtained by ATRP or RAFT are mostly used in bio-applications including drug delivery, bio-mineralization, and hydrogel applications [24]. Obtaining polymers by NMRP, block copolymers can be prepared to bemused in memory devices, pigment dispersions, and composite manufacturing [30].

2.1.1 Reversible Addition-Fragmentation Chain Transfer Polymerization (RAFT)

Reversible Addition-Fragmentation Chain Transfer polymerization has been one of the most frequently used method among CRP techniques in which molecular structure is controlled through a reversible deactivation which also provides the system living characteristics [27, 52, 53]. The main advantage of RAFT process compare to the other CRP processes is the applicability of unprotected functionalities pushing polymerization either in the neat monomer or by use of a solvent. This provides the system to be able to conducted in various reaction conditions where the surrounding can be either aqueous or protic [46, 54]. Moreover, applicability in different experimental conditions that belong to

the inexpensive techniques benefit from the simplicity of the processes compared to alternative ones. This property of the system makes it one of the most applicable processes for CRP techniques in synthetic polymer chemistry. Additionally, RAFT polymerization presents another feature being applicable for commonly used monomers which are suitable for radical polymerization (e.g. (meth)acrylates, styrene and its derivatives, and (meth)acrylamides). Another important advantage of this method is the ability to obtain polymers which show living properties and controlled molecular weight characteristics. However; there have been some disadvantages of this method because an appropriate RAFT agent has to be selected for the specific polymerization and process conditions. Additionally, the use of this method may be limited in some applications because of the undesired smell of the sulfur-containing compounds [53]. On the other hand, sulfur comprising materials possesses a certain biocompatibility making them more interesting if recycling of materials becomes an issue [55].

Living polymerization can be defined when all chains are initiated and grow at a similar rate. Functional groups which generates the initiating species remain during the polymerization which provides the end-groups. This property allows the re-initiate the polymerization from this reactive group at the end of the polymer chain. In RAFT polymerization, the living property can be provided by specific reagents called as RAFT agents. RAFT agents provides the reversible deactivation of propagating radicals which let the living chains are maintained during polymerization.

There are several types of RAFT agents available including dithiobenzoates, trithiocarbonates, xanthate and dithiocarbamates. Dithiobenzoates show very high transfer constants and may give retardation when used at high concentration. Trithiocarbonates, on the other hand, are really synthesized and more hydrolytic stable than dithiobenzoates. These compounds are most effective with more active monomers such as acrylates and styrene while xanthanes show more activity with less activated monomers such as *N*-vinylpyrolidine or vinyl acetate. These materials can be made more reactive by electron-withdrawing substituents. The substituents on nitrogen atom on the dithiocarbamates determine the activity for chain transfer. The effectiveness of RAFT agents strongly depends on alkyl group cleaving homolytically. Transfer constants decrease in the series where alkyl group depicts tertiary>>secondary>primary structural elements [56].

The general mechanism of RAFT process can be seen in Scheme 1. The RAFT agent behaves as a transfer agent in the reaction. Similar as the traditional free radical processes, initiation step occurs by an initiator which leads to the formation of propagating radicals. These radicals species are separated by linking to the RAFT agent and

fragmentation of the intermediating radicals. This gives rise to new radicals species and passive polymer RAFT-composition. The new active radical can be either the reinitiating radical R· of the new polymer chain or the other polymer chain P_n·. Monomers are added to these radicals to reinitiate the polymerization leading the formation of the new propagating radical. Ideally, all chains grow at same rate with the equilibrium between the propagating radicals and the dormant RAFT compound. This mechanism of the process leads to the preparation of the polymers with controlled structures and low molecular weight distrubitions. (*Đ*=1.1-1.2) [46, 57]. RAFT process also exhibits living character due to the remaining of the thiocarbonylthio functions at the end of the polymer chain. Living character of the system allows the syntheses of complex macromolecular structures including block copolymers and telechelic polymers [58, 59].

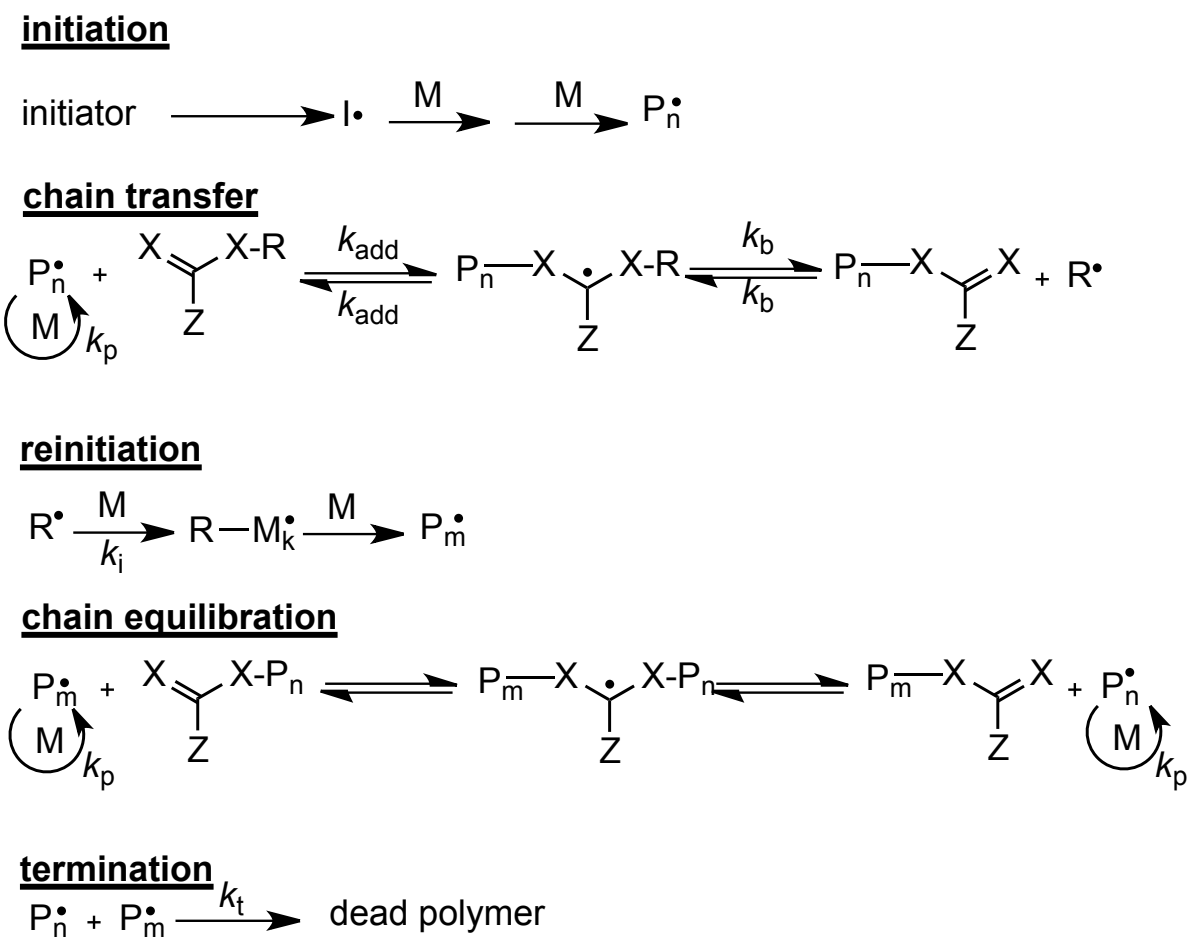

Scheme 1: General mechanism for RAFT polymerization.

2.1.2 Nitroxide-mediated Radical Polymerization (NMRP)

Nitroxide-mediated radical polymerization (NMRP) depicts a further approach of the controlled radical polymerization methods. This process can be thermally initiated which provides the use of no additional radical initiator. Additionally, no metal catalyst requirement makes this method to become one of the widely used CRP techniques. Another advantage of the system is the easy removal of alkoxyamine that provides both the initiating radicals and the mediating nitroxide radical [60].

In NMRP systems, stable radicals such as nitroxides are used to control the polymerization process. The free electron delocalizes between the nitrogen and the oxygen atoms and resulting mesomeric forms explaining the persistence of nitroxide radicals. In the presence of monomer, the radicals centered on the oxygen atom are very stable. They initiate the polymerization or form dimers by coupling. They can only react with a carbon radical to form an alkoxyamine. Solomon and Rizzardo found that alkoxyamines are stable at temperatures between 40°C and 60°C but they homolytically cleave at higher temperatures (>100°C) [61, 62]. The NO-C bond is labile regenerating a carbon radical by homolytic cleavage and a nitroxide radical [61]. Firstly, nitroxides were used in termination process of the polymerization after reacting with a radical source [62]. Later, they were recognized to be able to adjust the molecular weight was recognized. These approaches have been used to manufacture of block copolymers with low dispersity [29].

In contrast to other CRP processes, NMRP requires no metal catalyst or sulfur compounds. In NMRP, alkoxyamine compounds are used as unimolecular agent which generate both reactive initiating radicals and the mediating nitroxide radical. However, NMRP has some limitations for the applicability of methacrylates and slow polymerization kinetic [63].

The mechanism of NMRP follows a two-step mechanism as shown in Scheme 2. The initiation step consists of a conventional radical course and nitroxide such as 2,2,6,6-tetramethyl-1-piperidinoxyl (TEMPO). First, under the effect of the temperature initiator such as dibenzoyl peroxide generates initiating radicals that adds monomer and prefers before propagation starts to recombine with TEMPO radicals. Following to initiation, with the increased temperature the formed TEMPO adduct, which is an alkoxamine, rapidly cleaves and simultaneously forms the radicals comprising either nitroxide and carbon radio patterns. The carbon centered radical possesses the capability to add monomer while the nitride radical scavenges well carbon centered radicals. Finally, polymers showing narrow molecular weight distrubitions can be obtained [64]. There exist an equilibrium between

the dormant and active species during the reaction. Activation-deactivation equilibrium constant (*K) presents the equilibrium between the activation and deactivation process characterized.* If the equilibrium constant *K* is too high, the concentration of macro-radicals is also high facilitating irreversible termination reactions. If *K* is too low, the polymer chains remain in the form of macro-alkoxyamines resulting in inhibition of polymerization. The reaction temperature chosen and the structure of the nitroxide depicts important parameters to obtain well controlled polymerizations conditions.

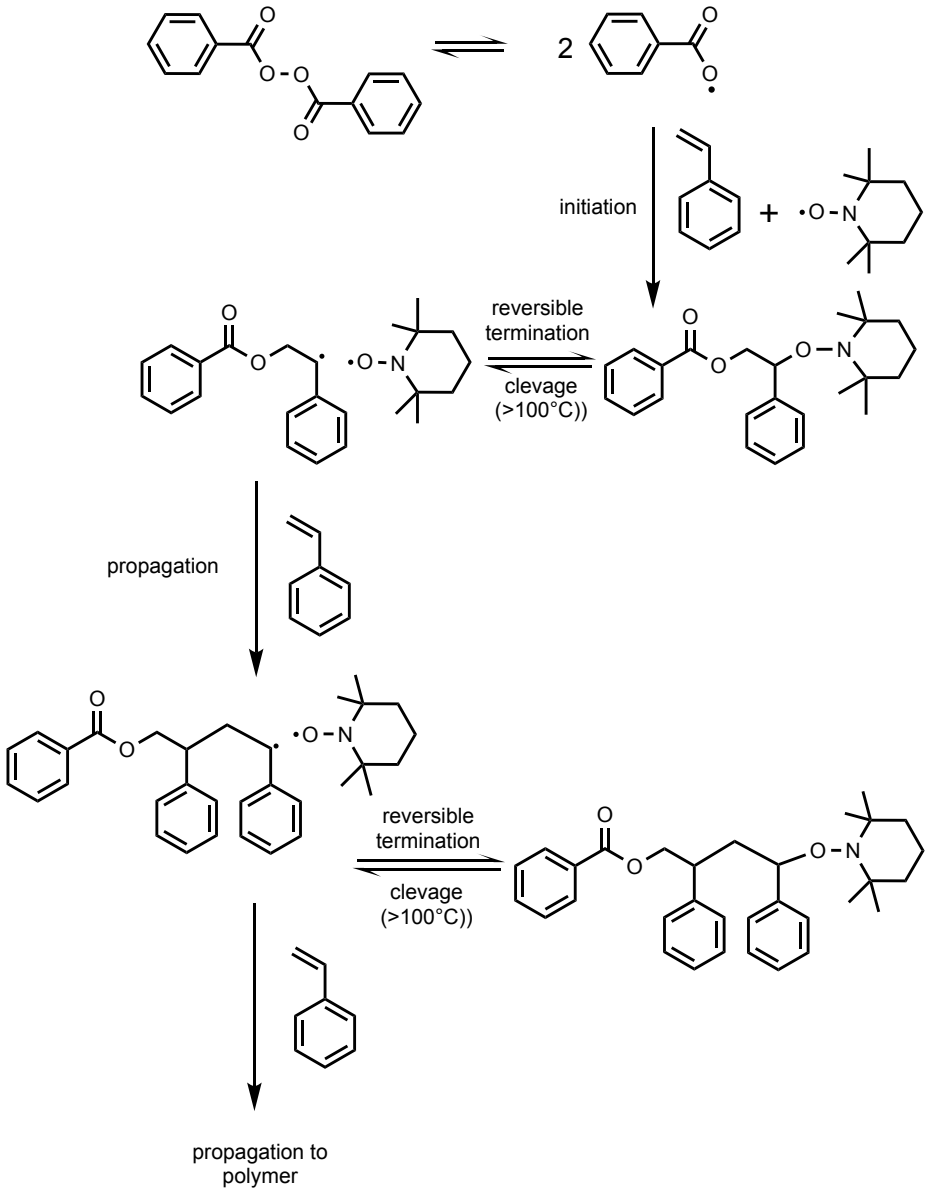

Scheme 2: Illustrated polymerization of styrene via NMRP process.

2.1.3 Atom Transfer Radical Polymerization (ATRP)

Atom transfer radical polymerization (ATRP) [26, 40, 65] has been the subject of much interest among the controlled radical polymerization methods developed one after the other for the last ten years [40, 43]. This reaction bases on the addition of species generated by in a catalyzed mechanism to olefins (Atom transfer radical addition (ATRA) comprising a metal/amine complex as catalyst and alkyl halides as initiating components [66]. In 1956, successful use of Fe^{III} or Cu^{II} salts was reported resulting in dramatical yield increase of the product in the reaction between alkyl halides and acrylonitrile. This new metal-catalyzed radical addition reaction required large amounts of metal catalyst [67].

By the inspiration from ATRA, ATRP was developed in 1995 and since then it has been the most extensively used method for the synthesis of polymers showing controlled properties including precise molecular weights, low dispersities, and excellent chain end functionalities [40]. It has become the most explored method in synthetic polymer chemistry due to its adaptability of a wide range of monomers [43].

ATRP depicts a catalytic process mediated by many transition metal complexes like Cu, Ru, Fe, Mo, Os, etc [68]. Among them copper has been the most successfully studied redox-active transition metal. As shown in Scheme 3, a metal complex in its low-oxidation state is used as catalyst (mostly Mt^mX/L, Mt^m is metal catalyst, X = halide, L = ligand) and an alkyl halide (P_n-X) in classical ATRP [69]. Initiating radicals are formed via halogen abstraction and donation processes between alkyl halide and low-oxidation state transition metal complex (Mt^m/L) results in the formation of its high-oxidation transition metal complex (X-Mt^{m+1}/L) and propagating radicals (P_n·). Monomers can add to the propagating radicals with the rate constant of propagation (k_p), and dormant species are formed by halogen abstraction from X-Mt^{m+1}/L by radicals where Mt^m/L and P_n-X are reversibly formed. Radicals terminate with the rate constant of termination (k_t). This equilibrium shows the reversible reaction and promotes halides at the end of the polymer chain. Fast initiation of the reaction and the reversibility of halide abstraction/donation processes during the reaction allow the formation of polymers with low dispersity and pre-determined molecular weights [70]. Reaction conditions (temperature, pressure, solvent), type of monomer, alkyl halide and ligand affects the values of activation and deactivation rate constants (k_{act} and k_{deact}) and thus their ratio, and the ATRP equilibrium constant.

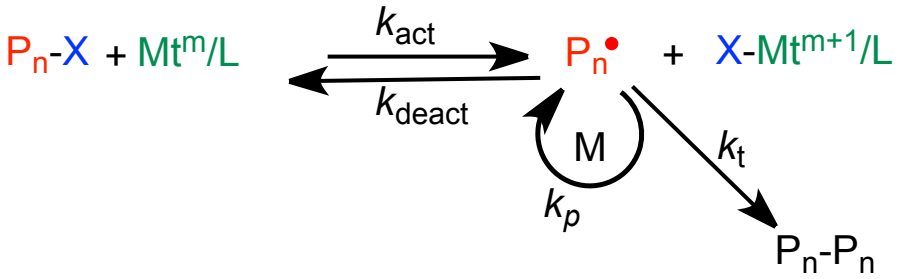

Scheme 3: General mechanism of ATRP, modified from [43].

Starting with the higher oxidation state transition metal complex (Mt^{m+1}-X_2/L) in conjuction with free radical initiators, “reverse” ATRP has been developed which facilitates to start ATRP reaction with most stable oxidative state (see Scheme 4) [40]. Higher oxidation metal complex (Mt^{m+1}-X_2/L) is then reduced to lower oxidation state (Mt^m) by generated free radicals. The high amount of catalyst needs to be removed and causes the purification steps of the polymer. Using Cu^0 which goes a proportionation reaction with Cu^{II} results in formation of Cu^I being an alternative reverse ATRP. This helped to handle the reaction conditions with less oxidatively stable Cu^I complex during the process [71].

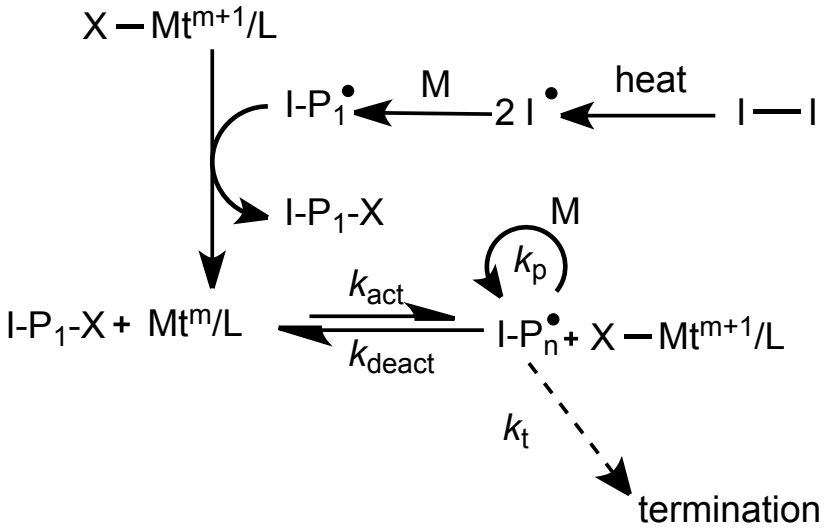

Scheme 4: Reverse ATRP by added free radical initiator (I) to form Cu^I activator and dormant species, modified from [43].

Following to these approaches, simultaneous reverse and normal initiation (SR&NI) ATRP has been proposed [72]. In this approach, more active catalyst complexes together with an alkyl halide are employed together with small amount of conventional radical initiator. However, the disadvantage of this approach can be still seen in the fact that additionally added radical initiator can initiate the polymerization resulting in the generation of new chains in the system (see Scheme 5).

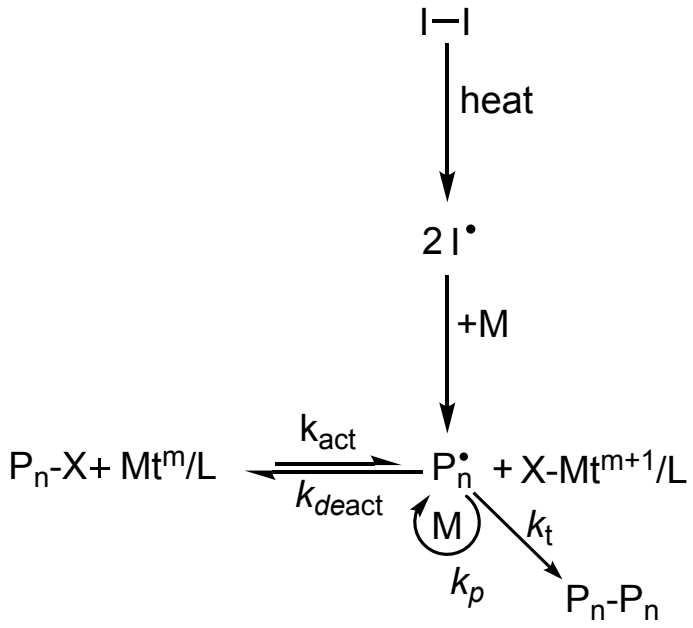

Scheme 5: SR&NI ATRP initiation mechanism, modified from [43].

SR&NI was derived into activator generated by electron transfer (AGET). Here, activation of Mt^{m+1}/L occurs by use of reducing agents rather than a radical initiator as shown in Scheme 6. The important point of this system is the added reducing agent, which should only generate Mt^{m} by electron transfer but not form any additional initiating species [73, 74].

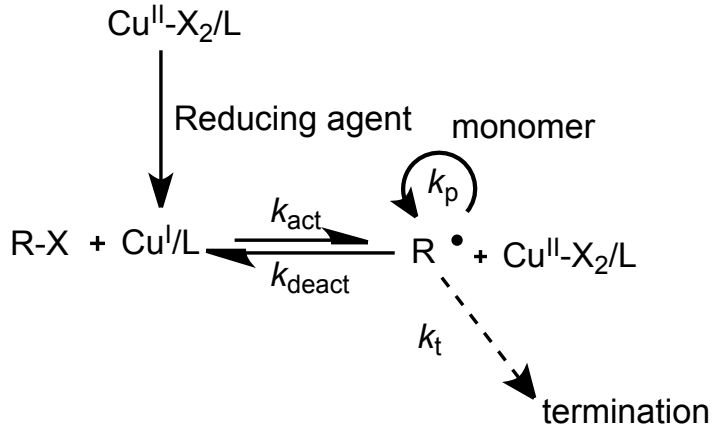

Scheme 6: AGET ATRP reaction by added reducing reagents, modified from [43].

Activator regenerated by electron transfer (ARGET) ATRP depicts a “green” procedure [75] in which only a small amount of catalyst is used together with reducing agent such as ascorbic acid [76], glucose [77], phenol [78], hydrazine [79] or Cu^0 [75]. This facilitates the use of only small amount of catalyst, which can be seen as the most important advantage of this system. It also prevents unnecessary side reactions such as chain termination reactions [63]. By the help of this technique, controlled synthesis of polymers can be succeeded with a very low catalyst concentrations (typically between 5-50 parts per million (ppm)). This facilitates to perform this technique for some applications because the catalyst removal should not be a problem. Another advantage of this technique is the fact that it prevents the formation of undesired radical formation generated by additional radical initiator during preparation of higher molecular weight polymers [80].

As mentioned before, Cu^0 functions as reducing agent and undergoes redox reaction with Cu^{II}. Thus, this procedure was called supplemental activator and reducing agent (SARA) ATRP. Other metal catalysts including magnesium, iron, silver and zinc have been shown to decrease the concentration of Cu^{II} complex in the process [81].

In all aforementioned processes, reducing agents oxidize resulting in formation of some side products. As an alternative, electrochemically mediated ATRP (e-ATRP) was developed [82]. In this concept of ATRP, the concentration of Cu^{I} and Cu^{II} are controlled by electrical current. Applied current, potential, and the passed total charge are the parameters which are needed to be considered in this process. Applied electrochemical potential affects the rate of e-ATRP reaction. The more negative potential shows the faster polymerization rate. Low oxidation state catalyst can be oxidized back to high oxidation state by electrical current [33]. Even though e-ATRP can be seen an option of the ATRP process, it possesses some limitations because of the requirement of the sufficient conductivity of the reaction and the necessity of using a counter electrode. Therefore, it has been suggested to use light to mediate ATRP; that is called as photo-ATRP [83, 84].

In all mentioned processes, Cu catalyst was used and this can be seen as one of the vital limitations of the ATRP procedures. Especially when the polymerization associates in the high concentration of catalyst, removal of metal catalyst should be considered. In order to remove the catalyst, there have been several approaches developed. Passing the polymer solution through including neutral alumina columns [85], stirring with an ion-exchange resin [86] orclay [87], using non-solvent for the precipitation [88] and the use of a heterogeneous catalysts [89] are the solution which have been proposed for the removal of the metal catayst.

Although catalyst loading can be decreased to ppm, there are still some limitations for its use for some special applications located in the field of biomaterials. Therefore, very recently, there have been successfully demonstrated some approaches to conduct the ATRP process in metal-free conditions. [90]. Photoinduced ATRP in the absence of metal catalyst was mediated by the help of light using several organic and inorganic photo-active materials [91, 92, 93]. This approach is going to be discussed in the following chapters.

2.2 Photoinduced ATRP (photo-ATRP)

Due to the limitations of large metal catalyst requirement and the possibility of oxidation of metal catalyst, researchers have developed additional approaches to eliminate those problems facilitating the operation at low catalyst concentration in ATRP by continuous regeneration of Cu^{I} activators. In order to do that, various strategies were investigated. The use of various chemical agents or photochemical and electrochemical processes have been applied for the generation the required Cu^{I} by the reduction of Cu^{II} complexes [94]. These methods include initiators for continuous activator regeneration ATRP (ICAR ATRP) [34], activators regenerated by electron transfer ATRP (ARGET ATRP) [80], supplemental activators and reducing agent ATRP (SARA ATRP) [95], and electrochemically mediated ATRP (e-ATRP) [79]. All of these system request either an excess of reducing agents or applied current.

By the introduction of light to initiate polymerization by photoactive compounds which are photoinitiators, photosensitizers, and photoredox catalysts [96, 97, 98], researchers have developed efficient methods for the syntheses of polymeric materials. Photoinitiators are able to convert light energy into chemical energy resulting in the formation of reactive species such as radicals or cations while photosensitizers can be defined as compounds acting either as donors or acceptors after absorption of light. Photoredox catalysts catalyze the reaction via single-electron transfer reactions. It is controlled by a regular photoinitiated electron transfer protocol where the redox potentials of participating substrates and the excitation energy depict important parameters [7]. Generation of reactive radicals by converting the light energy into chemical energy facilitates to use these compounds for preparation of well-defined polymers by CRP techniques in the past few years [48, 51]. The most important advantage of the these system is being fast reactions and allowing to be form thick polymeric films within a second upon irradiation [99, 100]. Additionally, polymerization can be easily controlled by turning the light on and/or off which provides spatial control into the process. Photopolymerization has become the most effective and technologically method for polymer coatings, inks, and photoresists [101, 102, 103].

It shows up as an energy saving method because photopolymerization mostly proceeds at room temperature resulting in removal of furnaces in thermal driven production processes [104]. This leads to saving of space being important for enterprises producing based on lean manufacturing. Thus, photopolymerization process is considered as an ecological alternative [46, 47, 105]. In addition, light induced polymerization enables the synthesis of patterned surfaces when the polymerization is performed on the surface. There are several light sources available which are cheap and practical can be used for photopolymerization processes. Halogen lamps, LEDs, laser diodes, UV lamps, and even sunlight was directly employed in photo-ATRP [106]. However, one should consider to scale the properties of sources, such as intensity of light source. Because time and light intensity directly affect the polymerization systems in photopolymerization reactions [107].

Several UV and visible light active compounds were used to initiate the ATRP reaction by photochemical approaches (see Scheme 7) [26, 108, 109]. Decreasing the copper catalyst concentration was succeeded by photoinduced ATRP approach [110]. One of the systems based on tris[2-phenylpyridinato-C^2,*N*]iridium(III) ($Ir(ppy)_3$) photoredox catalyst was presented for photo-ATRP [111]. In this system, highly responsive catalytic photoredox catalyst activates and deactivates by external visible light irradiation [42]. Additionally, dimanganese decacarbonyl ($Mn_2(CO)_{10}$)) showed to conduct ATRP by natural sunlight. In this system, $Mn_2(CO)_{10}$) abstracts halides from a number of alkyl halide upon visible light irradiation while Cu^{II} simultaneously reduces to Cu^{I} by the formed $Mn(CO)_5$• species. With this system, only ppm range of catalyst was employed resulted in conditions related to a controlled light-initiated system [112].

There have been demonstrated two different approaches either direct irradiation of copper catalysts or indirect irradiation in the presence of photoinitiators. In the direct approach, photoirradiation of Cu^{II} complexes was shown for the formation of Cu^{I} catalysts in the reaction media [113]. The mechanism can be explained by an electron transfer from ligand to the core metal yielding Cu^{I} complexes. In this system, $Cu^{II}X_2$/L was irradiated by light without additional photoinitiator to generate Cu^{I}X/L which can react with alkyl halide (Pn-X) and generate reactive radicals (Pn•) and high-oxidation state of Cu complex ($Cu^{II}X_2$/L) [100]. In the following step, these reactive radicals add monomer and are deactivated by the $Cu^{II}X_2$/L forming the dormant species and low-oxidation state copper complex (Cu^{I}X/L). In the indirect system, Cu^{I}X/L was generated by the reduction of $Cu^{II}X_2$/L under UV or Vis irradiation in the presence of photoinitiators [10, 112]

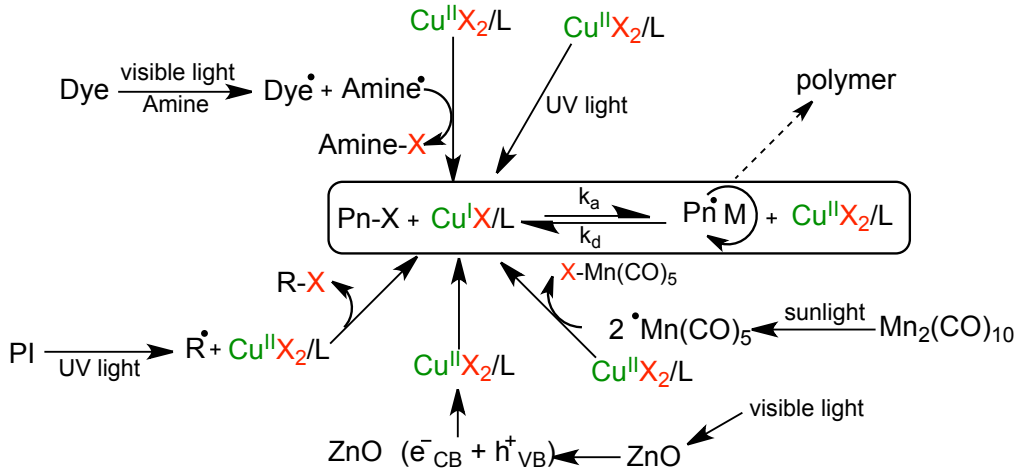

Scheme 7: Different types of photoinduced ATRP, modified from [114].

Even though, UV and visible light-induced polymerization systems have been efficiently demonstrated, these systems possess limitations. One of the drawbacks of using UV light can be seen in the poor penetration into materials, which can be tissues. UV light also possesses a scattering coefficient being about three times larger compared to NIR light [115, 116]. Additionally, UV light is harmful to cells and tissues [117]. Therefore, some applications limit its use as long as it bases on exposure with UV light. UV light also limits its applicability for these aforementioned reasons and especially for bio-applications using embedded collagen [118]. In addition, special precautions need to be considered while working under visible light to prevent the decomposition of light sensitive material by room or sunlight. This requires red light conditions for handling in industrial applications. Quite recently, the use of benefits of NIR light has successfully adapted into controlled polymerization systems [119]. These approaches will be discussed in the next chapters in this thesis.

2.2.1 UV Light-induced ATRP

The advantages of photochemical processes into the ATRP have been successfully adapted by Cu^{II} complexes under UV exposure. One of the first studies on UV-light initiated photopolymerization was shown by using 2,2-dimethoxy-2-phenylacetophenone (DMPA)/ferric tri(N,N-diethyldithiocarbamate)[$Fe(dtc)_3$] as photoinitiator for polymerization [120]. This system generates radicals by UV irradiation resulting in reduction of Fe^{III} to Fe^{II}. Another system in which the use of dithiocarbamates in conjuction with Cu catalyst was also investigated for photoinduced ATRP of methyl methacrylate (MMA) [83]. Without photoinitiators, photo-ATRP protocols were reported by direct photo-irradiation of Cu^{II} complexes [84, 100]. As shown in Scheme 7, Cu^{I} activator was formed by in-situ photo-

reduction of a more air-stable Cu^{II}/L complex. The formed Cu^{I} subsequently activates a halide initiator (P_n-X) providing the initiation of the polymerization of MMA at room temperature. Similar system also developed in which various photoactive materials such as photoinitiators or photosensitizers were employed together with Cu^{II}/L complex [84]. Scheme 8 shows the general mechanism of photo-ATRP by indirect UV exposure. The use of UV light in combination with Cu^{II}/L complex may lead to more or less polydisperse polymers. This is explainable by the possibility of photo-reduction based on a Cu^{II} system applying UV exposure. This may be the direct photolysis of Cu^{II} into Cu^{I}. Therefore, UV active materials have to be exposed in the range where Cu^{II} has no absorption. All of these studies, however, request a high concentration of copper catalyst while alternatives reported that UV light activates a reaction with lower concentrations of catalyst at ppm scale providing the desired properties of ATRP process [121].

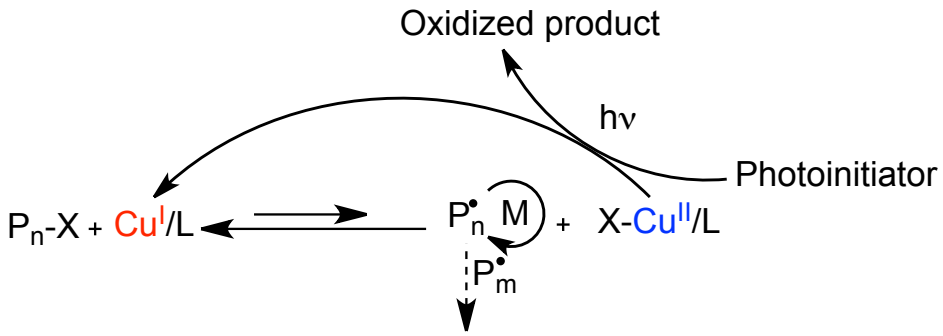

Scheme 8: Photoinduced ATRP by indirect irradiation of Cu^{II}/L complex, modified from [96].

2.2.2 Visible Light-induced ATRP

To overcome the damage of UV light and to discover more environmentally friendly alternatives, the use of visible light photoinitiators has taken a significant importance in recent years [122]. Additionally, visible light-induced systems can be employed with more simple light sources (e.g. easily accessible LEDs or sunlight) compared to UV systems. Several visible light active compounds have taken the place in the industry and have become commercial products. For example, camphorquinone (CQ) has used for dental curing [123] and certain adhesives [124] while titonocene depicts an alternative photocatalyst [125].

The wide range of absorption of sunlight has been an excellent natural energy source for several natural and synthetic polymerization reactions [126]. This might be important for countries having much more access to this natural available light source compared to

middle Europe region. Further advantage can be seen in the simplicity and free availability of sunlight.

Many light sensitive copper(II) complexes can initiate photochemical redox reaction under UV or visible light. Earlier spectroscopic investigations showed dominant absorption of Cu^{II} complexes in the UV with two bands at 250 nm and 300 nm and one band in the visible range at 650 nm and NIR range at 1000 nm [127, 128]. However, this absorption can be changed by respective ligands and the nature of the copper salt. Many photoinitiators used for free radical polymerization under visible light have been also mentioned as possible photocatalyst in ATRP process in combination with copper complexes. The use of visible light photoinitiors with Cu^{II} salts for CRP systems provides much simpler reaction conditions and overcomes the damage from the UV light.

Photoinitiated ATRP has been extended to visible range using various initiating systems operating in the visible part such as dyes (eosin Y and erythrosin B) and bis(2,4,6-trimethylbenzoyl)-phenylphosineoxide (Irgacure 819) photoinitiator [44, 129]. Acylphosphine oxide-type photoinitiators also showed to mediate photo-ATRP together with $CuCl_2$/PMDETA via PET reactions by visible light. Another copper(II) complex was developed comprising as counter anion acylphosphinate (AP) as a photoinitiator in the visible light [130]. $Cu^{II}(AP)_2$/PMDETA was able to catalyze ATRP by visible light irradiation either in organic or aqueous reactions media. Narrow bandwidth LEDs and sunlight induced photo-ATRP has been also shown with the use of copper catalyst in the ppm range. Furthermore, the photo-reduction of $CuBr_2$/L to CuBr/L was achieved using two different ligands which are tris(2-pyridylmethyl)amine (TPMA) and tris((4-methoxy-3,5-dimethylpyridin-2-yl)amine) (TPMA*) for the controlled polymerization of different monomers [122]. The proposed mechanism brings together ARGET ATRP and ICAR ATRP approaches.

In the case of dye system, as shown in Scheme 9, dye molecule absorbs the light, while an amine co−initiator reduced to the excited state of dye molecule. The photochemical reaction occurs between the excited state of dye molecule and amine by an electron transfer reaction to form radical−cation of amine and radical−anion of dye. While radicals generated from dye molecule undergoes other reactions leading to bleaching, radicals formed from amine molecule are generally reactive to initiate the polymerization [114].

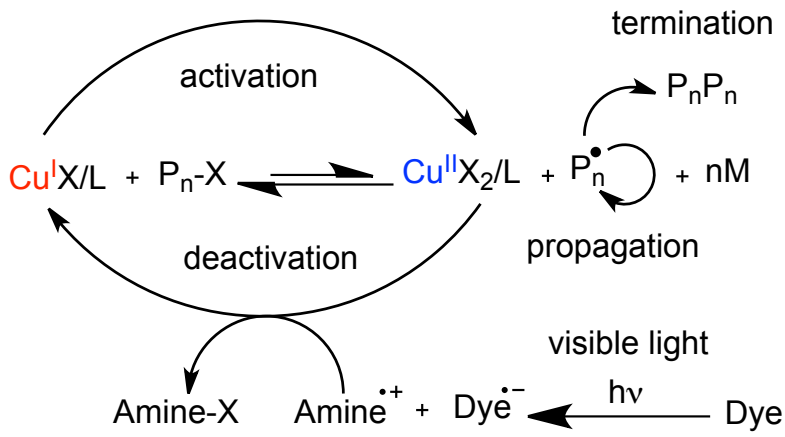

Scheme 9: Visible light-induced ATRP, modified from [44].

2.2.3 Photoinduced Metal-free ATRP

Followingly, the demand for new approaches for the decreasing the low-oxidation state transition metal catalyst concentrations including the use of reducing agents, electrical current or photochemical strategies have brought several benefits into the ATRP system. However, there still exist some limitations based on the fact that the presence of metals causes some undesired reactions such as oxidation reactions. Especially for biologic, microelectronics, pharmaceutical applications metal contamination can be very restricted [131]. Additionally, their costs and the requirements of purification to remove the metal ions are needed to be considered. To overcome these limitations associated with metal contaminations in conventional photo-ATRP, metal-free approaches were developed. The activation of the alkyl halides can be homolytically cleaved with various photocatalysts through oxidative and reductive pathways [132].

In 2014, the first attempt to conduct photo-ATRP in metal-free conditions was reported using 10-phenylphenothiazine (PTZ) as an organic photocatalyst [90]. The excitation of PTZ with 380 nm light resulted in the reduction of alkyl halide via oxidative quenching [133, 134]. After that, the formed alkyl radicals react with monomer and initiate the polymerization of several monomers. Following to this study, other PTZ compounds were also employed as photocatalysis for photoinduced metal-free ATRP [135]. Later, polynuclear aromatic compounds including perylene [97] and pyrene [136] were studied as successful photocatalysts in the visible and UV range, respectively. Both systems have been shown to activate photo-ATRP of conventional monomers in metal-free conditions. Living characteristics and chain end functionality of polymers were also showed by several kinetic studies and chain-extension experiments.

In a more recent study, dihydrophenazines [137] and phenoxazines [138] have also been shown to be a successful catalyst for the syntheses of monodisperse polymers by metal-free photo-ATRP [139]. Their light sensitivities at higher wavelengths allow ATRP process to be conducted at higher wavelengths. Very recently, thienothiohene derivatives have been used as photocatalyst for metal-free ATRP upon UV light irradiation [140].

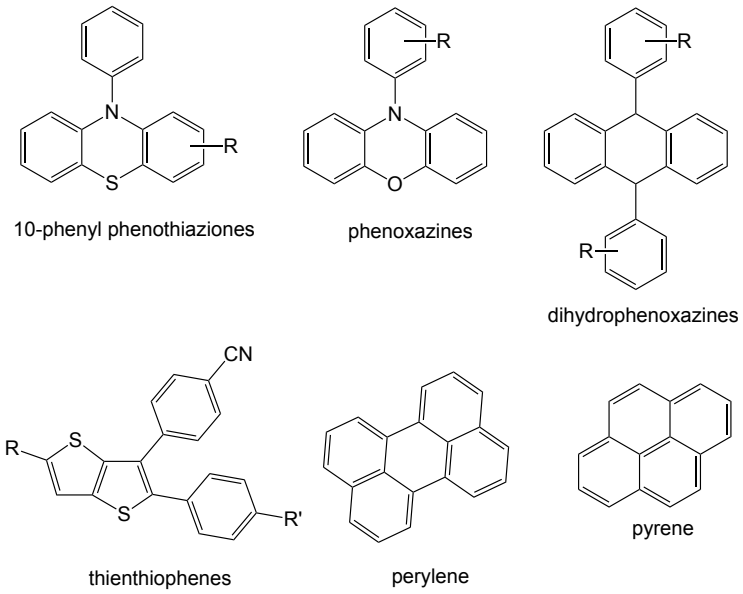

Chart 1: Structure of photocatalysis used in metal-free photo-ATRP through oxidative mechanism.

Scheme 10 shows the oxidative mechanism. The excited state of photosensitizer (PS) directly reduces the halide initiator to form the respective cation radical of the photosensitizer, bromide ion, and alkyl radicals. Monomer addition continues from these initiating radicals (P_n•). The back electron transfer from bromide ion to the cation radical of PS ($PS^{+\cdot}$) brings the PS back to the polymerization cycle and the formed bromine atom terminates the polymer chain showing the living character of the polymerization in the system.

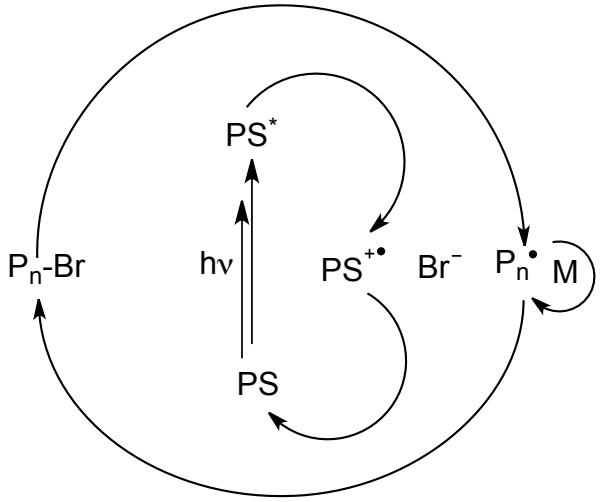

Scheme 10: General mechanism of metal-free ATRP, modified from [90].

Previously, common and commercially available dyes such as fluorescein, eosin Y and erythrosin B have been shown to catalyze ATRP together with amines in metal-free conditions through a reductive quenching mechanism [141, 142].

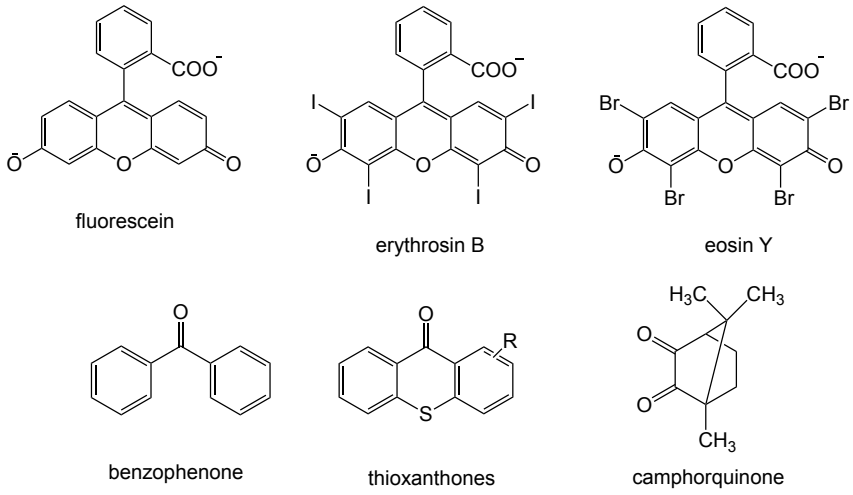

Chart 2: Structure of photocatalysis used in metal-free photo-ATRP through reductive mechanism.

In contrast the other systems, the mechanism follows a reductive quenching cycle based on PET from the electronically rich amine molecule to the excited state of the visible light active sensitizer as shown in Scheme 11. The formed anion radical of photosensitizer reduces alky halides to generate initiating radical species. Living characteristics and chain-end functionality was achieved by reversible electron transfer reactions in the process. The dye/amine system showed good efficiency under various colors of LED exposure [92, 141]. In another study, *Type II* initiators including benzophenone, thioxanthane, ITX and CQ were also shown as photocatalysts for the polymerization of vinyl monomers in the absence of Cu catalysts.

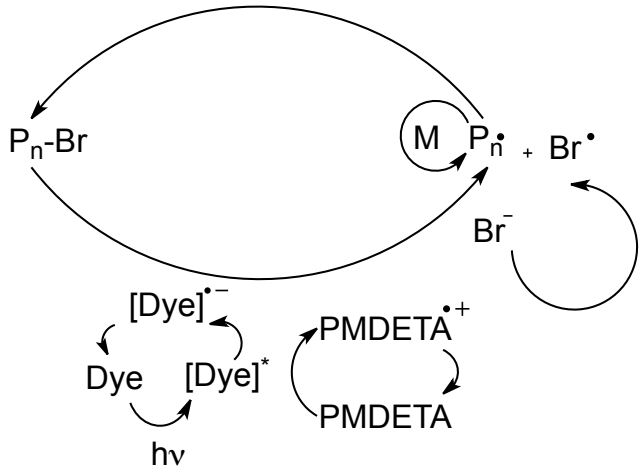

Scheme 11: Schematic mechanism of metal-free ATRP using dyes as reductive mechanism, modified from [141].

Photoinduced metal-free ATRP makes it possible to prepare well-defined polymers and their applications for example to manufacture tailor-made biomaterials [143]. Development of novel photocatalysts which are biocompatible and non-toxic, are still of big interest. Additionally, combination of other polymerization methods with metal-free ATRP might connect biological systems and polymer chemistry.

2.3 Click Chemistry

In 2001, a new concept of organic reactions was introduced for synthesis of materials with magnificent properties over the traditional routes which focus on high yields and great selectivities [144]. These reactions were called under the term of click chemistry being a green synthetic method [145, 146]. In general, “click” term means introducing molecules as easily as clicking together while no side reactions occur explaining why this synthesis is grouped to green chemistry [147]. These reactions result in very high chemical yields of product and result in the formation of no byproduct. They can be easily isolated by non-chromatographic methods and performed under mild conditions including aqueous and organic solvents [146].

Click chemistry provides an excellent strategy for the construction of carbon-heteroatom bond. Reactions matching the click chemistry criteria belong to highly selective processes. Starting materials and reagents for these reactions are mostly available. The required process features include very high yield of intended product easily removable by-products, showing regiospecificity and stereospecificity. These reactions have been able to perform in simple and mild reaction conditions. The solvent used (if necessary) should be easily

removable [144]. By showing chemoselective and single reaction pathways, click reactions possess great importance for the synthetic chemistry.

The most extensively employed reactions which succeed “click status” are Huisgen 1,3-dipolar cycloaddition, Copper catalyzed Azide- Alkyne (CuAAC) cycloaddition [148, 149], and Diels-Alder cycloaddition reactions (DA) [150, 151, 152, 153]. Additionally, thiol-ene reactions can be defined as click reactions because of their efficiency, and applicability in mild reactions conditions. However, thiol-ene reactions do not possess all click reaction properties [154, 155, 156]. The cycloaddition reactions of alkynes and azides (namely as Copper-catalyzed azide alkyne cycloaddition, CuAAC) resulting in the formation of 1,2,3-triazoles is the most commonly used and applicable method. The easy synthesis of alkyne and azide functionalities make CuAAC reactions the most attractive one. Even though click reactions take place in a wide range of applications, these reactions have some disadvantages which limit to be used in some applications. Similar to traditional ATRP system mentioned in Chapter 2.1.3 CuAAC needs copper catalyst which has the capability to oxidize by molecular oxygen. Therefore, specific experimental conditions need to be considered. Additionally, the concern about the safety of azide moiety is point that medical chemists have not given these reactions attention [157]. It has been growing the number of applications based on click chemistry in polymer science, bio-conjugation, materials science, and drug delivery [158, 159, 160].

2.3.1 Diels Alder Click Reactions

Diels-Alder (DA) reaction was explored and awarded by the Nobel Prize in 1950 for its discovery [161]. In this reaction, [4+2] cycloaddition reaction between an electron-rich diene and an electron poor dienophile introduces the formation of a stable cyclohexene as shown in Scheme 12. This reversible reaction allows the preparation and functionalization of several molecules. Decomposition of formed stable cycle can be controlled by temperature [162]. Some of Diels-Alder reactions serve the requirements of click reactions. The main advantage of these reaction is no requirement to use a metal catalyst.

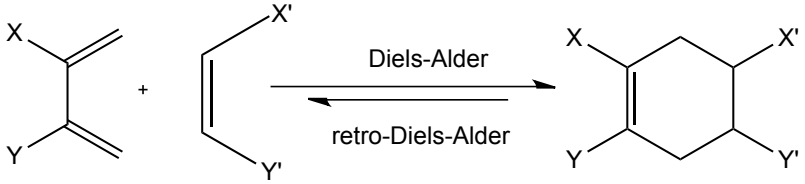

Scheme 12: General mechanism of Diels-Alder reaction of dienophile and diene.

The combination of living/controlled polymerization techniques with DA reactions facilitates preparation of different macromolecular structures including homopolymers or complex polymer structures. The polymerization system comprising diene and dienophile functional groups can be achieved by DA reactions. This approach can be extended to synthesize polymers containing reactive end groups and can go further polymerization or other reactions (also known as telechelic polymers). Preparation of maleimido-functionalized telechelic polymers was reported elsewhere [163]. Syntheses of block copolymers have been also successfully showed through DA reactions by several working groups [164, 165, 166]. The synthesis of polystyrene-*b*-(ε-caprolactone) (PSt-*b*-PCL) by just by increased temperature the dithioester-functionalized polystyrene and diene-functionalized poly(ε-caprolactone) has been investigated recently [167, 168]. These studies have shown the possibility of synthesis of block copolymers with high molecular weight to over 100000 g·mol^{-1} and narrow molecular weight distubution (*Đ*<1.2). Several groups also showed the synthses of graft copolymers by DA reactions [169]. Well-defined polystyrene-*g*-poly(ethylene oxide) (PSt-*g*-PEO) and polystyrene-*g*-poly(methylmethacrylate) (PSt-*g*-PMMA) copolymers were successfully synthesized via this method. For the complex macromolecular structures, it is also possible to combine DA reactions with other click-type reactions. As an example, a further approach reported synthesis of A_3 and ABC-type star polymers [170]. Preparation of polymer networks with DA click reactions resulted in a new cross-linked polymers [171] and hydrogels [172]. DA reactions were used to synthesize polymer networks with multifunctional polymers [173, 174, 175], linear polymers comprising furan and maleimide [176, 177] or cross-linker or an initiator [178, 179]. For the synthesis of thermoset networks and polymer gels, DA click chemistry has been the most commonly employed reaction [180, 181].

2.3.2 Thiol-ene Click Reactions

The new synthetic routes in chemistry promote the research of scientist in the polymer science. Click reactions are one of the best pathways which are one of the mostly studied strategies in chemistry. These reactions include cycloaddition reactions in general, the catalyzed and non-catalyzed coupling between an azide and alkyne, as well as a family of thiol-based chemistries such as thiol-ene [182, 183, 184], thiol-yne [185], thiol-isocyanate [186] and thiol-halo reactions [187]. Scheme 13 provides a general mechanism.

The reactions of sulphur comprising compounds with alkenes go back to mid-19th century. In the middle of the 20th century, thiol-ene chemistry was used to make cross-linked networks [188]. The benefits of thiol-ene coupling reactions such as tolerance of many

different reactions conditions, clearly defined reaction products or pathways make thiol-one chemistry being used in synthetic polymer chemistry. Similar to DA cycloaddition reactions, high reactivity of thiol compounds with carbon-carbon double bond also exhibit some properties of click chemistry. These reactions can be conducted in mild reaction conditions and exhibit orthogonality with other common synthetic procedures. In addition, thiol-ene click reactions result in high yields conditions in rapid reaction rates. These systems are not sensitive to water and often molecular oxygen therefore these reactions are easy to perform which as also a click criteria [189]. The nature of thiol-ene chemistry allows for the preparation of well-defined macromolecular structures such as network formation. This also allows the functionalization of the polymers with few synthetic pathway. Because this system is not sensitive the oxygen, mechanical properties of formed networks showed to have more regular structures [190]. Additionally, the use of this concept can be found in hydrogels, thin films and lithographic applications [191, 192]. These reaction take place in the application of surface modification, photolithography, and bio-conjugation systems due to the applicability to several functional groups [193].

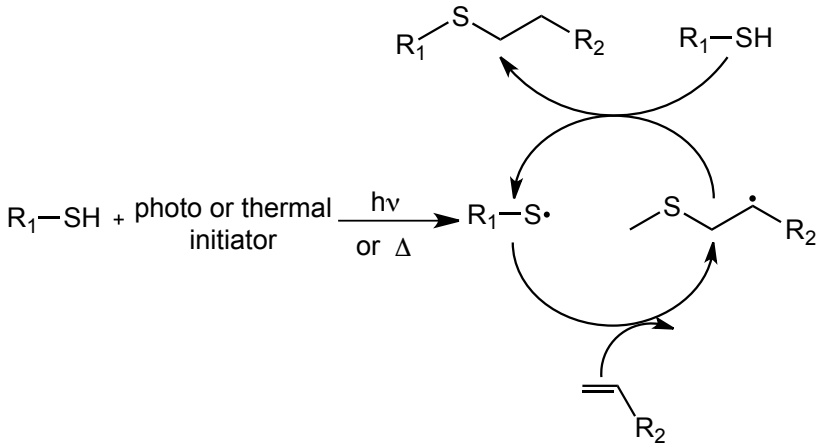

Scheme 13: Mechanism of radical thiol-one coupling reactions, modified from [194].

Photo-induced thiol-ene click reactions were also successfully shown between thiols and alcohols, amines and amino acids at ambient temperature. Visible light has been widely used for photoinduced thiol-ene click reactions. Being not harmful to the environment and bio-systems, visible lightinduced thiole-ene click reactions can be found in the application of bio-conjugations.

2.3.3 Conventional and Photoinduced Copper Catalyzed Azide-Alkyne Click Reactions (CuAAC and Photo-CuAAC)

Copper-catalyzed cycloaddition reaction between azides and alkynes has been the most studied click reactions [149]. Azides and alkynes are not reactive unless certain conditions are provided. They undergo cycloaddition reaction only at high temperatures without catalyst resulting in the formation of mixture of products. Cu(I)-catalyzed click reaction between organic azides and alkynes are much faster and highly regioselective reaction [148]. This reaction prompts the formation of triazole which is essentially stable to oxidation, reduction and hydrolysis. Triazoles do not hydrolytically cleave [195]. This reaction can even be carried out at ambient temperatures. Sharpless introduced the reduction of copper silicate pentahydrate for in situ generation of Cu for carrying out this reaction [145]. Other approaches have been shown using cuprous iodide together with peptides [196]. Both reactions showed the regioselective formation of 1,4-disubstituted 1,2,3,-triazoles. Applications of this reactions in synthetic polymer chemistry and materials science have been reviewed by Binder et al. [146] and Lutz [197].

A comprehensive mechanistic studies of click reaction demonstrated that the CuAAC reaction proceeds through a stepwise mechanism. An interaction between Cu^{I} and terminal alkynes result in the formation of Cu-alkyne π-bond complex followed by deprotonation of alkynes and formation of a copper acetylide. This complex then reacts with terminal nitrogen of the azide group to produce a metallacycle via a nucleophilic attack. The formed metallacycle then undergoes a ring construction. Cu triazolide is then formed by a fast transannular interaction between the lone pair of electrons on the substituted nitrogen of the azide and the C=Cu bond. Cu triazolide then undergoes protonation to produce the 1,4-disubstituted triazole and Cu(I) catalyst is generated [198].

Even though click reactions are known as efficient processes, they have some limitations. For example, CuAAC reactions require Cu^{I} catalyst that can oxidize in the presence of air. To overcome this problem, reducing agents (i.e. phenol derivatives, hydrazine, ascorbic acid) have been proposed for the reduction of Cu^{II} salts to form Cu^{I} species [199]. Electrochemical redox processes [200, 201] and photochemical techniques have been also developed as similar reduction processes.

Light-induced chemical reactions have been extensively adapted in synthetic chemistry including click reactions by combining the advantages of photochemical process and benefits of click reactions. Because light-induced reactions are spatially and temporally controlled, it is easy to reach the high level of control of the reaction. This is not possible with thermal processes [202, 203]. The control over the reaction can be succeeded by

changing the exposure time, wavelength, and intensity and by focusing photons on onto a given area. Furthermore, these reactions result in excellent synthetic strategies in chemistry, and tailored material fabrication. Light-induced reactions are introduced to click reactions, including photoinitiated thiol-ene/thiol-yne coupling [194], photoinduced 1,3-dipolar cycloaddition reaction of alkynes and nitrile imines [202], cycloaddition reactions of photochemically generated cycloalkanes and azides [204], photoinduced ester formation reactions of benzodioxinones with alcohols [205], and photoinduced DA reactions [206].

In particular, the necessity of Cu^{I} catalysts in CuAAC reactions promotes the scientist to find out several methods for the generation of the Cu^{I} catalyst by starting Cu^{II} salts. Some reducing agents are shown to reduce CuI^{I} species to generate Cu^{I} species [199]. These strategies also prevent the inhibition of molecular oxygen. Electrochemical redox techniques can be also applied for the similar reduction strategy [201]. Notably, these methods have also been employed for ATRP reactions that also requires Cu^{I} catalyst. Photochemical strategies for CuAAC reactions have been intensively and most efficiently used for several years. These works comprise the direct or indirect irradiation with UV and visible light. In direct photolysis, copper ligand complex absorbs the light and undergoes redox reactions with the ligand. This electron transfer results in the formation the radical complex of the ligand and Cu^{I} by reduction of Cu^{II}. The direct exposure method need longer time compare to the indirect photolysis. In indirect photocatalysis, photoinitiators act as light absorber. Excited state of the photosensitizer reduced Cu^{II} to Cu^{I} required for CuAAC reaction and generates the reactive intermediates such as initiating radicals or carbocations. Additionally, in indirect irradiation, the use of visible light can be another advantage because in this range Cu^{II} complex is also transparent.

More approaches exploited standard photolithographic techniques [207]. As summarized in Scheme 14, the use of Type I initiators including α,α-Dimethoxy-α-phenylacetophenone, 2-(Dimethylamino)-1-(4-morpholinophenyl)-2-benzyl-1-butanone, (2,4,6-Trimethylbenzoyl)diphenylphosphine oxide, and dicyclopentadienyl bis[2,6-difluoro-3-(1-pyrrolyl)phenyl]titanium which is well known as titocene in industry, polynuclear aromatic compounds and CQ, and bisacylgermane (namely dibenzoyldiethylgermane) successfully showed to follow this approach [208, 209, 210, 211]. Type I initiators directly decompose by light irradiation while CQ, for example, reaches to its triplet state and abstract hydrogen from co-initiators to form reactive radicals as well known in Type II initiators.

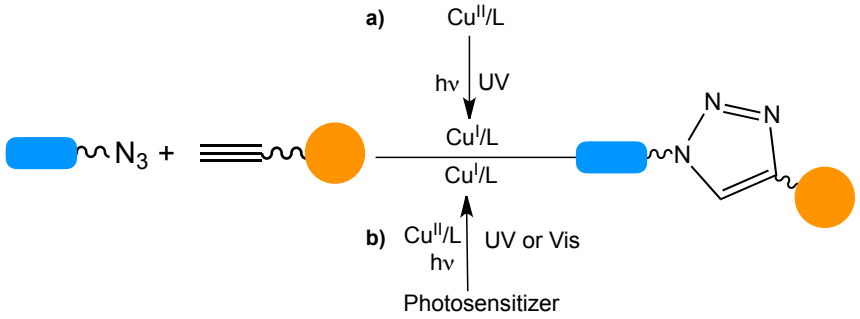

Scheme 14: Photoinduced CuAAC reactions by direct (**a**) or indirect irradiation (**b**), modified from [212].

Furthermore, these reactions can be completed a short UV irradiation or low catalyst concentration because the formed Cu^{I} is stable when the reaction mixture is kept in dark as explained by kinetic studies. CuAAC reaction can be easily stopped by simply opening the solution to the air which leads to oxidation of Cu^{I} to Cu^{II}. This reversible oxidation of Cu^{I} to Cu^{II} reaction can be followed by the change of the color of the solution to green. However, when the solution purged with inert gas and re-irradiated with UV light, reactions proceeds further [212]. This feature makes photo-CuAAC reactions an excellent method for many applications[158].

2.4 Upconversion Nanoparticle Assisted Photopolymerization

Photopolymerization in NIR region has gained a big interest because of the great advantages of the system [118]. One of the advantages of this system is that NIR light has lower photon energy and causes not to damage the formed polymeric materials or living cells needed for bioapplications [213, 214]. Moreover, NIR light provides deeper light penetration in materials due to lower scattering coefficient [116]. It also facilitates the deep or complete curing of the thick composites [215]. In addition, bio-applications prefer NIR light for processing due to the deep penetration through the deep tissue [117]. This is one of the main reasons why NIR light induced processes have become very important in both materials sciences and bio-related applications [216, 217, 218]. An appropriate photosensitizer has to be chosen in order to proceed a successful utilization of NIR light into photopolymerization techniques. These photoinitiators should not only possess an optimal absorption but also match with the emission of NIR light source. However, the drawback of NIR photo initiator compared to contrast to UV/visible light photoinitiator is the limited available amount NIR light photoinitiators. Typical NIR photoinitiators include Bacteriochlorophyll A [213], polymethines [119], NIR absorber-borate [219], and cyanine derivatives [220, 221, 222].

Upconverting nanoparticle-assisted photochemical reactions with NIR excitation has become increasingly important [223]. The upconversion process describes stepwise absorption of several photons at longer wavelength results in an emission in a shorter wavelength. Lanthanide-doped upconverting of phosphors in the form of glasses, crystals, and nanoparticles (**UCNP**s) provide unique spectroscopic properties such as relatively good photoluminescence efficiency, sharp emission and absorption spectra, and long lifetimes [217]. Lanthanide-doped materials convert NIR light into UV or blue light multiphoton absorption processes [223, 224]. This type of emission is also called as anti-Stokes emission. It should be emphasized that the function of **UCNP**s basically differs from the simultaneous two-photon absorption. Lantanide ions generate upconverted photons after excitation. Another dopant (e.g. Yb^{3+}) showing a large absorption in the NIR can be used to bring the system to NIR region. Different interactions between different dopants on the particle cause the emission of the **UCNP**s from UV to NIR.

Recently, NIR-light induced photopolymerization by **UCNP**s was introduced in polymer science [225, 226, 227, 228, 229, 230]. Excitation of **UCNP**s with high intensity sources such as NIR laser diodes results in the formation UV or visible light, which can initiate the photopolymerization rections with UV or visible light initiators. Upconversion nanoparticle assisted photopolymerization reactions have been applied to drug delivery [231] photolithography [232], and catalysis [233]. **UCNP**-assisted photopolymerization was successfully employed in macromolecular syntheses including traditional free radical polymerization [225] and thiol-ene photo-click coupling reaction [234]. Furthermore, **UCNP**-assisted polymerization has been recently employed for CRP techniques including photo-ATRP [226] and photo-RAFT [235]. Successful NIR-induced free radical and cationic photopolymerizations were also reported via electron transfer between visible light photoinitiator and *N*,*N*,*N*',*N*'',*N*''-pentanethyldiethylenetriamine (PMDETA) using upconverting glass together with iodonium salts [236]. Emitted light from the upconversion glass was successfully used for the excitation of fluorescein and excited state fluorescein was shown to undergo redox reactions with PMDETA resulting in the generation of reactive radicals. These radicals were able to add the monomers for the polymerization of methyl methacrylate. Very recently, it has been shown that the combination titanocene with diphenyl iodonium hexafluorophosphate has been demonstrated successfully for free radical-promoted cationic photopolymerization of oxirane and vinyl monomers such as cyclohexane oxide, *n*-butyl vinyl ether and *N*-vinyl carbazole in the NIR region [237]. In this system, visible light generated by **UCNP**s after exposure with NIR laser at 980 nm was absorbed by titanocene to form radicals. These radicals were shown to add the monomer

or to abstract hydrogen to form electron rich radicals. The cationic polymerization then initiated by after the oxidation of these electron donor radicals by iodonium salt. Furthermore, this system has been also employed for macromolecular systems using the emitted visible or UV light of NIR-excited **UCNP**s [238]. They showed that the activation of blue or UV light emission generated from the **UCNP**s by NIR light exposure can initiate the polymerization resulting in the formation of cross-linked polymeric materials. All of these examples require additional photoinitiator to activate the polymerization. Recently, another approach was developed with no request of an additional photoinitiator [239]. By surface modification of **UCNP**s with the photoactive chain transfer agent, they reported an efficient method for visible light-induced photopolymerization. Another example of this system for controlled radical polymerization, that is photo-RAFT, based on NIR light-induced RAFT polymerization of several monomers [235] using dithiocarbonyl compounds and **UCNP**s as internal light sources [235]. In the system, the RAFT agent absorbs the emitted blue light by **UCNP**s when they irradiated by 980 nm light. Well-defined macromolecular structures were synthesized and successful chain end functionality were demonstrated by spectroscopic methods.

Adaption of the reported photoinduced metal-free photo-ATRP systems to NIR region, it has been successfully demonstrated that **UCNP**s can be also used in photo-ATRP system without metal catalysts. The system comprising **UCNP**s as UV light generator, isopropyl thioxanthone (ITX) as photoinitiator and PMDETA as electron donor was able to activate the polymerization of methyl methacrylate through photo-ATRP strategy without metal catalyst. The living property of the system was approved by chain-extension experiment. This thesis shows the first results in this field [226] *vide infra* in Chapter 2.2.3.

2.5 Carbon Nanodots (CDs) Assisted Photopolymerization

Commonly used photosensitizers or photocatalysts for photoinduced polymerization base on synthetic materials may cause several problems considering environmental issues. They even cause a high carbon food print because they base on petrol chemicals. Therefore, there have been a great afford to replace these materials with sustainable photocatalysts or photosensitizers. Being a member of nano-carbon family, **CD**s promise to be used as green photosensitizers because of their low cost and toxicity. **CD**s show excellent photophysical properties as well as fascinating photostability [240, 241, 242]. Additionally, **CD**s derived from natural sources can substitute the role of the synthetic photosensitizers in photopolymerization systems. Because the synthetic routes are easy and cheap, recently, the synthesis and applications of these materials have been

intensively studied [242]. They also show a novel florescent properties and exhibit size below 10 nm [241]. Additionally, **CD**s demonstrated interesting electrochemical redox properties. Attributed to ultra-stable photoluminescence, easy preparation and sustainable raw materials, photoluminescent **CD**s can be applied in bioimaging, optoelectronics, and photocatalysis [240, 242]. In general, first lab results also showed tunability of absorption into the red part. In general, it may become possible to cover NIR part as well.

According to their photonics and electrochemical properties, **CD**s can be used to sensitize photoinitiated radical polymerization. They uptake the function as photosensitizer together with onium salts. Recently, it has been successfully shown that **CD**s took the role as effective photocatalyst for RAFT polymerization under visible light and natural sunlight irradiation resulting in effective polymerization of various monomers and narrow dispersity about 1.1 [243]. **CD**s also take place in photo-induced ATRP process by a broader available range of LED sources which has received big attention in academia and industry in order to replace existing mercury lamp with modern light sources. First results can be found in Chapter 5.5.

3. Materials and Methods

This chapter briefly discloses the experimental conditions used in this thesis. More details can be found in published material [119, 226, 244, 245].

3.1 Reaction Conditions

Photopolymerization reactions were carried out in dried glassware under inert atmosphere using standards *Schlenk* techniques. Room temperature refers to 22-25 °C. Temperatures of 0 °C were obtained using ice/water bath for the syntheses of clickable compounds.

3.2 Solvents

For moisture sensitive reactions, dry solvents are purchased and were used without further purification. Dimethylsulfoxide (DMSO) 99.8% extra dry, and *N*, *N*'-dimethylformamide (DMF), 99.8% extra dry were purchased from Sigma-Aldrich. Dry solvents are stored over activated molecular sieves (4Å). Deuterated solvents were received from ARMAR AG. The following solvents are commercially available and were used without further purification: Toluene, diethyl ether (Et_2O), dichloromethane, (CH_2Cl_2), methanol (MeOH), *n*-hexane (n-Hex), ethyl acetate (EtOAc) were used as received.

3.3 Reagents

Commercially available chemicals were purchased from the suppliers Across, Alfa-Aesar, Sigma-Aldrich (now Merck KGaA), and TCI, and were used without further purification. *N*,*N*,*N*′,*N*″,*N*″- pentamethyldiethylenetriamine (PMDETA, 99%), α,α-dimethoxy-α-phenylacetophenone (DMPA, 99%), 2-isopropyl thioxanthone (ITX) and ethyl α-bromo-2-methylpropionate (EBiP, 98%), ethyl α-bromophenylacetate (EBPA, 97%), and ethyl α-bromopropionate (EBP, 99%) were purchased from Sigma-Aldrich and used as received. Methyl methacrylate (MMA, 99%), styrene (S, 99%) and tri(propylene glycol) diacrylate (TPGDA) were bought from Sigma-Aldrich and passed through a plug of basic alumina before use to remove the inhibitor and stored under nitrogen atmosphere and stored in the fridge (0-5°C) before use. For the removing of the inhibitor from the monomers, basic alumina (Merck, aluminium oxide 90 active basic, 0.063-0.0200 mm) was used. Copper(II)bromide ($CuBr_2$), tris(2-pyridylmethyl) amine (TPMA, 98%), benzyl bromide (98%), phenylacetylene (98%), 9-(chloromethyl)anthracene (98%), 1-bromooctane (99%), sodium azide (NaN_3, 99%), 4-pentynoic acid (95%), poly(ethylene glycol) methyl ether (Me-PEG) (M_n=2000 g·mol^{-1},), *N*,*N*′-dicyclohexylcarbodiimide (DCC, 99%) and 4-

(dimethylamino)pyridine (DMAP, 99%,) were purchased from Sigma-Aldrich and used as received without any further purification. Sigma Aldrich and used as received. Chloroform (99%), 4-toluenesulfonyl chloride (98%), propargyl alcohol (99%) were purchased from Merck. In addition, sodium nitrite ($NaNO_2$), magnesium sulfate ($MgSO_4$, 99.5%), sodium bicarbonate ($NaHCO_3$, 99.9%), were also purchased from Sigma-Aldrich and used without any further purification. NIR sensitizers **1** (2-[2-[3-[2-(1,3-Dihydro-1,3,3-trimethyl-2H-indol-2-ylidene)-ethylidene]-2-(1-phenyl-1H-tetrazol-5-ylsulfanyl)-1-cyclohexene-1-yl]-ethenyl]-1,3,3-trimethyl-3H-indolium chloride), **2** (5-(6-(2-(3-Ethyl-1,1-dimethyl-1H-benzo[e]indol-2(3H)-ylidene)ethylidene)-2-(2-(3-ethyl-1,1-dimethyl-1H-benzo[e]-indol-3-ium-2-yl)vinyl)cyclohex-1-en-1-yl)-1,3-dimethyl-2,6-dioxo-1,2,3,6-tetrahydropyrimidin-4-olate), **3** ((E)-2-(2,2-bis((hexanoyloxy)methyl)-1H-perimidin-3-ium-4(2H)-ylidene)-4-(2,2-bis((hexanoyloxy)methyl)-2,3-dihydro-1H-perimidin-4-yl)-3-oxocyclobutanolate), and **4** (6-butyl-2-((1E,3E,5Z)-5-(5-butyl-3-cyano-2-methyl-4,6-dioxocyclohex-2-en-1-ylidene)penta-1,3-dien-1-yl)-4-cyano-3-methyl-5-oxocyclohexa-1,3-dienolate), and **5** (1,3-diethyl-5-((*E*)-6-((*E*)-2-(3-ethyl-1,1-dimethyl-1*H*-benzo[*e*]indol-2(3*H*)-ylidene)ethylidene)-2-((*E*)-2-(3-ethyl-1,1-dimethyl-1*H*-benzo[*e*]indol-3-ium-2-yl)vinyl)cyclohex-1-en-1-yl)-6-oxo-2-thioxo-1,2,3,6-tetrahydropyrimidin-4-olate) were received from FEW Chemicals as S 0507, S 2265, S 0821, and S 2483, and S 2344 respectively. All onium salts were **1a**, **1b**, and **2a** were received from FEW Chemicals as S 2617, S 2430, S 2615 respectively.

3.2.1 NIR Sensitizers

NIR sensitizers **1** (2-[2-[3-[2-(1,3-Dihydro-1,3,3-trimethyl-2H-indol-2-ylidene)-ethylidene]-2-(1-phenyl-1H-tetrazol-5-ylsulfanyl)-1-cyclohexene-1-yl]-ethenyl]-1,3,3-trimethyl-3H-indolium chloride), **2** (5-(6-(2-(3-Ethyl-1,1-dimethyl-1H- benzo[e]indol-2(3H)-ylidene)ethylidene)-2-(2-(3-ethyl-1,1-dimethyl-1H-benzo[e]-indol-3-ium-2-yl)vinyl)cyclohex-1-en-1-yl)-1,3-dimethyl-2,6-dioxo-1,2,3,6-tetrahydropyrimidin-4-olate), **3** ((E)-2-(2,2-bis((hexanoyloxy)methyl)-1H-perimidin-3-ium-4(2H)-ylidene)-4-(2,2-bis((hexanoyloxy)methyl)-2,3-dihydro-1H-perimidin-4-yl)-3-oxocyclobutanolate), and **4** (6-butyl-2-((1E,3E,5Z)-5-(5-butyl-3-cyano-2-methyl-4,6-dioxocyclohex-2-en-1-ylidene)penta-1,3-dien-1-yl)-4-cyano-3-methyl-5-oxocyclohexa-1,3-dienolate), and **5** (1,3-diethyl-5-((*E*)-6-((*E*)-2-(3-ethyl-1,1-dimethyl-1*H*-benzo[*e*]indol-2(3*H*)-ylidene)ethylidene)-2-((*E*)-2-(3-ethyl-1,1-dimethyl-1*H*-benzo[*e*]indol-3-ium-2-yl)vinyl)cyclohex-1-en-1-yl)-6-oxo-2-thioxo-1,2,3,6-tetrahydropyrimidin-4-olate) were received from FEW Chemicals as S 0507, S 2265, S 0821, and S 2483, and S 2344 respectively as stated in Table 1 and used without further purification. These patterns include sensitizers showing no charge (S 2265,

S 0821). Table 1 shows the respective structures. It was expected that these sensitizers might have an impact on sensitized photopolymerization based on their redox properties and excitation energy on the free reaction enthalpy of photoinduced electron transfer [7, 17].

3.2.2 Onium Salts

All onium salts were received from FEW Chemicals GmbH as commercially available materials **1a**, **1b**, and **2a.** as S 2617, S 2430, S 2615, respectively, and used without further purification. Table 2 shows the respective structures. They functioned as electron acceptors to generate initiating radicals. The different structures provided an improved compatibility with the surrounds derived from higher viscous multi-functional acrylates [246].

Table 1: Structures of NIR Sensitizers

NIR Sensitizers	Name[a]	Chemical Structure	
Cationic	S 0507	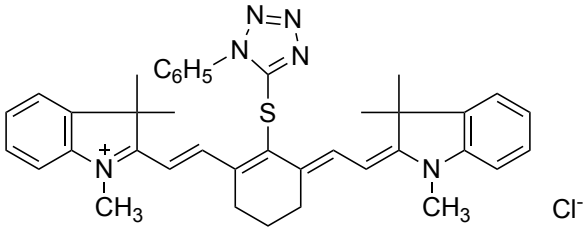	**1**
Zwitterionic	S 2265	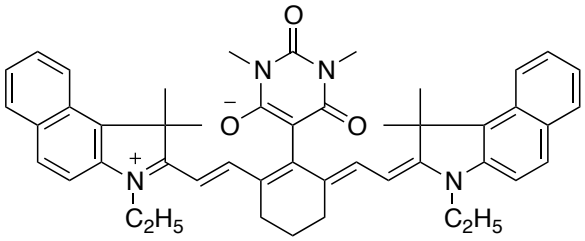	**2**
	S 0821	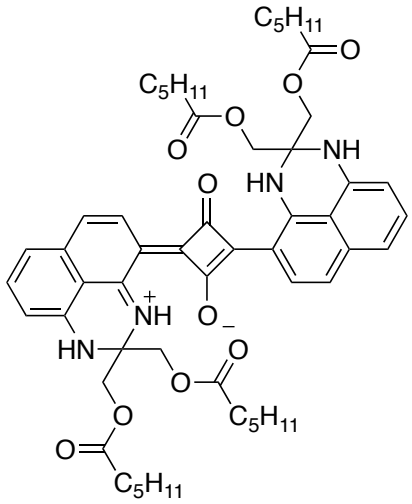	**3**
	S 2344	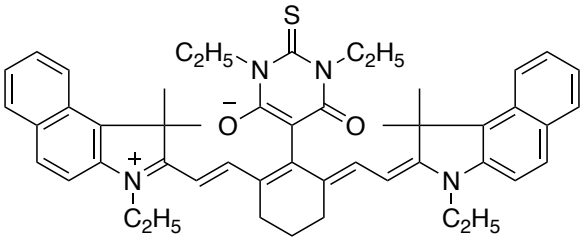	**5**
Anionic	S 2483	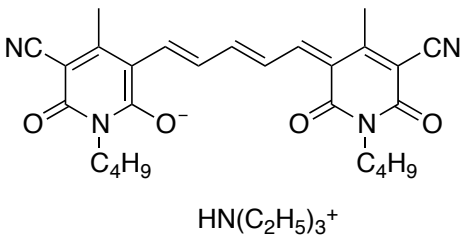	**4**

[a]Commercial names from FEW Chemical GmbH.

Table 2: Structures of Onium Salts

Name[a]	Chemical Structure	
S 2617	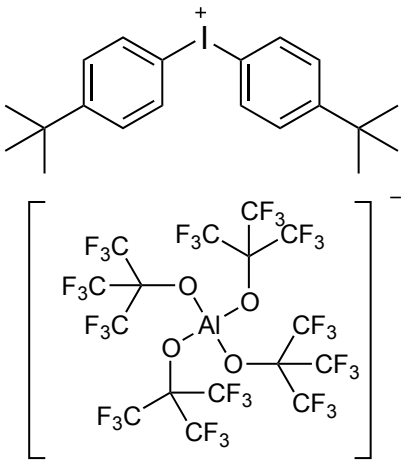	**1a**
S 2430	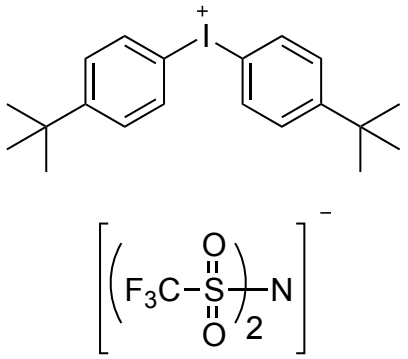	**1b**
S 2615	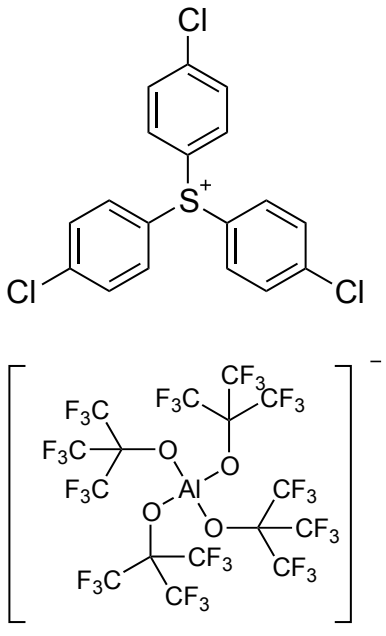	**2a**

[a]Commercial names from FEW Chemical GmbH.

3.2 Analytical Methods and Equipment

3.2.1 UV/Vis Spectroscopy

All characterizations were performed by Varian Cary 5000 UV/Vis/NIR spectrometer. Measurements of activation rate coefficients were performed on Agilent 8453 UV-Vis Spectrometer, with measurements every 5 s at 750 nm. The data were recorded using Varian UV Scan Application from Varian (version 3.00 (339)). The subsequent evaluation was carried out with Igor Pro Version 6.37 from Wave Metrics.

3.2.2 Nuclear Magnetic Resonance Spectroscopy (NMR)

To check the structure and purity of compounds synthesized nuclear magnetic resonance (NMR) spectroscopy was used. For this purpose, about 15 mg of the compound for a ^{1}H-NMR measurement were dissolved in 0.7 ml of deuterated solvent. Then ^{1}H-NMR spectra were recorded with a Fourier 300 NMR spectrometer from Bruker. The software "TopSpin 3.2" from Bruker was used to select the measurement method and data acquisition. Further evaluations (e.g. integration) were carried out using the software "MestReNova V8.1.1-11591" from Mestrelab Research S.L. performed.

3.2.3 Fourier-transform Infrared Spectroscopy (FTIR)

In this work, infrared spectra of the compounds synthesized were recorded using the “Alpha-P” device from Bruker. For the acquisition of the spectra, a small amount of the compound was transferred to the sample area of the “Alpha-P” device and then measured using attenuated total reflection (ATR). To obtain the spectra, 25 scans were carried out in the measuring range from 400 to 4000 cm^{-1}. The settings and data acquisition was carried out using "OPUS" (Bruker, Version 6.5).

3.2.4 Gel Permeation Chromatography (GPC)

GPC was used to determine number average molecular weight (M_n) and dispersity (M_w/ M_n) values of poylmers. GPC measurements were conducted with a GPC Viscotek 270 max using TGuard Col 10×4.6 mm and two T6000M general mixed 3000×7.8 mm columns, a column temperature of 30°C, a refractive index (RI) detector, and tetrahydrofuran (THF) as an eluent at a flow rate of 1 mL/min. The column system was calibrated with 7 linear poly(methyl methacrylate) standards of the company Shodex (1850 $g \cdot mol^{-1}$; 6380 $g \cdot mol^{-1}$; 20100 $g \cdot mol^{-1}$; 73200 $g \cdot mol^{-1}$; 218000 $g \cdot mol^{-1}$; 608000 $g \cdot mol^{-1}$; and 1050000 $g \cdot mol^{-1}$). GPC data were analyzed using Omni SEC 4.6.2:GPC.

3.2.5 Photo Differential Scanning Calorimeter (Photo-DSC)

Reference 220 discloses the setup [220]. To compare the reactivities of the different iodonium salts, the maximum polymerization rate and final conversions of the polymers were determined by Photo-DSC using blue LED emitting with an intensity of 100 mW/cm^2 at 405 nm and 0.5 mW/cm^2 at 470 nm available from Roithner for radical polymerization. Radiometric data were determined with a USB 4000 spectrometer from Ocean Optics. Light was trasnfered to the sample with a lens and projected into a y-fiber, which was connected with the head of the DSC (Q2000 from TA-Instruments). The output of each fibre arm was adjusted at the y-fibre with OmniCure HR4000 from TA-Instruments, coupled additionally to the DSC. This allows an almost equal intensity of both the sample and reference in the calorimeter. The LED-source was synchronized with the DSC by a shutter system placed between the fiber and the lens. It was controlled by an Arduino uno board, which was programed with the program Arduino 1.05 available from Arduino. The software of the DSC controls the event-output of this instrument functioning as digital switch. Change of resistance resulted in an ON (no resistance)/OFF (infinite resistance) modulation. This information went to the Arduino uno board controlling the shutter in ON/ OFF position by a servomotor [220].

3.2.6 Cyclic Voltammeter

Oxidation and reduction potentials of the sensitizers were recorded by cyclic voltammetry (VERSASTAT4-400 from AMETEK served as potentiostats) in acetonitrile (C = 10^{-3} M) with tetrabutylammonium hexafluorophosphate (0.1 mol/L) as a supporting electrolyte against ferrocene as an external standard. The data were taken with a scanning rate of 0.015 V·s^{-1} using platinum disc as a working electrode and Ag/AgCl as reference electrode.

3.2.7 Photoreactor

Figure 1 shows the schematic view of photoreactor used for photo-reactions. The photoreactor consists of an opaque vessel in which four identical NIR LEDs (LED790-66-60 from Roithner Lasertechnik, 790 nm) are attached at an angle of 90° each. There is a magnetic stirring plate under the vessel, which magnetically stirs the reaction mixture in the flask during the reaction. The LEDs are cooled under a continuous flow of air during the reaction. The light intensity of each LED was measured with the fiber optic spectrometer USB4000 from Ocean Opticsas and recorded as 100 mW·cm^{-2}. The sample

was cooled with an airflow around the tube and stirred with a magnetic mixer during the reaction.

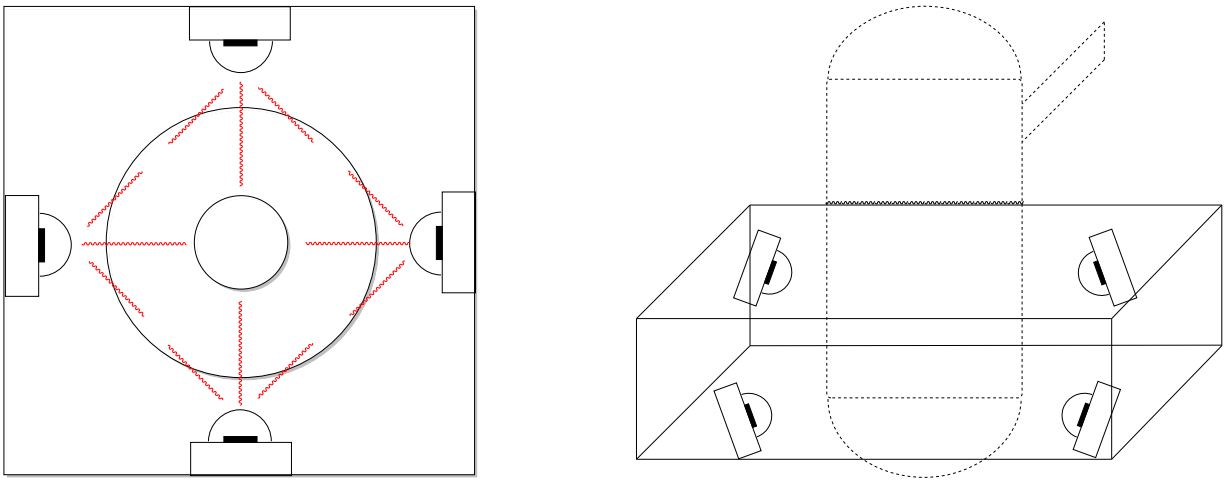

Figure 1: Schematic view of the photoreactor.

3.3 Light source

3.3.1 NIR LEDs

As can be seen in Figure 2, NIR LED which emits at 790 nm was used for the photopolymerization. The light intensity of LED was 100 mW·cm^{-2} within the exposed area in the middle height on the surface of the tube. The intensity was measured with the fiber optic spectrometer USB4000 from Ocean Optics.

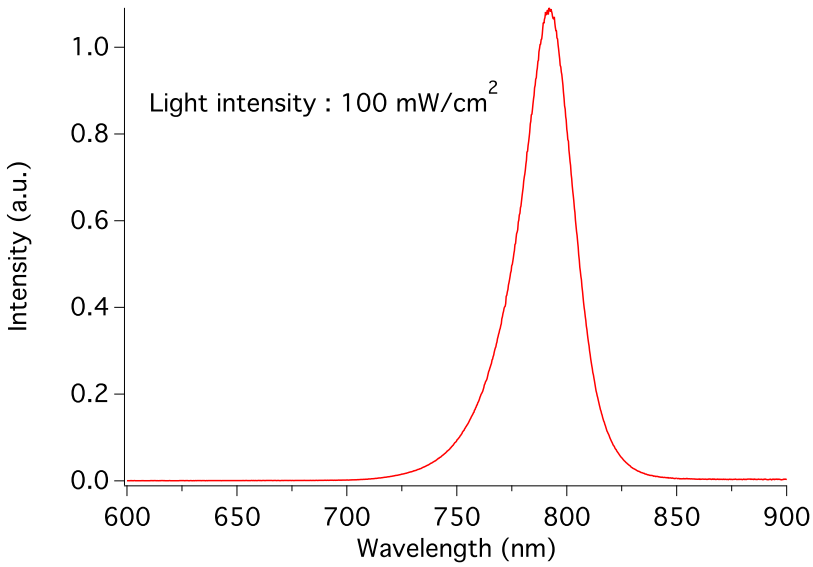

Figure 2: Emission spectrum of NIR LED at 790 nm.

3.3.2 LED at 405 nm

As can be seen in Figure 3, NIR LED which emits at 405 nm was used for the excitation of **CD**s. The light intensity of LED was 100 mW·cm^{-2} in a distance of 5 cm to reaction The intensity was measured with the fiber optic spectrometer USB4000 from Ocean Optics. LED at 470 nm was also used for the excitation of **CD**s. The intensity was measured 0.5 mW·cm^{-2}.

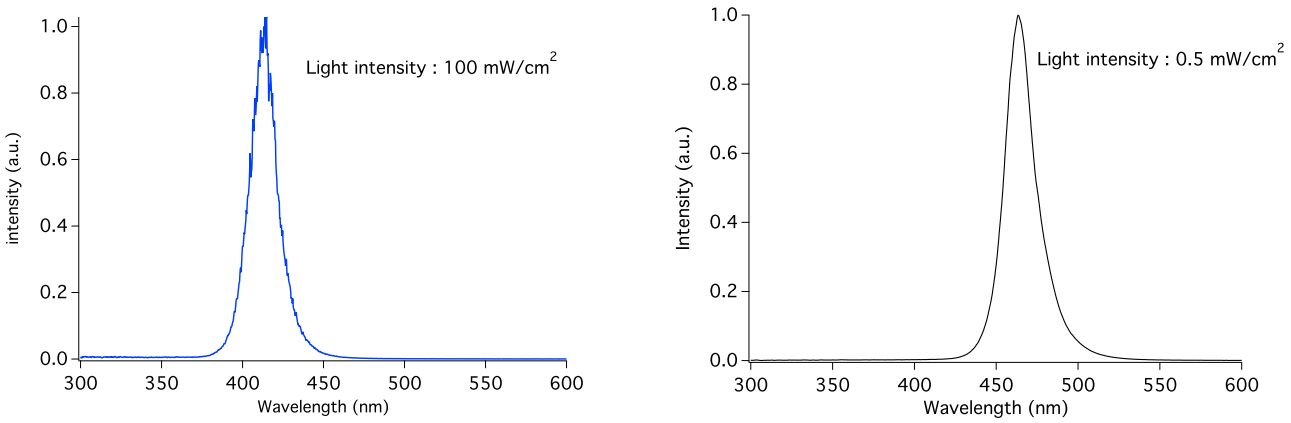

Figure 3: Emission spectrum of NIR LEDs at 405 nm and 470 nm.

3.3.3 Halogen Lamp

Halogen lamp was used for the irradiation of NIR sensitizer comprising anionic structure (**4**). Chemical structure of **4** was shown in Table 1. Halogen lamp was chosen for the exposure experiment because absorption of **4** and emission of the halogen lamp match well. Figure 4 shows the spectral profile.

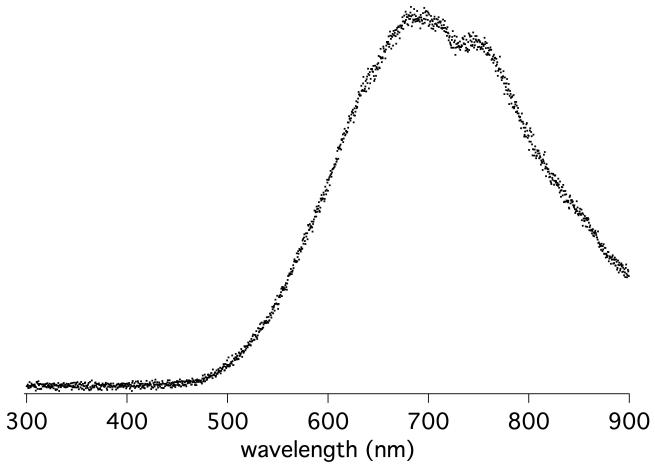

Figure 4: Emission spectrum of halogen lamp.

3.3.4 NIR Laser

An NIR laser at 974 nm (type P976MF, PhotonTec Berlin GmbH) was used as the light source for excitation of **UCNP**s. The laser was operated in a mode to be on for 1s and off for 2 s. It had a diameter of about 5 mm.

4. Experimental Part

This chapter briefly discloses the experimental conditions used in this thesis. More details can be found in published material [250][119, 226, 244, 245, 246].

4.1 Upconversion Nanoparticle Assisted Metal-free ATRP

In a typical experiment, a solution of UCNPs (20 g·L^{-1}) was dispersed in 1 mL of toluene in an ultrasonic bath for 15 min. After completion, MMA (200 eq.), EBiP (1 eq.), PMDETA (5 eq.) and ITX (1 eq.) were put into this mixture and transferred into *Schlenk* tube. This mixture was degassed by three freeze-pump-thaw cycles. After that, the solution was irradiated at 974 nm laser. After exposure, polymer was precipitated in cold methanol following by drying over night. Conversions were determined gravimetrically.

4.2 Chain Extension Experiment Using UCNPs

The bromide moiety in the polymers obtained was examined by chain extension experiment. For this purpose, precursor PMMA (40 mg) comprising bromide as chain-end group was used as the macroinitiator and mentioned polymerization conditions were applied for the chain extention with MMA monomer.

4.3 NIR Light-Induced ATRP Using Cu^{II} at ppm Scale

NIR sensitizer (45 µmol), ethyl α-bromophenylacetate (36.5 mg, 0.150 mmol), 25 µL of a 180 mM $CuBr_2$ stock solution in DMF (4.5 µmol) and 75 mL of a 270 mM TPMA stock solution in DMF (20.3 µmol) were transfered to a glass vial. To this mixture, MMA (4.51 g, 45 mmol) and DMF (4.53 g) were added. The solution was transferred to a *Schlenk* tube with a magnetic stirrer and degassed by four freeze-pump-thaw cycles. The reaction mixture was placed in a photoreactor irradiating at the either at 790 nm in case of **1**-**3**; or with halogen lamp exposure in the case of **4**. At the end of the irradiation, the resulted polymers were precipitated in cold methanol and then dried under reduced pressure. Conversion was determined gravimetrically.

4.4 Chain Extension Experiment Using NIR Sensitizers

A vial was charged with PMMA macroinitiator (0.676 g, 0.045 mmol), **2** (9.86 mg, 13.5 µmol), 7.5 µL of a 180 mM $CuBr_2$ stock solution in DMF (1.35 µmol) and 45 µL of a 270 mM TPMA stock solution in DMF (6.09 µmol). MMA (1.40 g, 13.5 mmol) and DMF (1.36 g)

were added to this mixture, and the solution was homogenized by vigorous stirring. The solution was transferred to a *Schlenk* tube (diameter 18.0 mm) with a magnetic stirrer and degassed by four freeze-pump-thaw cycles. The reaction mixture was placed in a photoreactor, and irradiated at 790 nm. At the end of the irradiation, the resulted polymers were precipitated in cold methanol and then dried under reduced pressure. Conversion was determined gravimetrically.

4.5 Block Copolymerization Experiment Using NIR Sensitizers

A vial equipped with a magnetic stir bar and fitted with a teflon screw cap septum was charged with PMMA macroinitiator (0.676 g, 0.045 mmol), **2** (9.86 mg, 13.5 μmol), 7.5 μL of a 180 mM $CuBr_2$ stock solution in DMF (1.35 μmol) and 45 μL of a 270 mM TPMA stock solution in DMF (6.09 μmol). Styrene (1.38 g, 13.5 mmol) and DMF (1.38 g) were added to this mixture, and the resulting solution was homogenized by vigorous stirring. The solution was transferred to a *Schlenk* tube (diameter 18.0 mm) comprising a magnetic stirrer and degassed by four freeze-pump-thaw cycles. The reaction mixture was placed in a photoreactor and irradiated at 790 nm. The resulted polymers were precipitated in cold methanol at the end of the irradiation, and then dried under reduced pressure. Conversion was determined gravimetrically.

4.6 Kinetic Studies of the Polymerization Using NIR Sensitizers

A vial equipped with a magnetic stir bar and fitted with a teflon screw cap septum was charged with **2** (32.9 mg, 45 μmol), ethyl α-bromophenylacetate (36.5 mg, 0.150 mmol), 25 μL of a 180 mM $CuBr_2$ stock solution in DMF (4.5 μmol) and 75 mL of a 270 mM TPMA stock solution in DMF (20.3 μmol). To this mixture MMA (4.51 g, 45 mmol) and DMF (4.53 g) were added, and the solution was homogenized by stirring. The solution was transferred to a *Schlenk* tube (diameter 18.0 mm) with a magnetic stirrer and degassed by four freeze-pump-thaw cycles. The reaction tube was exposed at 790 nm and every 6 hours 1 mL volumes of reaction mixture were syringed out from the polymerization media and precipitated in cold methanol. Next, the polymers were analyzed gravimetrically to determine the conversions. The molecular weight was analyzed by GPC.

4.7 Light on/off Experiment

Ethyl α-bromophenylacetate (36.5 mg, 0.150 mmol), **2** (32.9 mg, 45 μmol), 25 μL of a 180 mM $CuBr_2$ stock solution in DMF (4.5 mol) and 75 μL of a 270 mM TPMA stock solution in DMF (20.3 mol) were combined in a vial. MMA (4.51 g, 45 mmol) and DMF (4.53 g) were added to this mixture, and the solution was homogenized by stirring. The solution was

transferred to a *Schlenk* flask (diameter 18.0 mm) equipped with a magnetic stirrer and degassed by four freeze-pump-thaw cycles. The reaction tube was exposed to repeated cycles at 790 nm for 6 hours and kept in dark for 18 hours. In these subsequent intervals, certain volumes of reaction mixture were syringed out from the polymerization media and precipitated in cold methanol. Next, the polymers were analyzed gravimetrically to determine the conversions. The molecular weight was analyzed by GPC.

4.8 Photobleaching Experiments of photo-ATRP Using NIR Sensitizers

Ethyl α-bromophenylacetate (36.5 mg, 0.150 mmol), **2** (32.9 mg, 45 μmol), 25 μL of a 180 mM $CuBr_2$ stock solution in DMF (4.5 mol) and 75 μL of a 270 mM TPMA stock solution in DMF (20.3 mol) were combined in a vial. DMF (4.53 g) was added to this mixture, and the solution was homogenized by stirring. The solution was transferred into a 1 cm cuvette. The setup chosen used a NIR LED emitting at 790 nm whose light was coupled into a 1 cm cuvette placed in a sample holder CUV−ALL−UV from Ocean Optics. The spectrum was perpendicular measured with a fiber optical spectrometer USB HR4000 in combination with a HL-2000-FHSA (both from Ocean Optics). The solution was continuously stirred upon exposure while a Labview based shutter system allowed selective control of exposure and spectral data measurement. Each spectrum was taken after an irradiation period of 15 minutes.

4.9 Photoinduced ATRP Using Carbon Nanodots with Cu^{II} Catalyst At ppm Scale

A vial equipped with a magnetic stir bar and fitted with a teflon screw cap septum was charged with **CD**s (3 mg) and 1 mL of DMSO. To this mixture MMA (1 mL), 5.20 μL of a 180 mM $CuBr_2$ stock solution in DMSO and 15.6 mL of a 270 mM TPMA stock solution in DMSO and ethyl α-bromophenylacetate (5.5 μL) was added and the solution was homogenized by stirring. The solution was transferred to a *Schlenk* tube with a magnetic stirrer and degassed by four freeze-pump-thaw cycles. The reaction mixture was irradiated at 405 nm in a distance of 5 cm. Solution was stirred during exposure. At the end of the irradiation, the resulting polymer was precipitated in methanol and then dried under reduced pressure. Conversion was determined gravimetrically.

4.10 Block Copolymerization Experiment (PMMA-*b*-PSt) Using Carbon Nanodots

A vial equipped with a magnetic stir bar and fitted with a Teflon screw cap septum was charged with PMMA macroinitiator (0.676 g, 0.045 mmol), 7.5 μL of a 180 mM $CuBr_2$ stock solution in DMSO (1.35 μmol) and 45 μL of a 270 mM TPMA stock solution in DMSO (6.09 μmol). Styrene (1.38 g, 13.5 mmol) and DMSO (1.38 g) were added to this mixture, and

the resulting solution was homogenized by vigorous stirring. The solution was transferred to a *Schlenk* Flask comprising a magnetic stirrer and degassed by four freeze- pump-thaw cycles. The reaction mixture was placed in a photoreactor and irradiated at 790 nm. The resulted polymers were precipitated in methanol at the end of the irradiation, and then dried under reduced pressure. Conversion was determined gravimetrically. Exposure occurred under conditions as mentioned *vide supra*.

4.11 Kinetic studies of the Polymerization Using Carbon Nanodots

A vial equipped with a magnetic stir bar and fitted with a Teflon screw cap septum was charged with **CD**s (3 mg) and 1 mL of DMSO. To this mixture MMA (1 mL), 5.20 µL of a 180 mM $CuBr_2$ stock solution in DMSO and 15.6 mL of a 270 mM TPMA stock solution in DMSO and ethyl α-bromophenylacetate (5.5 µL) was added and the solution was homogenized by stirring. The solution was transferred to a *Schlenk* tube with a magnetic stirrer and degassed by four Freeze-Pump-Thaw cycles. The reaction tube was exposed at 405 nm and every 30 minutes 1 mL volumes of reaction mixture were syringed out from the polymerization media and precipitated in methanol. Next, the polymers were analyzed gravimetrically to determine the conversions. The molecular weight was analyzed by GPC. Exposure occurred under conditions as mentioned *vide supra*.

4.12 Light on-off Experiments of Photo-ATRP Using Carbon Nanodots

A vial equipped with a magnetic stir bar and fitted with a Teflon screw cap septum was charged with **CD**s (3 mg) and 1 mL of DMSO. To this mixture MMA (1 mL), 5.20 µL of a 180 mM $CuBr_2$ stock solution in DMSO and 15.6 mL of a 270 mM TPMA stock solution in DMSO and ethyl α-bromophenylacetate (5.5 µL) was added and the solution was homogenized by stirring. The solution was transferred to a Schlenk Flask with a magnetic stirrer and degassed by four Freeze-Pump-Thaw cycles. The reaction tube was exposed to repeated cycles at 405 nm for 30 minutes and kept in dark for 30 minutes. In these subsequent intervals, 1 mL volumes of reaction mixture were syringed out from the polymerization media and precipitated in methanol. Next, the polymers were analyzed gravimetrically to determine the conversions. The molecular weight was analyzed by GPC. Exposure occurred under conditions as mentioned *vide supra*.

4.13 Kinetic Studies of the Polymerization Using Carbon Nanodots

A vial equipped with a magnetic stir bar and fitted with a Teflon screw cap septum was charged with **CD**s (3 mg) and 1 mL of DMSO. To this mixture MMA (1 mL), 5.20 µL of a

180 mM $CuBr_2$ stock solution in DMSO and 15.6 mL of a 270 mM TPMA stock solution in DMSO and ethyl α-bromophenylacetate (5.5 μL) was added and the solution was homogenized by stirring. The solution was transferred to a *Schlenk* tube with a magnetic stirrer and degassed by four Freeze-Pump-Thaw cycles. The reaction tube was exposed at 405 nm and every 30 minutes 1 mL volumes of reaction mixture were syringed out from the polymerization media and precipitated in methanol. Next, the polymers were analyzed gravimetrically to determine the conversions. The molecular weight was analyzed by GPC. Exposure occurred under conditions as mentioned *vide supra*.

4.14 Synthesis of Azide Components

A round bottom flask equipped with a magnetic stir bar was charged with the corresponding bromide (benzyl bromide, 1-bromooctane, and 9-(chloromethyl)anthracene) compounds (15 mmol, 1.0 eq) and dissolved in DMSO (200 mL). Following dissolution of the bromide compounds, sodium azide was added in excess (1.5 eq.) and the solution was allowed to stir for 2 hours at room temperature. After this period the reaction, water (200 mL) was added to the mixture and after cooling down to room temperature, the aqueous solution was extracted with diethyl ether (3×100 mL). The organic layers were combined and washed with water (2×100 mL) and brine (2×100 mL). After the separation, the combined organic phase was dried over $MgSO_4$, filtered, and ether was removed under reduced pressure to yield azides.

4.14.1 Synthesis of ω-azido functionalized poly(ethylene glycol) (PEG-N_3)

The synthesis of azide functionalized poly(ethylene glycol) (PEG-N_3) was performed as follows: Me-PEG (M_n= 2000 g·mol^{-1}) was dissolved in 10 mL chloroform under a nitrogen atmosphere and cooled in an ice bath (0°C) and pyridine (7.5 mmol) was added. Then, 4-toluenesulfonyl chloride (5.3 mmol) dissolved in 10 mL of chloroform was slowly added to the cold reaction flask. The reaction mixture was stirred overnight at room temperature. The solvent was removed under vacuum and the viscous liquid tosylate obtained was used in the azidation reaction without any purification. Sodium azide (3.3 mmol) was added to a solution of the obtained tosylate (1.08 mmol) in DMF and the reaction mixture was stirred for 2 days at 65°C. After extraction of the crude product with CH_2Cl_2/water, the organic layer was concentrated and precipitated in to diethyl ether to give PEG-N_3. White powder. Yield 95%. ^{1}H NMR (300 MHz, CDCl3): δ 3.55 (t, 2H), 3.52 (t, 2H) 3.40 (s, 3H), 1.68 (t, 2H). FTIR: 2108 cm^{-1}.

4.14.2 Synthesis of ω-azido terminated polystyrene (PS-N_3)

A vial equipped with a magnetic stir bar and fitted with a Teflon screw cap septum was charged with ethyl(α-bromopropionate) (31.3 mg, 0.17 mmol), copper bromide (24.8 mg, 0.17 mmol), and PMDETA (29.46 mg, 0.17 mmol). To this mixture styrene (2 mL, 17 mmol) was added. The solution was transferred to a *Schlenk* flask with a magnetic stirrer and degassed by four Freeze-Pump-Thaw cycles. The mixture was heated and stirred at 110°C in an oil bath. After 30 min, the polymerization was ceased by opening the flask and exposing the catalyst to air. The final mixture was diluted in THF and passed through a neutral alumina column in order to remove copper catalyst. The mixture was concentrated by rotary evaporation and subsequently precipitated in cold methanol. The precipitated polystyrene was filtered and dried under vacuum. The obtained bromine-end functional polystyrene (3300 $g \cdot mol^{-1}$, 0.14 mmol), sodium azide (0.14 mmol) and 3 mL of DMF were added in a flask. The clear homogeneous solution was stirred at room temperature for 24 h. Then, polystyrene was precipitated in methanol, filtered and dried in vacuum ($M_{n,GPC}$ (PS-N_3) = 3000 $g \cdot mol^{-1}$, M_w/M_n = 1.09). White powder. Yield 95%. ^{1}H NMR (300 MHz, CDCl3): δ 7.32 (s, 1H), 7.28 (s, 1H), 7.21 (s, 1H), 7.19 (s,1H), 2.70-2.58 (m, 4H), 1,83 (t, 2H), 1.50-1.70 (m, 2H), 0.76 (t, 3H). FTIR: 2096 cm^{-1}.

4.16 Synthesis of Polymer Substrate Comprising Alkyne Component

α-Alkyne functional poly(ε-caprolactone) (Alkyne-PCL) was prepared according to modified literature procedures. Propargyl alcohol (37 mg, 0.67 mmol) was dissolved in ε-caprolactone (1.5 g, 13.1 mmol) and heated to 110 ºC. After addition of one drop of tin octoate, the solution was stirred for 3 hours at 110 ºC. The obtained solid was dissolved in CH_2Cl_2 and precipitated in methanol:water (2:1) resulting in the acetylene terminated poly(ε-caprolactone), as white solid (1.28 g, 82%). ($M_{n,GPC}$ (Alkyne-PCL) = 4000 $g \cdot mol^{-1}$, M_w/M_n = 1.26).

4.17 General Procedure for the NIR Photoinduced CuAAC

In a typical experiment DMSO-d_6 (0.5 mL) and azide compound (1 mmol, 1 eq.) were added to a *Schlenk* tube containing $CuBr_2$ (0.05 eq.), PMDETA (0.1 eq.), and sensitizer (0.05 eq.). After 1–2 min, alky^{n}e compound (1 mmol, 1 eq.) was added via a syringe. The reaction mixture was placed in a photoreactor irradiating at the desired wavelength (NIR-LED exposure at 790 nm).

4.18 Synthesis of Polystyrene-b-poly(ε-caprolactone) by Photoinduced CuAAC

To a *Schlenk* tube equipped with a magnetic stirrer, PS-N_3 (0.15 mmol, 1 eq.), Alkyne-PCL (1 eq.), $CuBr_2$ (0.05eq.), PMDETA (0.05 eq.) and 2 (0.05 eq.) were added and dissolved in 8 mL DMSO. The tube was degassed by three freeze–pump–thaw cycles. The reaction mixture was placed in a photoreactor and irradiated at 790 nm. At the end of 48 h, the mixture was diluted with CH_2Cl_2. Then, the copper complex was removed out by passing through a neutral alumina column, and CH_2Cl_2 was removed by rotary evaporation. The mixture was precipitated in cold methanol, and the solid was collected after filtration and dried at room temperature under vacuum overnight. ($M_{n,GPC}$: 6000 g·mol^{-1}, M_w/M_n: 1.22).

5. Results and Discussion

Within the scope of this thesis, new photochemical routes for the preparation macromolecular structures under favorable energetic conditions, *i.e.,* high wavelength irradiation and temporal conditions have been developed. These routes include the use of **UCNP**s, **CD**s and selected NIR absorbers for photo-ATRP and photo-CuAAC click processes. In the following subsections, each methodology is described and mechanistic details are discussed.

5.1 UCNPs Assisted Metal-free Photo-ATRP

Some of the results discussed in this subchapter were previously published [226]. $NaYF_4$:TmYb@$NaYF_4$ UCNPs, emits at 338 nm, 355 nm, 444 nm and 468 nm upon excitation with *cw*-laser at 974 nm (see emission in Figure 5). They also show only minor intensity emission in the red and green part of the visible spectrum as previously reported [230]. In general, this approach facilitates access to UV and blue absorbing photoinitiating systems by nonlinear absorption of 3-4 photons upon excitation at 980 nm [226, 230].

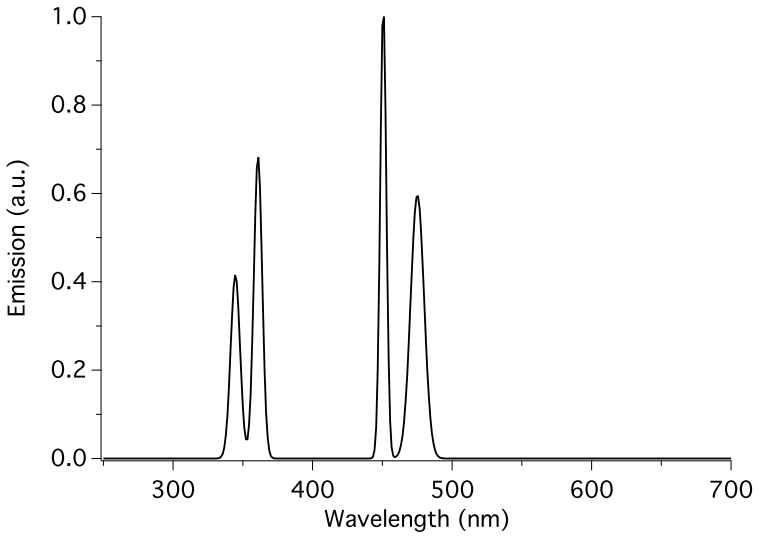

Figure 5: Emission spectrum of NaYF4;YB3*@NaYF4 **UCNP**s taken in n-hexane, modified from [230].

Initiation of the polymerization by **UCNP**s is possible with a good overlap between the emission of the **UCNP** and the absorption of the photosensitizer. Therefore, for the sensitization of radical formation, one should consider to choose the appropriate photosensitizer or photocatalyst for the desired wavelength matching the emission. The use of several visible and UV photoinitiators together with **UCNP**s for the radical and

radical promoted cationic polymerization was previously reported [226, 230, 236, 237]. Furthermore, the adaptation of already reported system into the CRP using **UCNP**s in conjunction with ITX and PMDETA was successful for the polymerization of MMA via ATRP process in the absence of metal catalyst [247]. As can be seen in Figure 6, the absorption of ITX at 345 nm and 361 nm covers well the emission lines of the **UCNP**s. This overlap between the emission of the **UCNP** and the absorption of ITX facilitates the light-induced polymerization in the UV range [226].

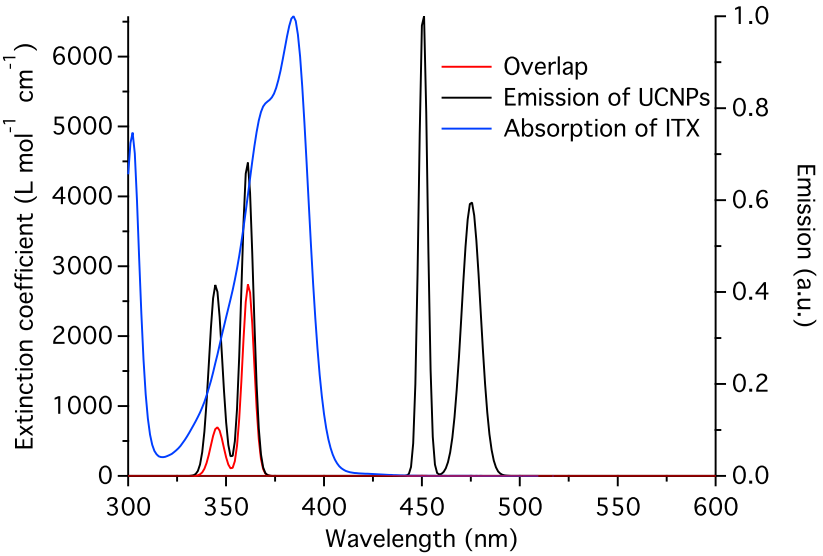

Figure 6: Comparison of the emission of NaYF4:TmYb@NaYF4 **UCNP**s with the absorption profile of the ITX taken in *n*-hexane and acetonitrile, respectively, modified from [226].

Polymerization of MMA by metal-free photo-ATRP using **UCNP**s together with an initiator system comprising ITX as photoinitiator and EBiB as alkyl halide resulted in polymers with dispersity of about 1.3. This result shows that this initiating mechanism mainly follows a controlled mechanism as shown in Scheme 15. This system successfully worked in previous studies applying UV exposure [247]. Photoexcitation of ITX together with EBiP and PMDETA generates radical anion ($ITX^{-\bullet}$), bromine ion (Br^-) and the alkyl radical ($(CH_3)_2(CO_2Et)C\bullet$) derived from EBiB according to an oxidative reaction mechanism while reduction of photoexcited ITX (ITX*) with PMDETA leads to the oxidized amine species $PMDETA^{+\bullet}$. These reactive radicals are able to initiate the monomer addition. Termination occurs by recombination with formed bromine radical (Br•) which goes the end of the polymer chain $(CH_3)_2(CO_2Et)C\text{-}(MMA)_n\text{-}Br$). The polymerization can be initiated again, which provides to extend the polymer chain either with the same monomer or with another monomer.

$$\mathbf{UCNP} \xrightarrow{974\,nm} \mathbf{UCNP^*} \xrightarrow[\mathbf{UCNP}]{365\,nm\ +\ \mathbf{ITX}} \mathbf{ITX^*}$$

$$\mathbf{ITX^* + PMDETA \rightarrow ITX^{-\bullet} + PMDETA^{+\bullet}}$$

$$\mathbf{ITX^{-\bullet} + \alpha\text{-}BrBuEt \rightarrow (CH_3)_2(CO_2Et)C\bullet + Br^- + ITX}$$

$$\mathbf{(CH_3)_2(CO_2Et)C\bullet} + n\ \mathbf{MMA \rightarrow EtCO_2C(CH_3)_2\text{-}(MMA)_n\bullet}$$

$$\mathbf{PMDETA^{+\bullet} + Br^- \rightarrow PMDETA + Br\bullet}$$

$$\mathbf{EtCO_2C(CH_3)_2\text{-}(MMA)_n\bullet + Br\bullet \rightarrow EtCO_2C(CH_3)_2\text{-}(MMA)_n\text{-}Br}$$

Scheme 15: Mechanism of metal-free photo-ATRP using **UCNP**s in conjunction with ITX as photoinitiator and PMDETA as electron donor, modified from [226].

Experiments were also done with the initiator system comprising ITX, EBiB and PMDETA by UV-LED at 395 nm. The polymers obtained in the presence **UCNP**s by NIR laser exposure showed narrower dispersity. The obtained results can be seen in Table 3. Molecular weight distrubition shows a shift to free radical polymerization. The polymers synthesized exhibited high molecular weight using **UCNP**s. This may be explained by higher radical concentration generated by UV light due to the higher light intensity. Exposure with NIR light needs shorter time to reach the similar conversion. As shown before, the metal-free systems can show broader dispersity when ITX is used as photosensitizer to activate the system [247].

Table 3: Photoinitiated Radical Polymerization of Methylmethacrylate (MMA) in Toluene Using NaYF4:TmYb@NaYF4 UCNP/ITX/PMDETA/EBiB as initiating system[a]

λ (nm)	UCNP	Time (h)	Conv.[b] (%)	M_n[c] (g·mol^{-1})	$Đ$[c]
974	20 g·mol^{-1}	2	37	26000	1.8
395	-	20	35	5300	1.9

[a]Exposure was carried with NIR laser at 974 nm (laser power: 24 W, diameter: 5 mm, V_{MMA} = 1 mL, $V_{Toluene}$ = 1 mL,$[MMA]_0/[EBiB]_0/[PMDETA]_0/[ITX]_0$: 200/1/5/1,[**UCNP**] = 20 g·L^{-1}). [b]Determined gravimetrically. [c]Number-average molecular weight (M_n) and molecular weight distrubution ($Đ$) were determined by GPC using PMMA standards.

A typical ATRP reaction results in the formation of polymers with chain end functionality. Therefore, the polymer obtained in optical conditions can be used to extend the chain using the same monomer or to form block copolymers using another monomer. In this system, chain-end fidelity was approved by chain extension experiment. For this purpose, the polymer obtained using **UCNP**s was used as macroinitiator and ideal polymerization conditions were performed as indicated in Table 3. As expected, GPC chromatograms of the precursor and chain-extented polymer showed a clear shift to the higher molecular weight region indicating the presence of halide terminal group in polymer chain as shown in Figure 7. This increase of molecular weight proves the living character of the system. This can be applied for the preparation of new structures with UV and visible photoinitiating systems applying NIR exposure. Furthermore, the laser wavelength at 974 nm additionally brings such systems to new applications such as laser drying [23][12]. NIR light possesses also deeper penetration into materials due to the lower scattering coefficient, which can be seen as an additional benefit [248].

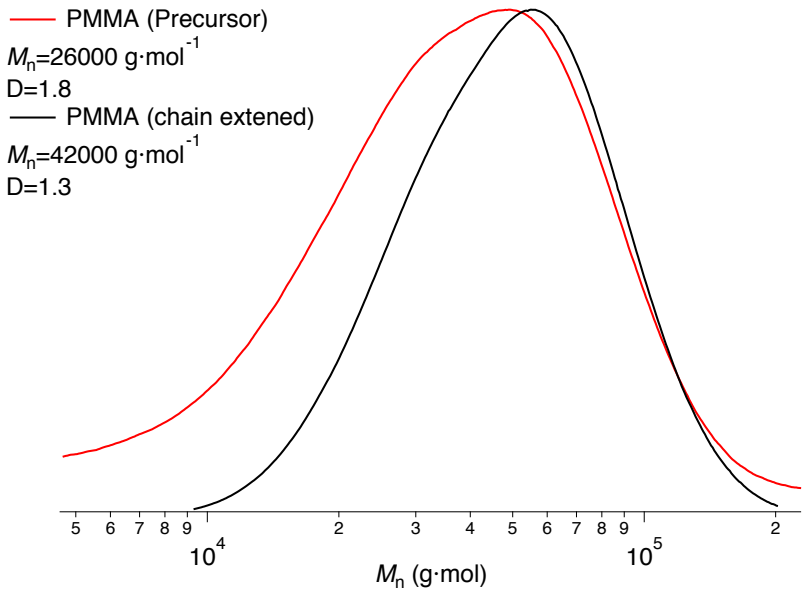

Figure 7: GPC traces of PMMA of the precursor and PMMA synthesized by chain extension made under controlled conditions, adapted from [226].

5.2 NIR Light-induced Metal-free ATRP using NIR Sensitizers

Some of the results discussed in this subchapter were previously discussed [119]. On the basis of the state of art, new photoactive systems with a defined absorption and redox characteristics should facilitate design of a new metal-free photo-ATRP system. Preference will be given in NIR-sensitized systems because this system allows to operate under moderate room light conditions. They also facilitate embedding of functional

materials exhibiting an absorption either in UV or Vis part of light. Particular of interest is biological materials carrying collagen having an intrinsic absorption up tp 650 nm. Combination of tailor-made polymerization such as metal-free ATRP allows the synthesis of tailor-made biomaterials being useful for several applications.

First of all, NIR sensitizers were selected and tested as photoactivators and the photophysical and redox properties for the suitability were investigated. Typical sensitizers being the target of the investigations were selected from polymethines. The initiating system comprising NIR sensitizers with different structural patterns, which are shown in Table 1 in conjunction with ethyl α-bromopropionate (EBP) as alkyl initiator and *N*,*N*,*N*,*N*',*N*'' pentamethyldiethylenetriamine (PMDETA) as electron donor, were tested for photo-ATRP without metal catalyst. Even though NIR sensitizers comprising zwitterionic (**2**, **3**, **5**) and anionic patterns (**4**) showed some polymerization activity, cationic structure (**1**) was not able to initiate the polymerization process. As can ben seen in Table 4, this system has failed to exhibit living character. The polymers obtained presented high molecular weights and broad molecular weight distributions indicating that the mechanism follows mostly the free radical polymerization. Exposure was carried with NIR LEDs for cationic (**1**) and zwitterionic sensitizers (**2**, **3**, **5**), see Figure 1 for the setup. Halogen lamp was chosen for the exposure of anionic sensitizer (**4**) because this matched better the absorption of the sensitizer compared to available LED-systems. As reported previously, the system comprising a NIR sensitizer and an iodonium salt (**1b**) was successfully employed for several acrylates for free radical polymerization [220, 246]. The results demonstrated that polymers obtained from the initiator system comprising NIR sensitizer, EBP and PMDETA without metal catalyst resulted in comparable molecular weight characteristics with the system including NIR sensitizer in conjunction with an iodonium salt (**1b**) as initiator. However, polymerization of methyl methacrylate using an iodonium salt as initiator showed better reactivity in contrast to the initiator system using an alkyl halide (EBP) [220]. These results indicated that metal-free photo-ATRP approach was not efficient enough using NIR sensitizers in the absence of copper catalyst. Initiation efficiency could not be able to form the reactive radicals from the reduced ally halide with excited **Sens** because of the low energy of the NIR light. One reason can be seen in the fact that the NIR sensitizers do not form a triplet state from our best knowledge whose lifetime should high enough to facilitate controlled polymerization.

Table 4: Photoinduced Metal-free ATRP of MMA Using NIR Sensitizers Under Different Experimental Conditions[a]

Sens	[MMA]/[RI]/ [PMDETA]/[Sens]	RI	Light Source	Conv.[b] (%)	M_n[c] (g×mol^{-1})	Đ[c]
1	200/1/1/0.05	EBP	NIR-LED	-	-	-
2	200/1/1/0.05	EBP	NIR-LED	14.2	239000	2.50
2	200/1/1/0.1	EBP	NIR-LED	12.8	160000	2.40
2	200/1/1/1	EBP	NIR-LED	12.0	109000	1.90
2	200/1/1/0.05	**1b**	NIR-LED	78.9	40500	2.09
2	200/1/0/0.05	EBP	NIR-LED	12.8	324500	2.70
2	200/1/5/0.05	EBP	NIR-LED	-	-	-
2	200/1/1/2	EBP	NIR-LED	12.0	109000	1.90
4	200/1/1/0.05	EBP	Halogen lamp	50.2	264000	2.70

[a]V_{MMA} = 1.75 mL, V_{DMF} = 1.75 mL, time = 24 h. [b]Determined gravimetrically. [c]Determined by gel permeation chromatography using PMMA standards.

5.3 NIR-Light Induced ATRP with ppm Range Copper (II) Catalyst

Some of the results discussed in this subchapter were previously published [119]. This subchapter shows first results for photopolymerization of MMA via ATRP process with the initiation system comprising NIR sensitizers, ethyl α-bromopropionate (EBP), and *N*, *N*, *N',* *N*'', *N*'' pentamethyldiethylenetriamine (PMDETA) with copper catalysts in the ppm range following in general the approach introduced for the ARGET ATRP as aforementioned in subchapter 2.1.3. More details can be found in a previous published report [119]. In order to test the ability of NIR sensitizers to conduct ATRP, methyl methacrylate was polymerized using ethyl α-bromophenylacetate (EBPA) and tris(2-pyridylmethyl)amine (TPMA) under NIR irradiation for 24 hours. Table 5 presents polymerization results. Adding copper(II) catalyst into the system showed an excellent efficiency by shifting the system to a controlled mechanism. With this work, it was reported for the first time a new photoinitiated system for the synthesis of well-defined polymers via ATRP strategy under NIR irradiation.

Table 5: NIR light-induced ATRP of Using NIR Sensitizers[a]

Sens	[MMA]/[EBPA]/ [$CuBr_2$]/[L]/[Sens]	Cu content (ppm)	Time (h)	Conv.[c] (%)	M_n[d] (g×mol^{-1})	Đ[d]
1	300/1/0.03/0.135/0.3	100	24	-	-	-
2	300/1/0.15/1.65/0.15	500	24	30.1	16400	1.52
2	300/1/0.15/1.65/1.5	500	24	27.2	14000	1.47
2	300/1/0.03/0.135/0.3	100	24	44.3	13000	1.17
2	300/1/0.03/0.135/0.3[b]	100	24	-	-	-
2	300/0/0.03/0.135/0.3	100	24	-	-	-
2	300/1/0.03/0.135/0	100	24	-	-	-
2	300/1/0/0/0.3	100	24	26.7	400000	2.47
3	300/1/0.03/0.135/0.3	100	24	-	-	-
4	300/1/0.03/0.135/0.3	100	24	-	-	-
5	300/1/0.03/0.135/0.3	100	24	-	-	-

[a]Irradiations were performed at 790 nm at room temperature. [b]Mixture was kept in the dark for 24. [c]Determined gravimetrically. [d] Determined by gel permeation chromatography using PMMA standards.

The results demonstrated that NIR sensitizer with zwitterionic structure (**2**) displayed good efficiency for the polymerization of MMA. Polymers obtained showed narrow molecular weight characteristics. To understand the polymerization mechanism in more detail, similar experiments were performed without copper catalysts, NIR sensitizer, or alkyl initiator. However, no polymer was obtained, which proves that the all components of the initiating systems are needed for the polymerization. In addition, the polymerization was not possible in the dark indicating that the light energy is needed for the initiatation.

As stated in Figure 8, the absorption of **1**,**2** and **3** matches well with the emission of the light source used for the polymerization. **4** was used in this study for comparison.

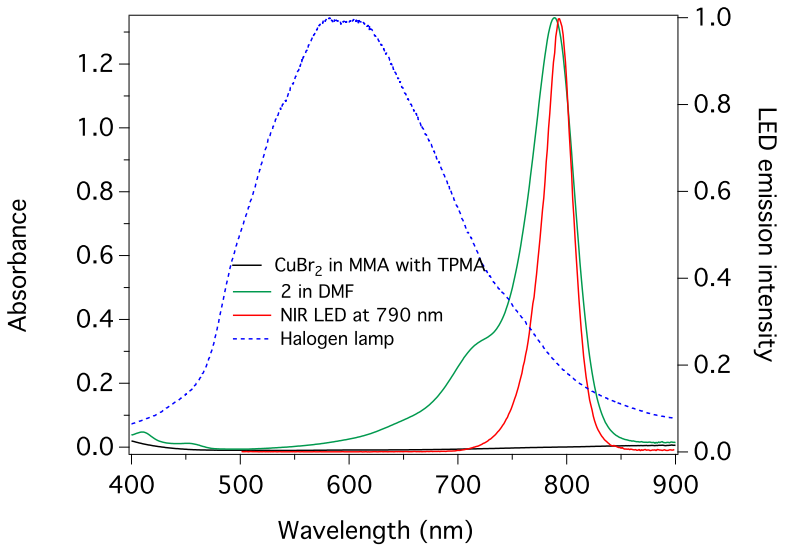

Figure 8: Comparison of NIR-LED emission with halogen lamp used as light sources. The absorption spectrum of **2** was taken in DMF. Cu^{II}/L complex is completely transparent in the NIR ([MMA]/[L]/[$CuBr_2$]=10^{-1}M/3×10^{-5}M/10^{-5}M), adapted from [119].

NIR sensitizers comprise either cationic (**1**), zwitterionic (**2**, **3** and **5**) or anionic (**4**) structures which can form initiating species through reductive or oxidative mechanism. While cationic sensitizer (**1**) may prefer to undergo electron transfer with electron rich compounds, anionic sensitizers (**4**) may select electron withdrawing groups. Neutral structures (**2, 3** and **5**) brings the system toward either reductive or oxidative pathways. Electrochemical data of all the sensitizers can be seen from Table 6. According the these data, **2** can be considered to be oxidize while **1** and **4** are suitable for the reduction. Additionally, for the exposure experiments NIR LED which emits at 790 nm was chosen for **1**, **2**, **3**, **5** while halogen lamp was used for the exposure of **4**. The light sources were chosen according to maximum absorption of the sensitizers.

Table 6: Absorption and electrochemical characteristics of **1**-**4**.

Sens	λ_{max} (nm)	ε_{max} ($M^{-1}cm^{-1}$)	E_{ox} (V)	E_{red} (V)
1	798[a]	224000[a]	0.69	-0.34
2	791[a] 798[b]	306000[a] 263000[b]	0.48	-0.97
3	800[a]	156000[b]	0.80	-0.59
4	693[a] 706[a]	196000[c] 171000[b]	0.57	-0.27

[a] In MeOH. [b]In DMF. [c]In MeOH. [d]Cyclovoltametric studies were pursued in acetonitrile.

Light on/off cycles were perform to investigate the effect of light in the polymerization. In order to do that, the polymerization mixtures were placed in a *Schlenk* tube, irradiated at 790 nm for 6 hours, and kept in dark for 18 hours in repeated cycles. 1 mL of polymerization mixture were taken out from *Schlenk* tube after the given time and precipitated into cold methanol for gravimetric determination of the conversion. After drying, polymers were analyzed by GPC for the molecular weight characteristics. The results showed irradiation dependence of the polymerization, and no polymer formation was observed in the dark (see Figure 9). These results show light is necessary for the formation of initiating radicals.

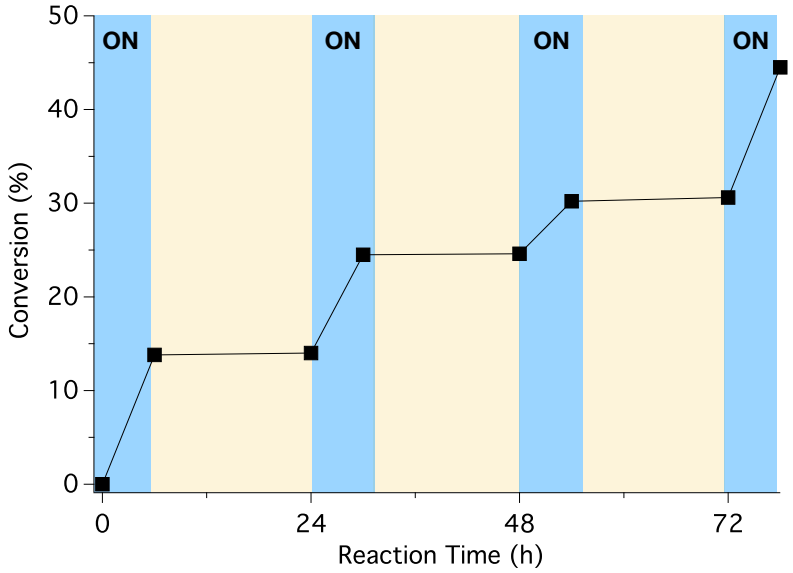

Figure 9: Monomer conversation (%) vs. Time using **2** to determine the light dependency of polymerization system ($[MMA]_0/[EBPA]_0/[CuBr_2]_0/[TPMA]_0/[\mathbf{2}]$=300/1/0.03/0.135/0.3), adapted from [119].

Kinetic studies were also examined to prove that polymerization follows controlled mechanism by following the first-order kinetic. A linear increase in the conversion by irradiation time was observed which indicates the growing radical concentration was stable during process (see Figure 10).

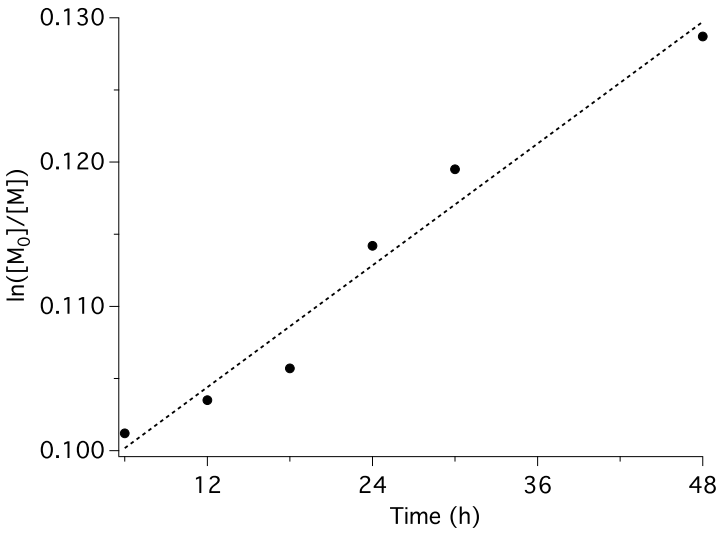

Figure 10: Kinetic plot for the polymerization of NIR light-induced ATRP of methyl methacrylate ($[MMA]_0/[EBPA]_0/[CuBr_2]_0/[TPMA]_0/[2]=300/1/0.03/0.135/0.3$), adapted from [119].

As can be seen in Figure 11, number average molecular weight linearly increases upon irradiation showing another property of living radical polymerization. Dispersities (*Đ*) remains in acceptable range between 1.17-1.27. The results of molecular weights of the polymer obtained with different exposure time are shown in Table 7.

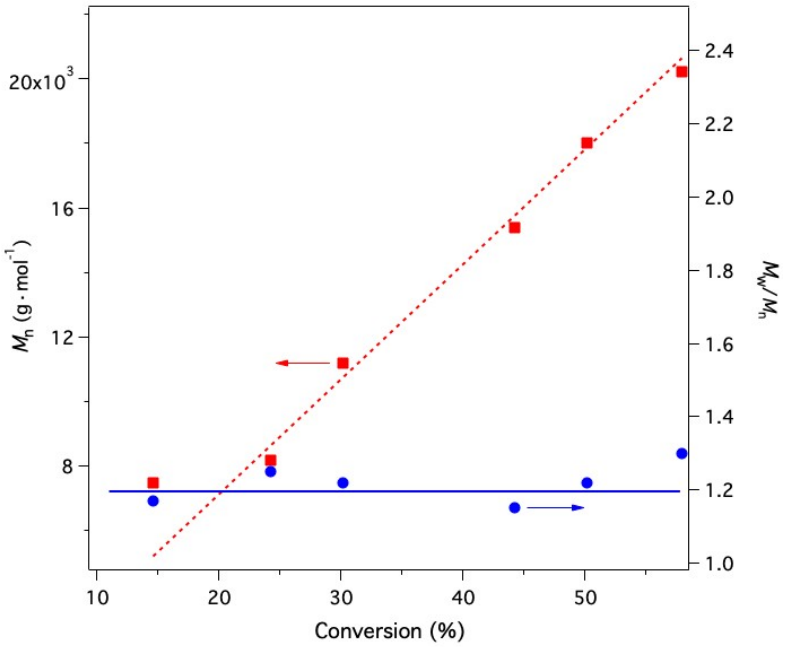

Figure 11: Number average molecular weights (M_n) and molecular weight distributions (M_w/M_n) of the polymers as a function of degree of conversion ($[MMA]_0/[EBPA]_0/[CuBr_2]_0/[TPMA]_0/$ [**2**]=300/1/0.03/0.135/0.3), adapted from [119].

Table 7: Effects of time on NIR light-induced ATRP of MMA using EBPA[a]

Runs	Time (h)	Conv.[b] (%)	M_n[c] (g×mol^{-1})	$Đ$[c]
1	6	14.6	7500	1.17
2	12	24.3	8200	1.25
3	18	30.2	11200	1.22
4	24	44.3	15400	1.15
5	30	50.2	18000	1.22
6	48	58.0	20200	1.30

[a] Time: 24 h, λ: 790 nm, polymerization conditions: [MMA]/[EBPA]/[$CuBr_2$]/[TPMA]/[**2**]= 300:1:0.03:0.135:0.3 with 50 vol % DMF at room temperature, [b]Determined gravimetrically. [c]Determined by gel permeation chromatography using PMMA standards.

In order to confirm chain-end functionality, chain extension experiment was performed. In order to do that, PMMA obtained by previously mentioned process was used as macroinitiator comprising halide functionality to extend the chain with the same monomer. GPC analyses showed an increase on the molecular weights (shifting to lower retention volumes) proving the living nature in the polymerization system. The molecular weight is shifted from 13000 g/mol to 22000 g/mol without contamination of the initial block (see Figure 12). Moreover, similar experiment was also performed for block copolymerization synthesis. For block copolymerization, styrene was chosen in the second step and identical polymerization conditions were applied. Again, as can be seen in Figure 12, clear shift to higher molecular weight region was observed (from 10800 g/mol to 15300 g/mol). This indicates the possibility of the system for the synthesis of block copolymers.

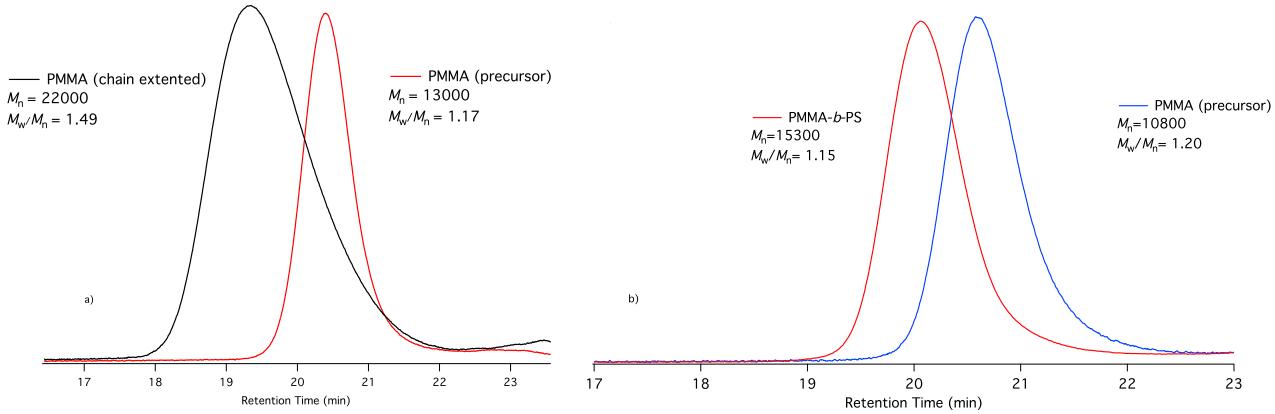

Figure 12: Comparison of GPC traces of precursor MMA with a) chain extended PMMA and b) PMMA-*b*-PS. Polymerization conditions in both cases:$[MMA]_0/[EBPA]_0/[CuBr_2]_0/[TPMA]_0/$[**2**]=300/1/0.03/0.135/0.3. Reactions were done in 50 vol% DMF at room temperature with 790 nm LED, adapted from [119].

By these investigations, the mechanims can be proposed as schown in Scheme 16. Initially, Cu^{II} complexes should be reduce to Cu^{I} as catalyst in photo-ATRP systems [80]. Similar to the reported studies in the UV and Vis region, electron trasnfer reaction took place after the NIR exitation of **Sens**. When it reaches the excited state (**Sens***), the reduction of Cu^{II} results in the formation of Cu^{I} complex and the cation radical of the sensitizer ($\mathbf{Sens}^{+\bullet}$). Cu^{I} starts the ATRP reaction in a usual way. Another electron transfer between $\mathbf{Sens}^{+\bullet}$ and Br^- brings the **Sens** back to the cycle in its ground state and bromine atom which terminates the propagating radical ($P^{\cdot}$) resulting in halide terminal polymer, P-Br (see Scheme 16).

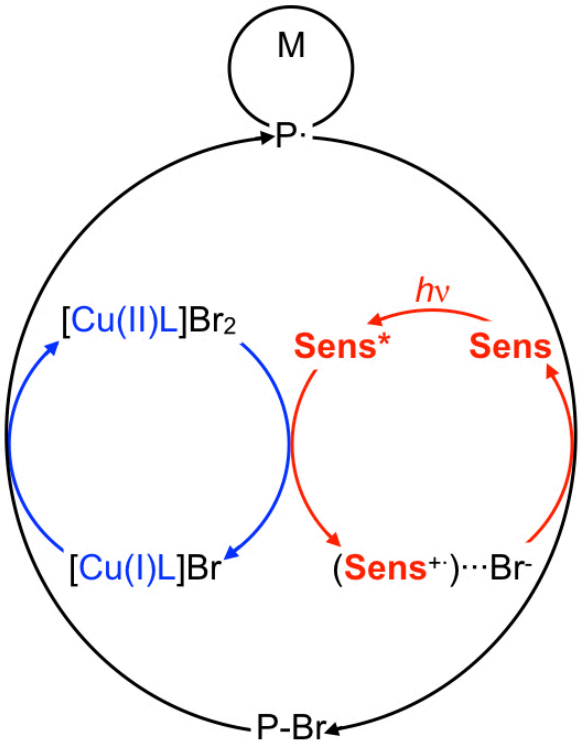

Scheme 16: Mechanism of NIR sensitized photoinduced ATRP using a polymethine (**2**) as sensitizer (**Sens**), adapted from [119].

As explained from the proposed mechanism, it was expected that this process shows a photocatalytic system. Because the **Sens** produced reversible by electron trasnfer reactionin the polymerization, the absorption should not change during the process. In order to do that, photobleaching experiment was performed. A solution comprising **2**, [Cu(TPMA)]Br_2, and EBPA was exposed to NIR lightfor 90 min. As can be seen in Figure 13, the absorption did not change significantly indicating successful photocatalytic cycle. Therefore, the high photostability of this system is the additional advantage of the system. It should be mentioned that **2** and bis-(4-*t*-butyl-phenyl)-iodonium bis(trifluoromethylsulfonyl)imide (**1b**) was previously shown to undergo fast bleaching by irreversible decomposition of $\mathbf{2}^{+\bullet}$ [220]. This system was also stable applying exposure under air. However, polymerization only occurred under anaerobic conditions.

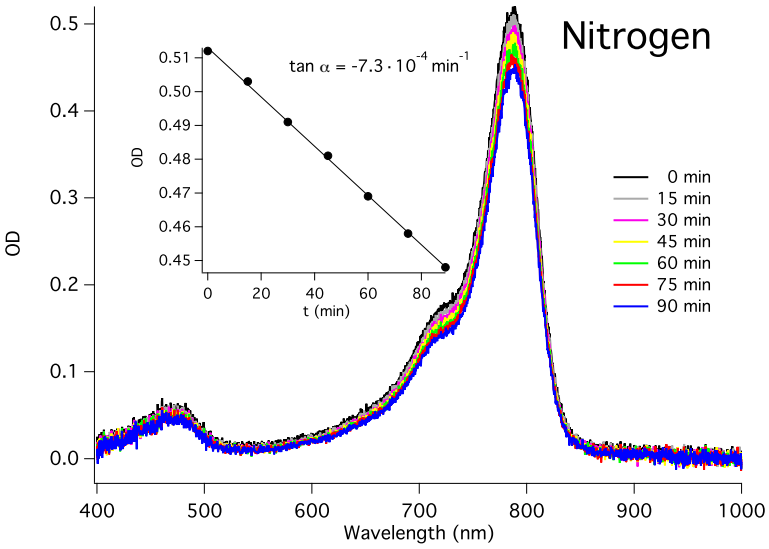

Figure 13: Spectral changes of the solution of **2** in the presence of $[Cu(L)]Br_2$ and ethyl α-bromophenylacetate (EBPA) in DMF upon irradiation at 790 nm obtained under nitrogen ($[MMA]_0/[EBPA]_0/[CuBr_2]_0/[TPMA]/[\mathbf{2}]$=300/1/0.03/0.135/0.3), adapted from [119].

A closer view on the spectra in Figure 13 shows an additional band between 400-500 nm which can be attributed the complex formation between the barbiturate moiety of the sensitizer and the copper catalyst. This was not observed without Cu(II) catalyst. Such interactions were almost reported in the 30s of the last century to quantify barbituric acid [249]. A separate titration of sensitizer **2** with Cu(II) showed complex formation but the probably low complex formation constant did not result in reliable quantities. Nevertheless, the fact that some parts of Cu(II) can be complexed with barbiturate sensitizer brings both substrates together while diffusion to them is less important. This might additionally explain why particular sensitizers comprising barbiturate work for the photo-ATRP approaches while other sensitizers carrying a barbiturate group.

5.4 NIR Light-Induced ATRP of Monomers Comprising UV Absorbing Moiety

Some of the results discussed in this subchapter were previously published [250]. Successful NIR light-induced ATRP process as discussed in Chapter 5.3 was employed for the polymerization of UV active monomers. Every attempt to excite them in the UV fails because of the moieties included in their structure which function as inner filter. Efficient photopolymerization of monomers as shown in Chart 3 namely 2-[3-(*2H*-benzotriazol-2-yl)-4-hydroxyphenyl] ethyl methacrylate (**M1**), phenylacrylate, cinnamyl methacrylate (**M2**), and 2-(4-benzoyl-3-hydroxyphenoxy)ethyl-acrylate (**M1**) was activated by NIR light following a photo-ATRP protocol. Solution of **2**, $CuBr_2$/TMPA complex and monomer in DMF resulted in the formation of well-defined polymers. Polymerization of these monomers were also tested under UV light irradiation using 2,2-dimethoxy-2-phenylacetophenone (DMPA) as photoinitiator together with $CuBr_2$/PMDETA complex and EBP as halide source. However, UV light-induced ATRP of these monomers failed as expected on contrary to NIR light. Free-radical polymerization of monomers were also performed for the comparison of the molecular weight charachteristics of the polymers. Polymerization results can be seen in Table 8.

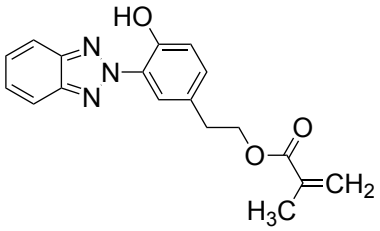

2-[3-(2H-Benzotriazol-2-yl)-4-hydroxyphenyl]ethyl methacrylate
(M1)

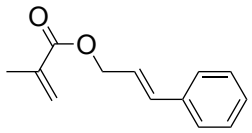

cinnamyl methacrylate
(M2)

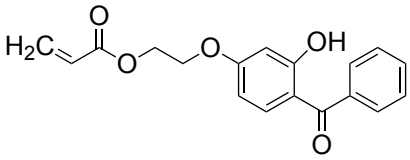

2-(4-Benzoyl-3-hydroxyphenoxy)ethylacrylate)
(M3)

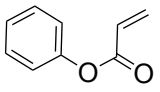

phenylacrylate
(M4)

Chart 3: Structure of monomers used in NIR light-induced photo-ATRP

Table 8: Photoinduced and Free Radical Polymerization of Monomers Using DMPA or Under Different Experimental Conditions[a]

M	NIR Light-induced ATRP			UV Light-induced ATRP			Free Radical Polymerization		
	Conv. (%)	M_n[b] (g/mol)	$Đ$[b]	Conv. (%)	M_n[b] (g/mol)	$Đ$[b]	Conv. (%)	M_n[b] (g/mol)	$Đ$[b]
M1	52	9400	1,5	No polymer obtained			50	22000	3,0
M2	3	2800	1,4				5	75200	2,5
M3	6	3400	1,4				97	9300	2,5
M4	8	2200	1,2				77	19600	2,6

[a][M]:[EBPA]:[$CuBr_2$]:[TPMA]:[**2**]: 300:1:0.03:0.135:0.3, Time= 24 h for NIR light-induced ATRP, [M]:[EBP]:[$CuBr_2$]:[PMDETA]:[DMPA]: 4000:5:1:3:1, Time= 5 h for UV light-induced ATRP, [AIBN]=0.3 mol%, Time=6 h, T=70°C for free radical polymerization. Conversions determined gravimetrically. [b]Determined by gel permeation chromatography using PMMA standards.

As demonstrated in Table 8, UV light induced ATRP was not successful for the polymerization of monomers in Chart 3. This can be explained intrinsic monomer absorbance of UV light. The monomer uptakes therefore the function of a inner filter resulting in inefficient generation of initiating radicals. Consequently, lack of initiating radicals interferes the polymerization process. On the other hand, these monomers can be polymerized efficiently by the help of NIR light. In this case, NIR light is directly absorb by NIR sensitizer to form its excite state. Excited state of **Sens** undergoes electron transfer reaction with the Cu^{II} to reduce to Cu^{I}. After generation of Cu^{I} species, ATRP process proceeds as aformentioned explained in detail in Chapter 2. As expected, free radical polymerization of these monomers resulted in polymers with broader molecular weight distributions ($Đ$>2) compared to polymers obtained by NIR-light induced photo-ATRP. This underlines the possibility of synthesis of monodisperse polymers by photo-ATRP.

Block copolymer synthesis was also performed with this strategy. In order to do that, MMA was polymerized by NIR light-induced ATRP and used as macroinitiator. Identical experimental conditions were applied using M1 as second monomer. GPC analyses showed an increase on the molecular weight indicating the success of polymerization from the halide function at the end of PMMA obtained. Additionally, the influence of the macroinitiator in the beginning of the synthesis were also examined. For this purpose, a

monomer with UV- absorbing moieties was first polymerized by NIR-light and used as macroinitiator to form block copolymer. In both cases, it can be seen that dispersity of polymers remain acceptable range (<1.5). However, the increase of the M_n was significantly different. Figure 14 shows GPC chromatograms of polymers obtained. These differences with respect to molecular weight can be explained by different propagation rate constants of each monomer as already discussed with alternative monomers.

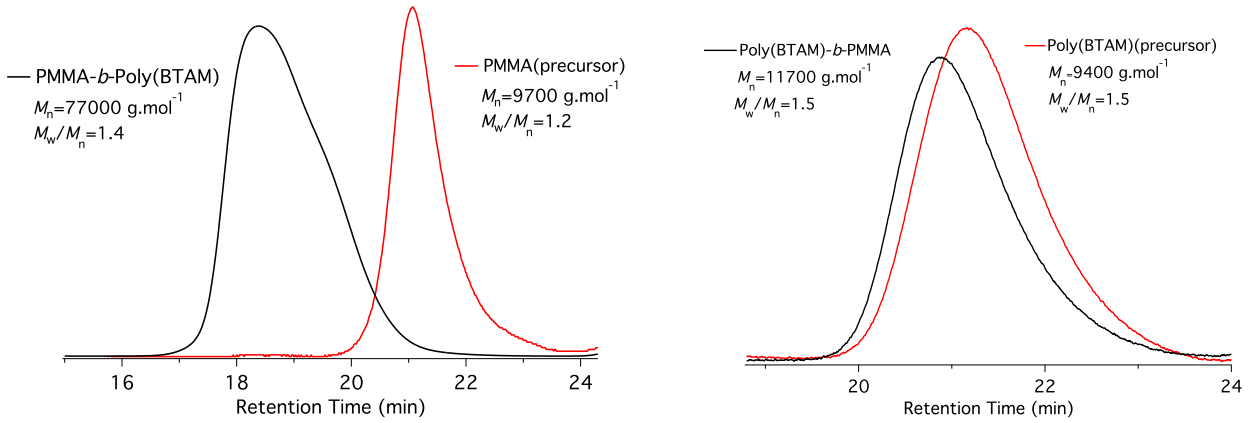

Figure 14: GPC traces of precursor PMMA and PMMA-*b*-P(BTMA) (left) and precursor P(BTAM) and P(BTAM)-*b*-(PMMA) (right):[M]/[EBPA]/[$CuBr_2$]/[TPMA]/[**2**]: 300/1/0.03/0.135/0.3. Both reactions are done in 50 vol% DMF at room temperature at 790 nm exposure, adapted from [250].

5.5 Carbon Dots as Green Photocatalyst for Photoinduced ATRP

Some of the results discussed in this subchapter were previously published [245]. As an alternative, efficiency of **CD**s for photopolymerization by LEDs was also investigated in this thesis. **CD**s have been shown as an excellent photocatalyst for photoinitiated free radical and controlled radical polymerization. First attempts were to test these materials in free radical polymerization with onium salts as oxidizing agents. The structures of onium salts used in this thesis have been shown in Table 2. This was the first report being part of these thesis [245]. Iodonium salts and sulfonium salts comprising low coordinating anions have received increased attention due to their efficient properties in polymerization systems [246].

CDs that are used in this study show broad absorption spectra, covering UV and slightly visible spectral region below 600 nm as can be seen in UV-Vis spectrum in Figure 15. Therefore, for the light source, blue LEDs that emit at 405 nm and 470 nm was used for the exposure. More lab work has been in progress to examine to explore **CD**s exhibiting significant red-shifted absorption. The synthesis pursued to fabricate these materials facilitates in general synthesis of **CD**s with absorption in the NIR as well. These properties could be the focus of future investigations. This thesis just included these materials to show the feasible use for free radical polymerization and photo-ATRP.

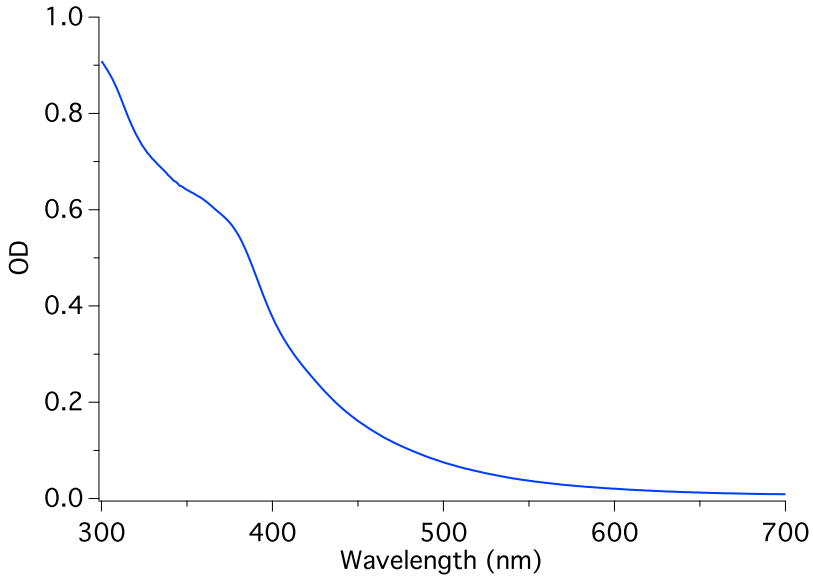

Figure 15: Absorption spectrum of **CD**s in DMSO, adapted from [251].

For free radical polymerization, the initiating system comprising iodonium and sulfonium salts as free radical initiator and **CD**s as photocatalyst was chosen for the polymerization of tri(propylene glycol) diacrylate (TPGDA). The anions were selected from aluminates and bis(trifluoromethylsulfonyl) imides due to their efficiency disclosed previously [246]. These anions have received an important attention as counter ion of onium salts because they can rule out the HF-issue caused by PF_6^- anion under certain conditions [252]. Figure 16 shows the polymerization rate of TPGDA with an initiator system using **CD**s together with onium salts by LED irradiation at 405 nm as determined by photo-DSC. Acceptable values for the polymerization rate of each system showed a good reactivity. This does not differ significantly though the molar concentration of **1a** was lower. Among the onium salts used, sulfonium salt (**2a**) showed less reactivity. However, R_p^{max} was similar time.

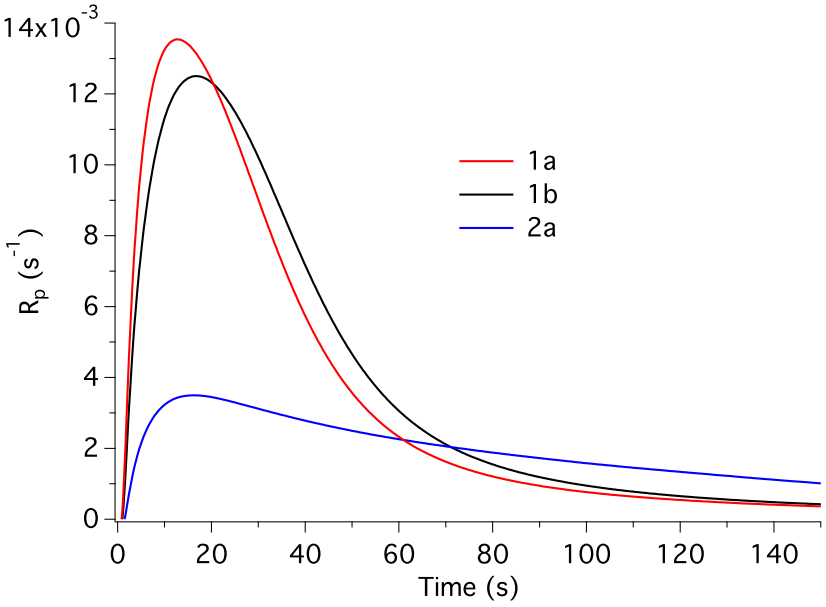

Figure 16: Polymerization as a function of exposure time obtained in free radical polymerization of TPGDA using **CD**s with different onium salts in combination with a blue LED emitting at 405 nm (light intensity: 100 mW×cm^{-2}), adapted from [251].

As stated in Table 9, **CD**s has exhibited similar reactivities with LED exposure at 470 nm. Polymerization reactivity measured by photo-DSC resulting in both a similar final conversion and R_p^{max}. However, although the t_{max} was significantly larger accompanied with a remarkable inhibition time because of the less intensity of LED used (0.5 mW×cm^{-2}). Comparable results indicate the applicability of this system in the light-regulated applications, for example in dental applications.

Table 9: Blue LED (405 nm and 470 nm) initiated free radical polymerization of TPGDA with onium salts **1a**, **1b**, and **2a** using **CD**s.

Onium salt	R_p^{max} (s^{-1})	t_{max} (s)	x_∞	λ_{exc} (nm)
1a	13,5	12,8	0,59	405
1b	12,5	16,8	0,64	405
2a	3,5	16,3	0,41	405
1a	12,1	597 (414)	0,64	470

After the successful efficiency of **CD**s as photocatalyst, activity of these materials was tested for controlled radical polymerization via ATRP process as described previously. As proposed in Scheme 17, **CD**s act as photocatalyst and absorbs the light emitted by LED at 405 nm. After reaching the excited state **CD***, it reduced Cu^{II} to generate $Cu^{I,}$ which is needed for ATRP. The cation readical of **CD** (**CD**$^{+\bullet}$) undergoes reversible electron transfer reaction with bromide which brings back the **CD in** its ground state. This is similar as previously introduced for photo-ATRP applying NIR exposure [119]. There exist similarities between Scheme 17 and the aforementioned shown Scheme 16. Both comprise two complementing redox equilibria; that is the Cu(II)-Cu(I) equilibrium and the **Sens**-**Sens***-**Sens**$^{+\bullet}$ cycle where bromide uptakes in both schemes a key function to close the cycle.

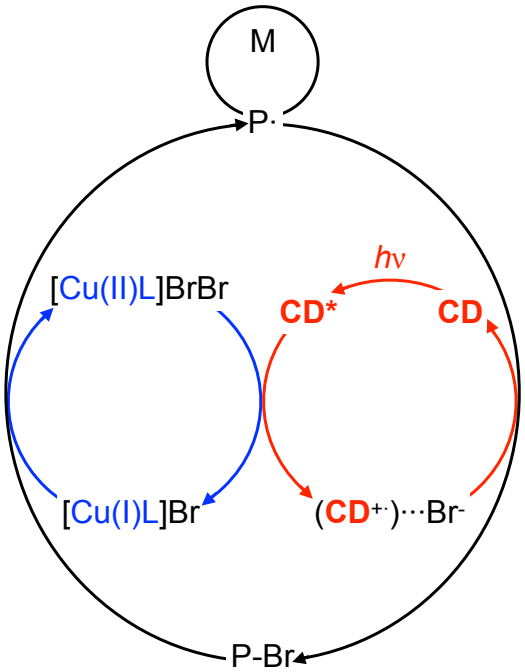

Scheme 17: Proposed mechanism of photoinduced ATRP using **CD**s as photocatalyst, adapted from [251].

Polymerization conditions insist of **CD**s as photocatalyst, EBPA as alkyl initiator, and $CuBr_2$/TPMA complex as catalyst for the polymerization of MMA in DMSO. This mixture was exposed at 405 nm under nitrogen atmosphere in different polymerization conditions as can be seen in Table 9. The polymers obtained using **CD**s showed low dispersity (runs 1 and 2 in Table 10). In order to understand the system, some experiments were performed in the absence of **CD**s and Cu^{II} catalyst (runs 3 and 4 in Table 10). In the absence of Cu^{II} catalyst the polymerization followed free radical protocols by obtaining high molecular weight and broad molecular weight dispersity. This explains the importance of Cu^{II} catalyst to push the polymerization into the contorolled manner. No polymer was obtained without the use of **CD**s. In addition, decreased concentration of **CD**s failed to form polymer even in longer exposure as shown in run 5 in Table 10.

Table 10: Blue LED induced ATRP of MMA using **CD**s under different experimental conditions (*t* = exposure time)[a]

Run	[MMA]/[RX]/[CD]/[$CuBr_2$]/[L]	Time (h)	Conv[b] (%)	M_n[c] (g·mol^{-1})	Đ[c]
1	300/1/0.3/0.03/0.135	0,5	5,5	23000	1,3
2	300/1/0.6/0.03/0.135	2,5	30	6000	1,2
3	300/1/0/0.03/0.135	1	-	-	-
4	300/1/0.3/0/0.135	1	<1	400000	2,4
5	300/1/0.15/0.03/0.135	4	-	-	-

[a]Polymerization experiments were performed at 405 nm at room temperature. [b]Conversions determined gravimetric. [c]Determined by gel permeation chromatography using PMMA standards.

Figure 17 and Figure 18 show the characteristics of polymers obtained in this process. ^{1}H-NMR spectrum of the obtained polymer proved the structure additionally showing the corresponding peaks of the PMMA.

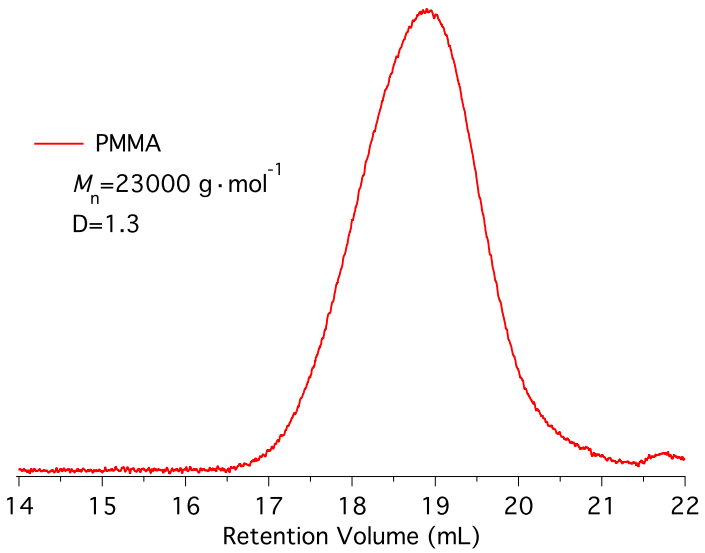

Figure 17: GPC trace of PMMA obtained after 30 min exposure. Reaction conditions:[MMA]/[EBPA]/[**CD**s]/[$CuBr_2$]/[L]:300/1/0.6/0.03/0.135, adapted from [251].

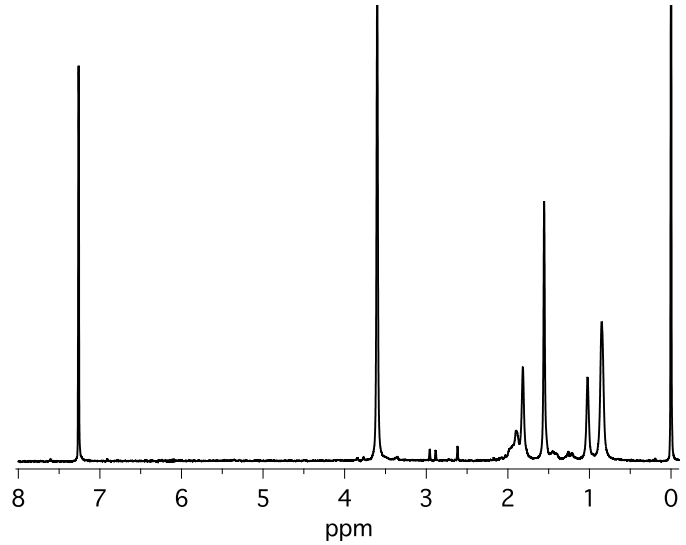

Figure 18: ^{1}H-NMR spectrum of the PMMA taken in $CDCl_3$, adapted from [251].

As shown in Figure 19, light on-off experiments were performed with the experimental conditions as indicated in Table 10, run 2. To achieve this, the polymerization mixture was irridiated to repeat cycles of LED exposures in which light exposed on the sample for 30 min while it was kept in dark for 30 min. After every repetition, certain amount of sample was taken from the tube and precipitated in cold methanol and kept in vacuum. Polymer conversion was gravimetric calculated. Molecular weight characteristics were investigated by GPC. Polymer formation observed when the light is on, however; in the dark period no polymerization occurred. This experiment proved that the initiating radicals were generated by a photonic mechanism.

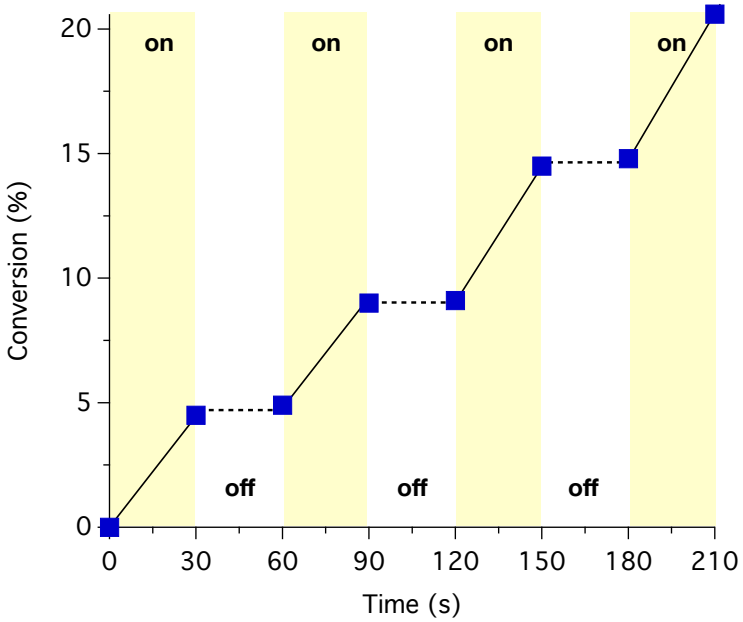

Figure 19: Monomer conversion (%) vs. time using **CD**s to determine the dependency on irradiation: light on (blue regions) light off (yellow regions). (Reaction conditions:$[MMA]_0/[EBPA]_0/[CuBr_2]_0/[TPMA]/[$**CD**s$]=300/1/0.03/0.135/0.3$), adapted from [251].

For kinetic studies similar experiments were performed without turning the light off. Conversion was increased linearly during the irradiation time. Linear relationship between $\ln([M]_0/[M])$ by time was presented indicating first order kinetics (see Figure 20). GPC data of the polymer obtained indicated the molecular weight increase upon irradiation while the dispersities remained around 1.5 (see Figure 20). Chain breaking can explain broad dispersity values. Similar results were obtained with the system comprising up-conversion nanoparticles whic may be because of the heterogeneous nature of the photocatalyst Nevertheless, this topic has been still under consideration.

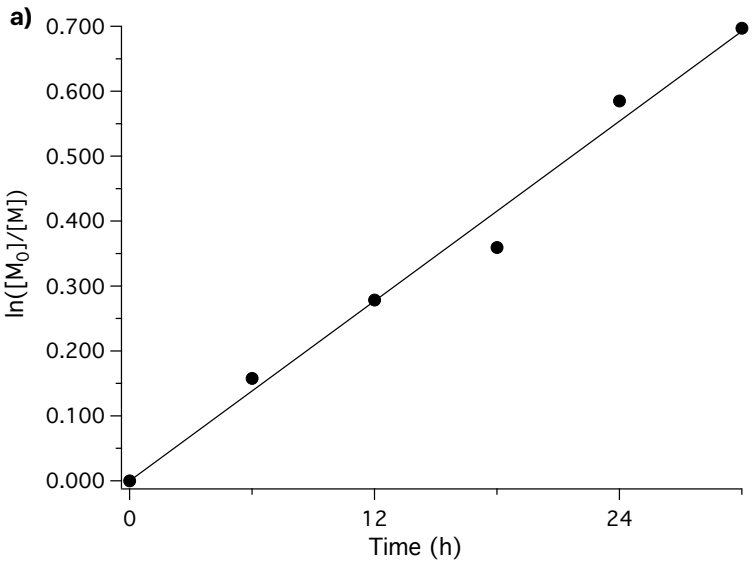

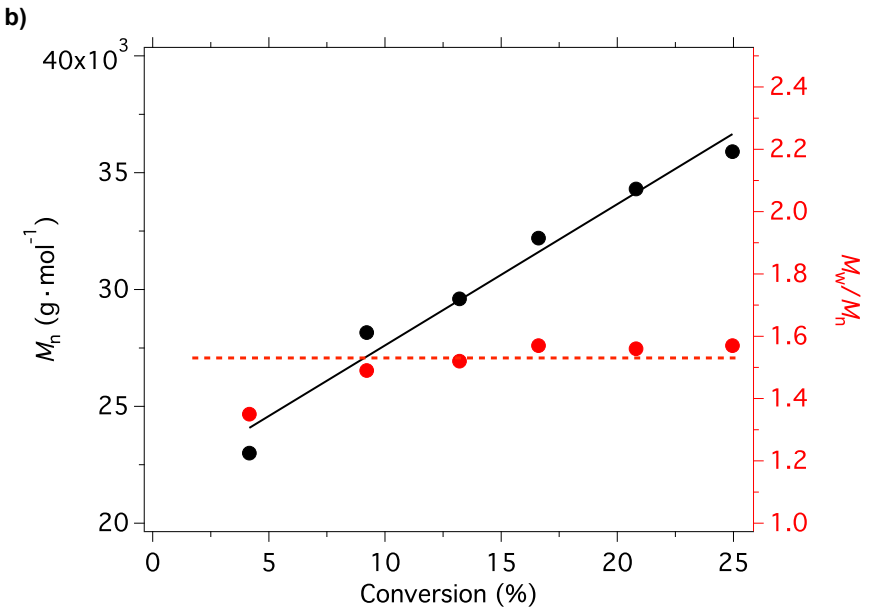

Figure 20: Kinetic plot of the polymerization system using **CD**s (**a**) and molecular weight characteristics and dispersity of PMMA vs irradiation time (**b**). ([MMA]$_0$/[EBPA]$_0$/[Cu^{II}Br$_2$]$_0$/[TPMA]/ [**CD**s]/ =300/1/0.03/0.135/0.3), adapted from [251].

As shown in Figure 21, block copolymerization experiment was performed to prove the halide-end functionality at the end of the polymer obtained by this process. To do that, PMMA was obtained in the first step and used as macroinitiator for block copolymer synthesis. Styrene was employed as second monomer and identical polymerization conditions were employed. GPC chromatograms shifted from 6000 g/mol to 12000 g/mol which indicates the living character of the system. Furthermore, ^{1}H-NMR spectrum also evidenced the expected end group between 4-4.5 ppm in the block copolymer as can be seen in Figure 21.

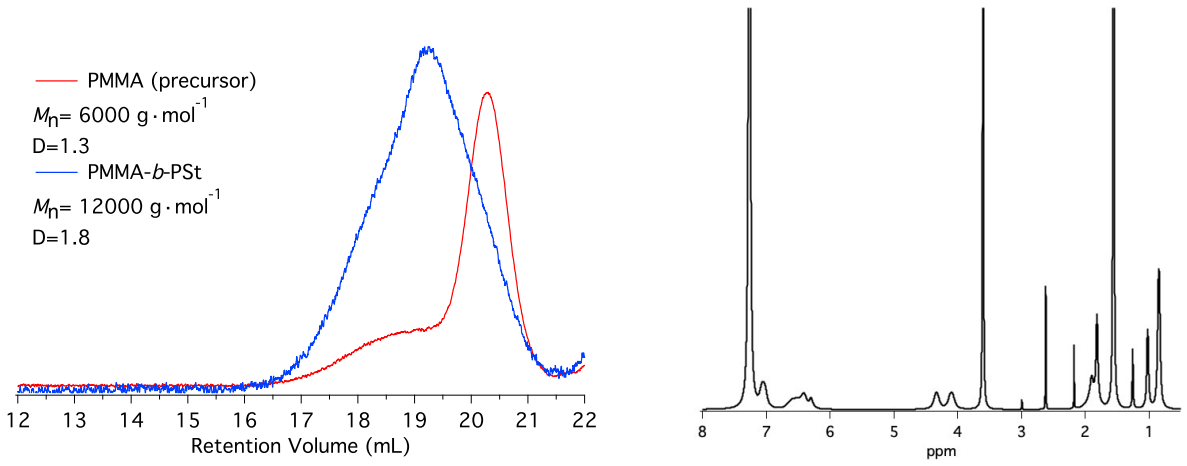

Figure 21: Comparison of GPC traces of precursor PMMA with PMMA-*b*-PSt (left) and ^{1}H-NMR spectrum of the block copolymer (PMMA-*b*-PSt) taken in $CDCl_3$ (right), adapted from [251].

5.6 NIR-Light Induced CuAAC Click Reactions

Some of the results discussed in this subchapter were previously published [244]. Successful PET between excited state of **Sens** and Cu^{II} has given an idea to use the same approach for CuAAC reactions. In order test that, benzyl azide and phenyl acetylene were chosen as model compounds. The solution of NIR sensitizer (**1** or **2**), $CuBr_2$/PMDETA complex, benzyl azide, and phenyl acetylene in DMSO was irradiated with LEDs at 790 nm under nitrogen atmosphere. Similar as photo-ATRP process, NIR sensitizer with cationic structure (**1**) was not successful in this process. However, the formation of triazole ring was successful with using **2** together with $CuBr_2$/PMDETA complex as stated in Scheme 18.

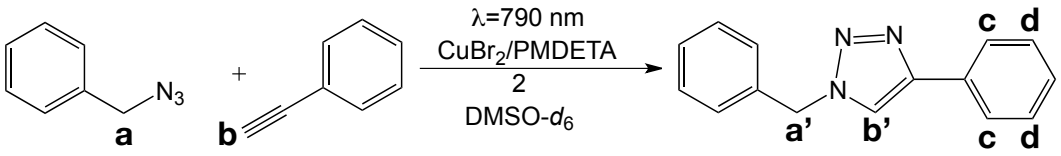

Scheme 18: Photoinduced CuAAC reaction between benzyl azide and phenyl acetylene using **2.**

Click strategy between benzyl azide and phenyl acetylene (shown in Scheme 18) was followed by ^{1}H-NMR spectroscopy as stated in Figure 22. Disappearance of propargyl proton at 4.22 ppm and the observation of signals at 8.69 ppm corresponding to the triazole confirms successful CuAAC reaction with NIR light. Reaction yield was calculated by the integration of the proton in the starting molecule (**a**) and corresponding photon in the product (**a'**). Click reaction with **2** is summarized in Scheme 19. As should be noted, reaction mixture comprising **2**, Cu^{II}/ PMDETA, azide and alkyne was also tested in the dark. However, no triazole formation was observed without NIR exposure.

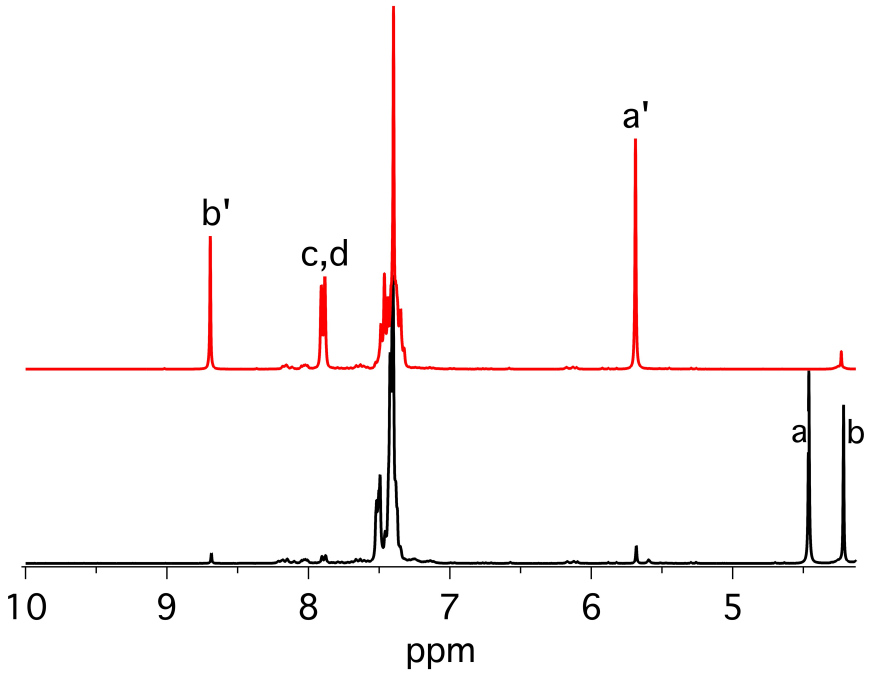

Figure 22: ^{1}H NMR spectra of the reaction between benzyl azide and phenyl acetylene before (black) and after (red) exposure using **2** under NIR LED with emission at 790 nm, adapted from [244].

This reaction preferentially worked again with **2** comprising the barbiturate moiety approving again that the interaction between Cu(II) and barbiturate takes control over these reactions [249]. The fact that it did not react with the neutral sensitizer **4** either rules out any assumption that the charge of the substrate has an impact on the reactivity.

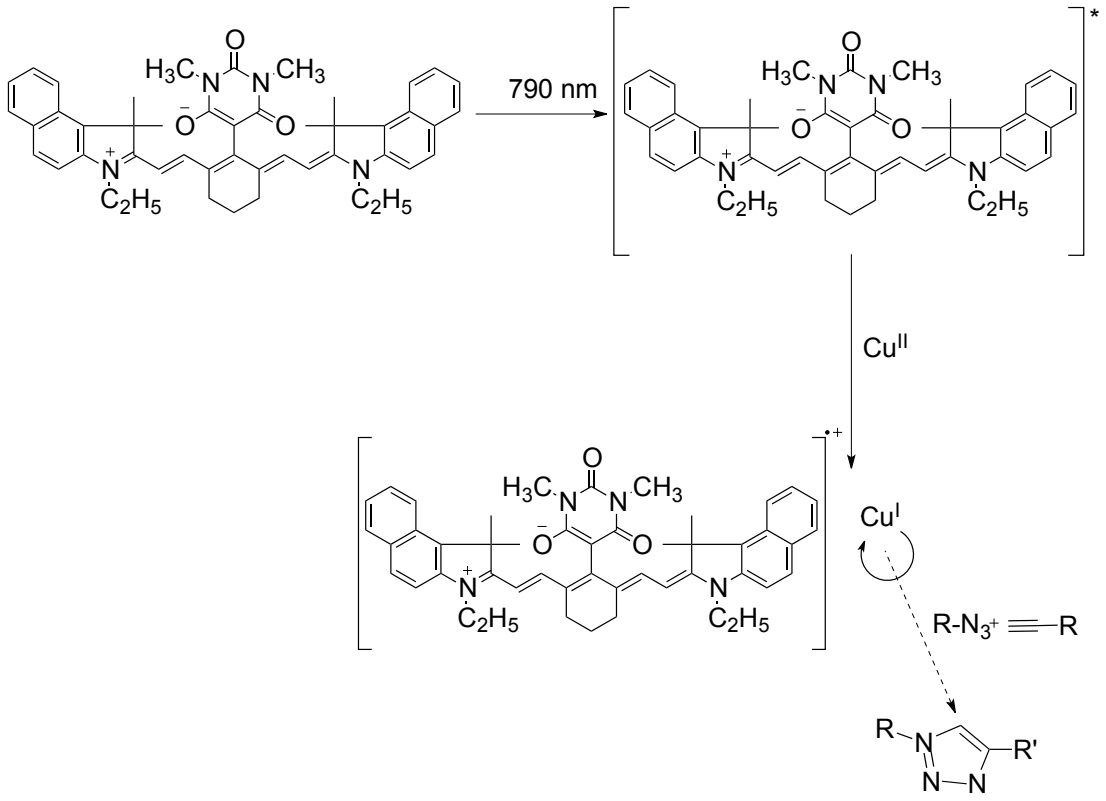

Scheme 19: Schematic view of photoinduced click reaction using **2** and Cu^{II} salt.

The ability of the photoinduced reduction process of Cu(II) by photoexcited **2** with several low molar mass compounds were tested under ideal experimental conditions using phenyl acetylene in the presence of **2** and $CuBr_2$/PMDETA as shown in Table 11. Different compounds either the components comprising aromatic (Runs 1 – 2 using **A2** and **A3**, respectively) or aliphatic moieties (Run 3 – 4 with **A3** and **A**4, respectively) showed good efficiency as can be seen by the conversion. Additionally, an azide compound comprising UV sensitive moiety, that is 9-azidomethylanthracene, exhibited successful CuAAC reaction upon NIR irradiation (Table 11, run 2). This compound can undergo[4+4] cycloaddition upon irradiation with UV-light. In addition, polymer functionalization was succeeded by photoinduced CuAAC using **2**. Azide functional polyethylene glycol (**A4**), and azide functional polystyrene (**A5**) were clicked with phenyl acetylene by photoinduced CuAAC reactions in the NIR region. Scheme 20 shows end-group functionalization of PS-N_3 and PEG-N_3.

Table 11: Photoinduced CuAAC between various phenylacetylenes and various organic azides using **2**[a]

Run	R-N_3	Product	Conv.[b] (%)
1	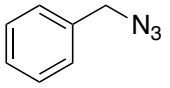 **A1**	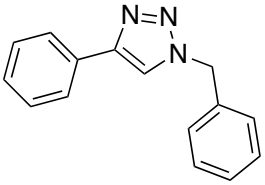 **P1**	99
2	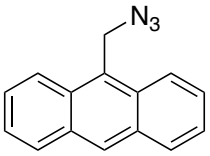 **A2**	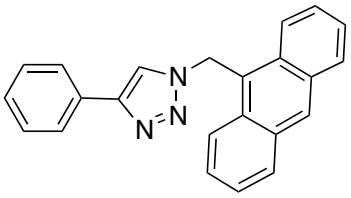 **P2**	98
3	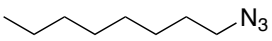 **A3**	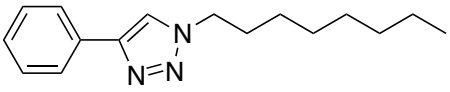 **P3**	95
4	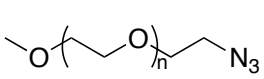 **A4**	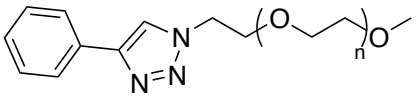 **P4**	95
5	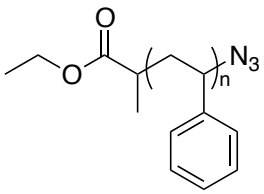 **A5**	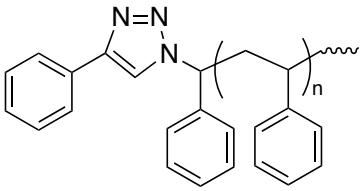 **P5**	98

[a]All reactions were carried out under irradiation at 790 nm at room temperature, in DMSO-d_6 for 2 hours. [b]Conversions were determined by ^{1}H-NMR spectroscopy.

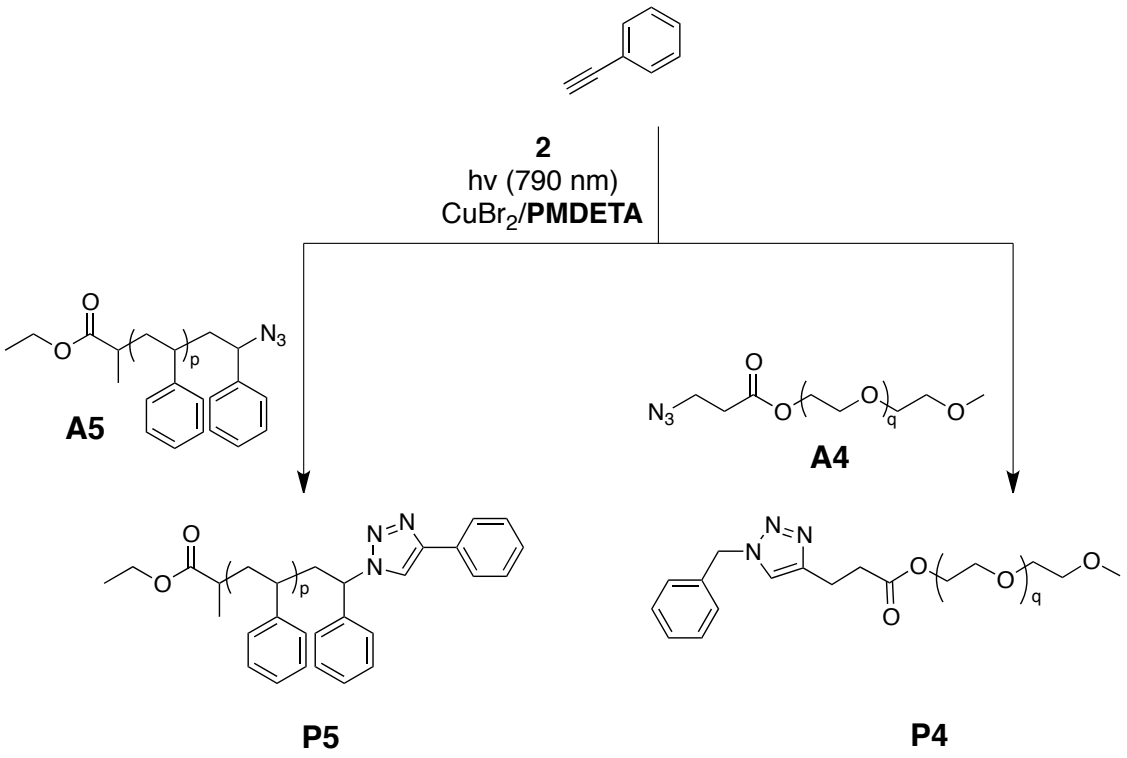

Scheme 20: End-group functionalization of polymers via photoinduced CuAAC click reaction, adapted from [244].

The applicability of described process for the synthesis of high molecular weight compounds was also demonstrated by preparation of block copolymer via NIR photosensitized CuAAC reaction. For that, clickable polymers poly(ε-caprolactone) (Alkyne-PCL) and polystyrene (PS-N_3) were prepared by ring opening polymerization (ROP) and ATRP, respectively. After obtaining polymers with controlled molecular weight characteristics, esterification and azidation reactions were processed for alkyne functional poly(ε-caprolactone) (Alkyne-PCL) and azido functional polystyrene (PS-N_3), respectively. Click reaction between PS-N_3 and Alkyne-PCL using **2** in conjuction with $Cu^{II}Br_2$/PMDETA was accomplished for selective formation of polystyrene-b-poly(ε-caprolactone) (PS-*b*-PCL) upon exposure at 790 nm (Scheme 21). The corresponding block copolymer was formed with the yield of 94%.

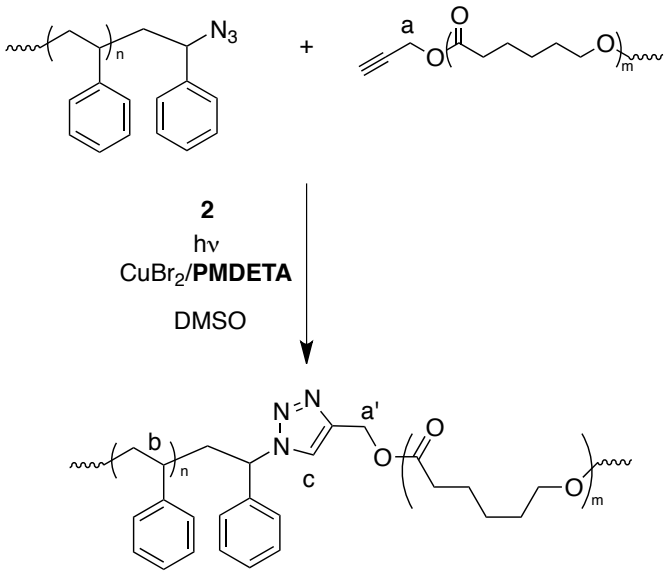

Scheme 21: Synthesis of PS-*b*-PCL block copolymer using **2** by photoinduced CuAAC click reaction, adapted from [244].

Figure 23 exhibits the GPC chromatogram of alkyne-PCL and PS–N_3, and the block copolymer (PS-*b*-PCL). The observation of molecular weight of the block copolymer together with a new signal at 7.48 ppm corresponds to the triazole ring in the ^{1}H-NMR spectrum of the block copolymer proves the successful block copolymer formation through photoinduced click reaction using NIR sensitizer.

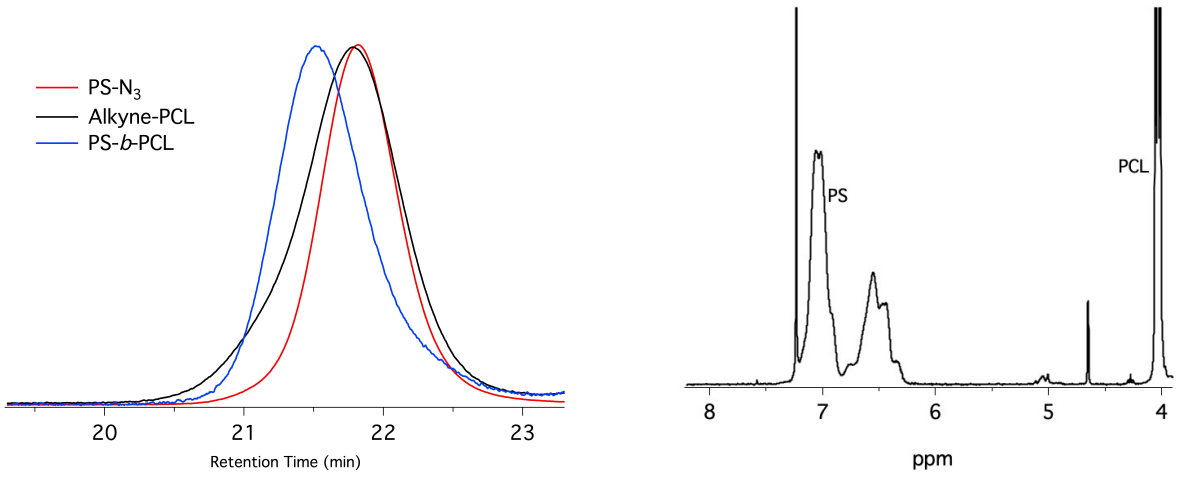

Figure 23: GPC traces of PS-N_3, Alkyne-PCL and PS-*b*-PCL (left) and ^{1}H-NMR spectrum polystyrene-b-poly(ε-caprolactone) copolymer (PS-b-PCL) (right) by photoinduced CuAAC click reaction at 790 nm, adapted from [244].

Kinetic plot of the reaction between phenylacetylene and benzyl azide at 790 nm can be seen shown in Figure 24. As stated, almost complete conversion was attained in a in 2 hours irradiation. This might explained the concentration of formed Cu^{I} by photoinduced electron transfer reactions remains similar during the reaction.

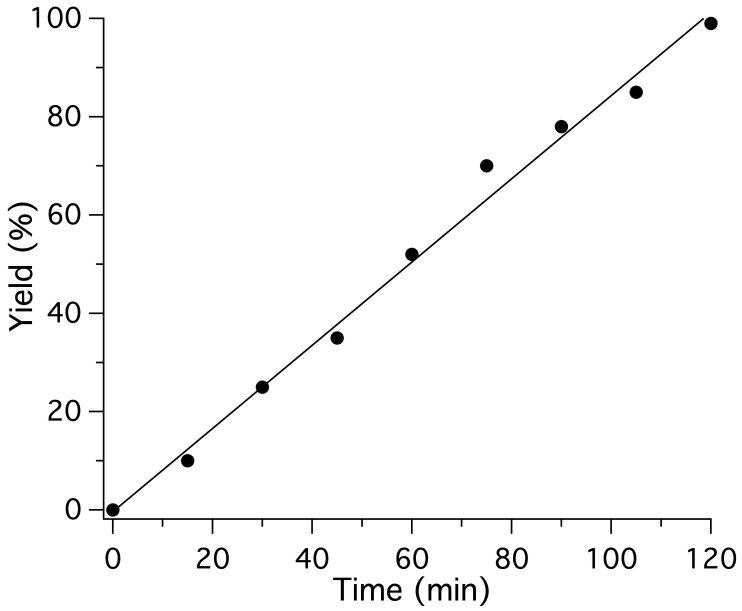

Figure 24: NIR light-induced click reaction of benzyl azide and phenyl acetylene at 790 nm irradiation using Cu(II) in conjunction with **2**. Yields were determined by ^{1}H NMR spectroscopy, adapted from [244].

Furthermore, the reactivity of Cu^{I} generated successful photoinduced electron transfer reaction was examined by light on/off experiment. It was expected to observe an increase of the conversion even when the mixture is kept in the dark after a short irradiation in the beginning. As shown in Figure 25, conversion increases with irradiation time indicating that formed Cu^{I} catalyst upon irradiation protected its activity in dark. This indicates that Cu^{I} is not oxidized back if it is formed in the reaction mechanism shown in Scheme 22 *vide infra*.

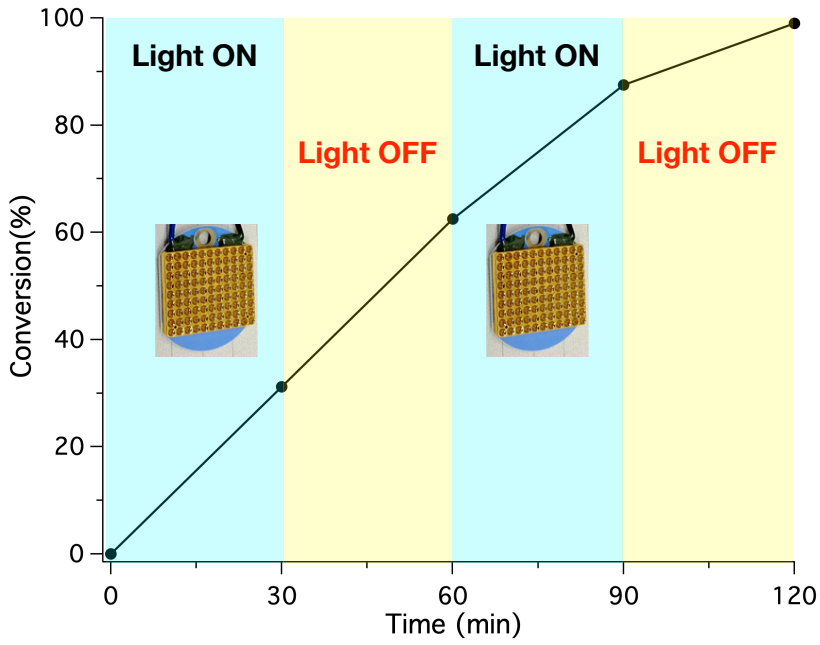

Figure 25: Light on-off cycles of click reactions between benzyl azide and phenyl acetylene using **2** as NIR sensitizer, adapted from [244].

With the light of these investigations and photochemical behaviour of **2**, Scheme 21 explains photoinduced electron transfer reaction in which **2** as photocatalyst. First of all, the reaction starts with NIR irradiation of **2** to be able to reach its excited state. Excited state (**Sens***) reacts with Cu^{II} generating the cation radical of **Sens**$^{\bullet+}$, and Cu^{I} species upon NIR irradiation. The formation of Cu^{I} in the reaction media catalyzes the click reaction as described previously in detail. **Sens**$^{\bullet+}$ go through electron transfer reaction with PMDETA to go back the reaction cycle as its ground state (**Sens**). It can also decompose resulting in oxidation products. This was examined by photobleaching experiments . Photolysis of reaction mixture comprising **2** as photosensitizer, phenyl acetylene, benzyl azide, and Cu^{II}/PMDETA exhibited a slow bleaching.

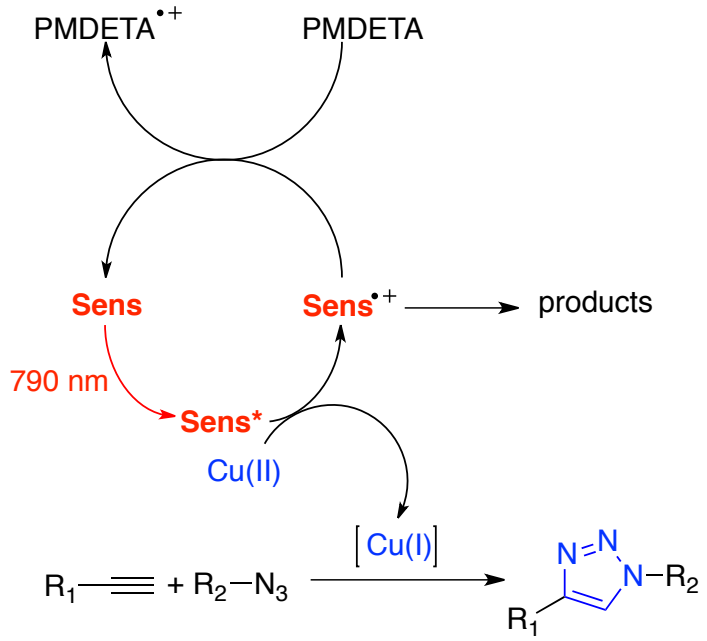

Scheme 22: Proposed mechanism of photoinduced click reaction using **Sens**, adapted from [244].

In this scenario, **Sens** slowly bleaches upon photoexcitation as a result of decomposition of **Sens**$^{\bullet+}$. Thus, it was assumed that some **Sens**$^{\bullet+}$ comes back to **Sens** while some parts of **Sens**$^{+\bullet}$ irreversibly leave the cycle shown in Scheme 22. From this point of view, it was considered that this mechanism rather as a semi-catalytic cycle regarding the function of **Sens**. Figure 26 depicts a different pattern indicating that the reaction does not follow a unique route. The mechanism shown in Scheme 22 might support the kinetics observed in Figure 26 explaining the decrease of the spectra.

In general, this chemistry can be expanded in future works with azides and alkynes comprising a number of reacting groups resulting in cross linked materials; that is a functionality of at least three. Such materials should exhibit outstanding material properties such as reduced brittleness and enhanced elastic modulus [253, 254].

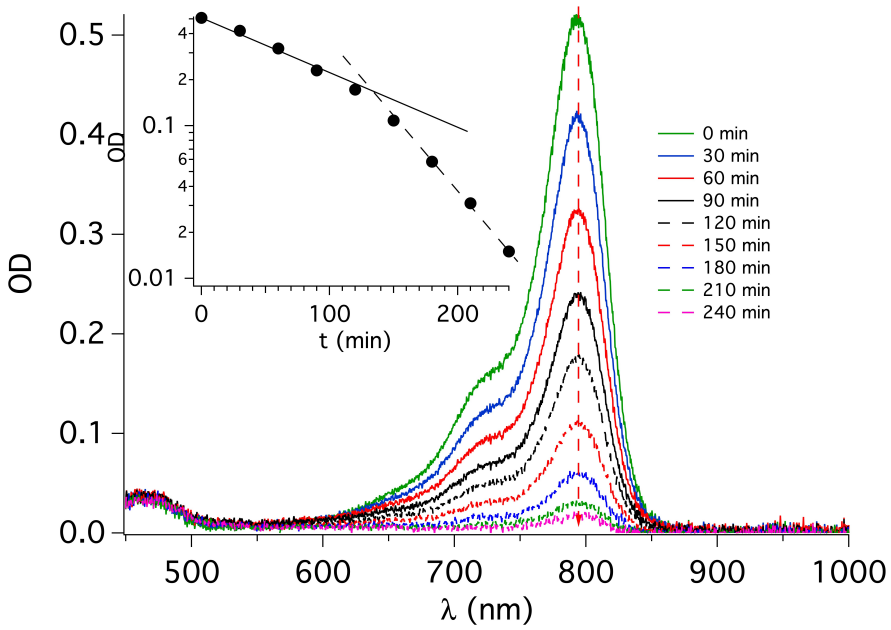

Figure 26: Spectral changes of the solution of **2** in the presence of PMDETA, phenylacetylene and benzyl azide in DMSO upon irradiation at 790 nm (under nitrogen). Cu^{I} formed does not react with **2** in the time frame chosen, adapted from [244].

6. Conclusion

Photoinduced systems have gained significant attention in many fields. These approaches offer several advantages over the thermal processes by being low cost, adaptable to several conditions regarding the desired applications, and by requiring low energy. Additionally, photochemical strategies have been applied in the construction of macromolecular compounds in polymer chemistry. These methods additionally provide alternatives to synthesize tailor-made polymeric materials. Both, the new photo-ATRP and click chemistry approaches possess potential to make also crosslinked materials if appropriate multi-functional materials would be available. This might become a point a fire research to put new impetus in material science.

Photopolymerization has become an important field in the synthetic polymer chemistry. Photoinduced processes provide spatiotemporal control over the process in mild reactions conditions. Additionally, many studies have been presented for the use of photoinduced reactions for the synthesis of well-defined polymers in terms of structure and functionality. Light as a reagent and tool provides the possibility to turn ON/OFF processes just on demand.

In general, UV light has been used to generate the initiating radicals or electrophilic species which can initiate the polymerization. There exist also examples of photopolymerization with sensitizers in the visible range from 400 nm to 600 nm, which have been described in detail in the literature. However, there have been great efforts to discover new initiating systems in longer wavelengths such as in the NIR in which NIR LEDs and NIR diode laser are an alternative to mercury lamps. It complements therefore regulations of the EU to find alternative light source for technologies using mercury lamps. Applications of NIR light are already used in lithographic printing plates, but have not been transferred any other areas yet because of lack of understanding of NIR initialing systems. One of the most advantages of the system is the generation of heat which can be used for chemical and/or physical drying processes. Therefore, NIR initiating systems have started to get revitalized interest recently. These system generally consists of an NIR sensitizer and onium salts or triazine derivatives as initiator. Initiating radicals and cations are generated by an electron transfer reaction between sensitizer and initiator by the use of different light sources. The new onium salts investigated in this thesis fit well in the requirements. This facilitates to replace those onium salts comprising hexafluoro-phosphates by less harmful and less toxic aluminates. The new iodonium salts can be applied for both applications using sensitizers in the NIR and UV. Furthermore, the big

potential to use NIR radiation can be also seen to polymerize monomers comprising UV absorbing moieties.

In this thesis, synthesis of tailor-made materials by photoinduced ATRP and CuAAC processes were shown as simple routes through the process light can be used for the generation of reactive species in the NIR region. Basically, both processes require lower oxidation state metal complexes and need several precautions in the synthesis. It was demonstrated that Cu^{I} can be generated in an in situ manner starting from Cu^{II} salts by using NIR sensitizers by photoinduced electron transfer reactions. As a result of starting the reaction with higher air stable salts, the possibility of oxidation of low oxidation state CuI can be eliminated. These studies clearly demonstrate the feasibility to connect hydrophobic and hydrophilic polymers by just one click.

In the first part of the thesis, **UCNP**s assisted metal-free ATRP approach is successfully shown with initiating system comprising ITX and *N*,*N*,*N'*,*N''*,*N'''*-pentamethyldiethylen-triamine (PMDETA) and ethyl α-bromo-2-methylpropionate (EBiP) for the polymerization of methyl methacrylate (MMA) via ATRP process in metal free conditions. This system results in polymers with a living character and controlled molecular weight characteristics. Chain end functionality is also proved by chain extension experiment. GPC chromatograms of the precursor and chain extended polymer clearly show the increase of the molecular weight. It was shown for the first time the use of NIR laser irradiation for metal-free photo-ATRP systems.

In the second part, metal-free approaches were tested using **Sens** instead of **UCNP**s with NIR LEDs. NIR sensitizers in combination with ethyl 2-bromopropionate (EBP) and PMDETA in the absence of metal catalyst showed no efficiency for well-defined polymers. Polymers obtained by this strategy showed high molecular weights and no controlled termination. This system was compared with the initiating system comprising **Sens** and an iodonium salt for the molecular weight characteristics. The polymers obtained by both systems exhibited comparable results which indicates that metal-free approaches using NIR sensitizers was not efficient for the synthesis of well-defined polymers as the polymerization proceeds through conventional free radical polymerization.

In the next part, metal-free systems using NIR sensitizers were improved by adding ppm scale of copper catalysts to the polymerization solution of MMA to convert the process ATRP. Using copper catalyst shifted the system to controlled mechanism in which living nature of the system was proven by chromatographic and spectroscopic analyses. Polymers with controlled molecular weight, low dispersity and chain-end functionality were obtained upon NIR irradiation. The used polymethine with zwitterionic structure reacts with

Cu^{II} via photoinduced electron transfer reactions for the generation of Cu^{I} catalyst that catalyzes ATRP reaction. This system exhibited a photocatalytic mechanism as **Sens** goes back to the cycle facilitating continuous initiation of the initiating the polymerization. Chain extension and block copolymerization experiments confirmed the existence of the halide functionality at the chain end of the polymer chain which allows to initiate the polymerization at any time. The temporal control of the polymerization was demonstrated by turning the light on-off. This strategy can be an efficient way to prepare well defined polymers in NIR region. This may open a new pathways for biological applications. It was also successfully demonstrated that synthesis of block copolymers consisting of UV-active monomers can be synthesized by NIR light induced ATRP. The results suggested that a basic polymerization of UV-active monomers is possible with this approach. However, the solubility of the monomer in the chosen solvent plays a crucial role in the conversion. With these results, it was clearly confirmed that NIR light can be used for the photopolymerization of monomers with UV-absorbing elements.

Alternatively, **CD**s was shown as an effective photocatalyst to initiate free radical and ATRP reactions upon irradiation by blue LEDs. Polymerization of tri(propyleneglycol) diacrylate (TPGDA) was examined using **CD**s as photocatalyst and onium salts as initiator by photo-DSC. Irradiation of **CD**s with LED emitting at 405 nm exposure in combination with iodonium and sulfonium salts showed efficient reactivity for the polymerization of TPGDA with acceptable final conversions. Same initiating system was exposed also with 470 nm LED and the results obtained showed similar reactivity regarding the final conversion which may be an alternative pathway for dental applications. Future work is going to provide alternative **CD**s covering the absorption in the NIR as well. They are cheap easy affordable since also waste originating from food waste.

NIR sensitized photo-ATRP approach was adapted to this system. Similar catalytic system was found using **CD**s instead of NIR sensitizers upon 405 nm exposure. **CD**s used as photocatalyst together with Cu^{II} catalyst and an alkyl halide as radical initiator. Polymers obtained with this approach showed well-defined structures. Living characters of the polymers including chain end functionality, linear increase of molecular weight with conversion or irradiation time, and the controlled molecular weight characteristics were proven by several experiments. Initiating species were active only when the light is on and polymerization did not occur in dark. With all of these characteristics, **CD**s was shown as an alternative and green photocatalyst for photopolymerization for free radical polymerization or controlled radical polymerization procedures. This synthetic routes can be classified as green and sustainable routes in polymer synthesis.

In the last part of the thesis, employment of NIR sensitizers were employed as photo reducing agents for the reduction of Cu^{II} in order to form Cu^{I}, which is a catalyst in CuAAC reactions. With this strategy both low molecular compounds and polymeric materials were clicked together resultin in the formation of triazole ring. It complements available green methods of polymer syntheses since click chemistry also belongs to green methods in synthetic macromolecular chemistry.

In conclusion, the photochemical methodologies presented this thesis focused on the use of various visible and NIR sensitive initiating systems that provide formation polymers in more energetically favorable and green manner. It is anticipated that the approaches presented here and their combinations have the potential to fabricate materials with desired structures and properties.

References

[1] H. Staudinger, “Makromolekulare Chemie und Biologie”, **1947**.

[2] H.-G. Elias, Macromolecules, Vol. 1-4, Wiley-VCH, Weinheim, **2005**.

[3] A. Shrivastava, Introduction to Plastics Engineering, Elsevier, Cambridge, **2018**.

[4] N. J. Turro, *Modern Molecular Photochemistry*, University Science Books, Sausalito, **1991**.

[5] N. J. Turro, V. Ramamurthy, J. C. Scaiano, *Principles of Molecular Photochemistry*, University Science Books, Sausalito, **2009**.

[6] V. Balzani, P. Ceroni, A. Juris, *Photochemistry and Photophysics*, Wiley-VCH, Weinheim, **2014**.

[7] S. Dadashi-Silab, S. Doran, Y. Yagci, “Photoinduced Electron Transfer Reactions for Macromolecular Syntheses”, *Chemical Reviews* **2016**, *116*, 10212-10275.

[8] R. Dessauer, Photochemistry, History and Commercial Applications of Hexaarylbiimidazoles: All about HABIs, Elsevier, **2006**.

[9] J. W. Stansbury, M. J. Idacavage, “3D printing with polymers: Challenges among expanding options and opportunities”, *Dental Materials* **2016**, *32*, 54-64.

[10] G. Yilmaz, Y. Yagci, “New Photochemical Processes for Macromolecular Syntheses”, *Journal of Photopolymer Science and Technology* **2016**, *29*, 91-98.

[11] R. Schwalm, UV Coatings. Basics, Recents Developments and New Applications, Elsevier, Oxford, **2007**.

[12] H. Baumann, “Lithographische Druckplatten für Laserbelichtung”, *Chemie in unserer Zeit* **2015**, *49*, 14-29.

[13] H. Baumann, T. Hoffmann-Walbeck, W. Wenning, H.-J. Lehmann, C. D. Simpson, H. Mustroph, U. Stebani, T. Telser, A. Weichmann, R. Studenroth, in *Ullmann's Encyclopedia of Industrial Chemistry*, Wiley-VCH Verlag GmbH & Co. KGaA, **2015**, pp. 1-51.

[14] H. Böttcher, J. Bendig, M. A. Fox, G. Hopf, H. J. Timpe, *Technical Applications of Photochemistry*, Deutscher Verlag für Grundstoffindustrie, Leipzig, **1991**.

[15] A. M. Braun, M. T. Maurette, E. Oliveros, *Photochemical Technology*, Wiley, Chichester, **1991**.

[16] J. Zhang, P. Xiao, “3D printing of photopolymers”, *Polymer Chemistry* **2018**, *9*, 1530-1540.

[17] B. Strehmel, C. Schmitz, K. Cremanns, J. Göttert, “Photochemistry with Cyanines in the Near Infrared: A Step to Chemistry 4.0 Technologies”, *Chemistry – A European Journal* **2019**, *25*, 12855-12864.

[18] W. A. Green, Industrial Photoinitiators: A Technical Guide, CRC Press, **2010**.

[19] M. Sangermano, G. Malucelli, E. Amerio, A. Priola, E. Billi, G. Rizza, “Photopolymerization of epoxy coatings containing silica nanoparticles”, *Progress in Organic Coatings* **2005**, *54*, 134-138.

[20] K.-H. Pfoertner, T. Oppenländer, in Ullmann's Encyclopedia of Industrial Chemistry, Wiley-VCH, Weinheim, **2012**, pp. 2-45.

[21] R. Podsiadły, K. Podemska, A. M. Szymczak, “Novel visible photoinitiators systems for free-radical/cationic hybrid photopolymerization”, *Dyes and Pigments* **2011**, *91*, 422-426.

[22] J. P. Fouassier, J. Lalevée, Photoinitiators for Polymer Synthesis, Wiley-VCH, Weinheim, **2012**.

[23] J. Lalevée, J. P. Fouassier, Photopolymerisation Initiating Systems, Royal Society of Chemistry, **2018**.

[24] D. J. Siegwart, J. K. Oh, K. Matyjaszewski, “ATRP in the design of functional materials for biomedical applications”, *Progress in Polymer Science* **2012**, *37*, 18-37.

[25] T. E. Patten, J. Xia, T. Abernathy, K. Matyjaszewski, “Polymers with Very Low Polydispersities from Atom Transfer Radical Polymerization”, *Science* **1996**, *272*, 866.

[26] N. V. Tsarevsky, K. Matyjaszewski, “"Green" atom transfer radical polymerization: From process design to preparation of well-defined environmentally friendly polymeric materials”, *Chemical Reviews* **2007**, *107*, 2270-2299.

[27] G. Moad, E. Rizzardo, S. H. Thang, “Living radical polymerization by the RAFT process”, *Australian Journal of Chemistry* **2005**, *58*, 379-410.

[28] L. Barner, S. Perrier, in *Handbook of RAFT Polymerization* (Ed.: C. Barner–Kowollik), **2008**, pp. 455-482.

[29] D. Benoit, V. Chaplinski, R. Braslau, C. J. Hawker, “Development of a universal alkoxyamine for "living" free radical polymerizations”, *Journal of the American Chemical Society* **1999**, *121*, 3904-3920.

[30] Y. Guillaneuf, D. Bertin, D. Gigmes, D. L. Versace, J. Lalevee, J. P. Fouassier, “Toward Nitroxide-Medlated Photopolymerization”, *Macromolecules* **2010**, *43*, 2204-2212.

[31] S. Shanmugam, C. Boyer, “Stereo-, Temporal and Chemical Control through Photoactivation of Living Radical Polymerization: Synthesis of Block and Gradient Copolymers”, *Journal of the American Chemical Society* **2015**, *137*, 9988-9999.

[32] B. Strehmel, S. Ernst, K. Reiner, D. Keil, H. Lindauer, H. Baumann, “Application of NIR-Photopolymers in the Graphic Industry: From Physical Chemistry to Lithographic Applications”, *Z. Phys. Chem.* **2014**, *228*, 129-153.

[33] A. J. D. Magenau, N. C. Strandwitz, A. Gennaro, K. Matyjaszewski, “Electrochemically Mediated Atom Transfer Radical Polymerization”, *Science* **2011**, *332*, 81.

[34] S. Okada, S. Park, K. Matyjaszewski, “Initiators for Continuous Activator Regeneration Atom Transfer Radical Polymerization of Methyl Methacrylate and Styrene with N-Heterocyclic Carbene as Ligands for Fe-Based Catalysts”, *Acs Macro Letters* **2014**, *3*, 944-947.

[35] B. Strehmel, S. Ernst, K. Reiner, D. Keil, H. Lindauer, H. Baumann, in *Zeitschrift für Physikalische Chemie, Vol. 228*, **2014**, p. 129.

[36] B. Strehmel, C. Schmitz, C. Kütahya, Y. Pang, A. Drewitz, H. Mustroph, “Photophysics and photochemistry of NIR absorbers derived from cyanines: key to new technologies based on chemistry 4.0”, *Beilstein Journal of Organic Chemistry* **2020**.

[37] D. A. Shipp, “Reversible-Deactivation Radical Polymerizations”, *Polymer Reviews* **2011**, *51*, 99-103.

[38] A. D. Jenkins, R. G. Jones, G. Moad, “Terminology for reversible-deactivation radical polymerization previously called "controlled" radical or "living" radical polymerization (IUPAC Recommendations 2010)”, *Pure and Applied Chemistry* **2010**, *82*, 483-491.

[39] T. Otsu, A. Matsumoto, “Controlled synthesis of polymers using the iniferter technique: Developments in living radical polymerization”, *Microencapsulation - Microgels - Iniferters* **1998**, *136*, 75-137.

[40] J. S. Wang, K. Matyjaszewski, “Living Controlled Radical Polymerization - Transition-Metal-Catalyzed Atom-Transfer Radical Polymerization in the Presence of a Conventional Radical Initiator”, *Macromolecules* **1995**, *28*, 7572-7573.

[41] M. Chen, M. Zhong, J. A. Johnson, “Light-Controlled Radical Polymerization: Mechanisms, Methods, and Applications”, *Chemical Reviews* **2016**, *116*, 10167-10211.

[42] B. P. Fors, C. J. Hawker, “Control of a Living Radical Polymerization of Methacrylates by Light”, *Angewandte Chemie-International Edition* **2012**, *51*, 8850-8853.

[43] K. Matyjaszewski, “Atom Transfer Radical Polymerization (ATRP): Current Status and Future Perspectives”, *Macromolecules* **2012**, *45*, 4015-4039.

[44] M. A. Tasdelen, M. Ciftci, Y. Yagci, “Visible Light-Induced Atom Transfer Radical Polymerization”, *Macromolecular Chemistry and Physics* **2012**, *213*, 1391-1396.

[45] J. F. Yan, B. Li, F. Zhou, W. M. Liu, “Ultraviolet Light-Induced Surface-Initiated Atom-Transfer Radical Polymerization”, *Acs Macro Letters* **2013**, *2*, 592-596.

[46] J. F. Quinn, L. Barner, C. Barner-Kowollik, E. Rizzardo, T. P. Davis, “Reversible addition-fragmentation chain transfer polymerization initiated with ultraviolet radiation”, *Macromolecules* **2002**, *35*, 7620-7627.

[47] M. A. Tasdelen, Y. Y. Durmaz, B. Karagoz, N. Bicak, Y. Yagci, “A new photoiniferter/ RAFT agent for ambient temperature rapid and well-controlled radical polymerization”, *Journal of Polymer Science Part a-Polymer Chemistry* **2008**, *46*, 3387-3395.

[48] M. K. Ham, J. HoYouk, Y. K. Kwon, Y. J. Kwark, “Photoinitiated RAFT polymerization of vinyl acetate”, *Journal of Polymer Science Part a-Polymer Chemistry* **2012**, *50*, 2389-2397.

[49] G. H. Liu, H. Shi, Y. R. Cui, J. Y. Tong, Y. Zhao, D. J. Wang, Y. L. Cai, “Toward rapid aqueous RAFT polymerization of primary amine functional monomer under visible light irradiation at 25 degrees C”, *Polymer Chemistry* **2013**, *4*, 1176-1182.

[50] S. Hu, J. H. Malpert, X. Yang, D. C. Neckers, “Exploring chromophore tethered aminoethers as potential photoinitiators for controlled radical polymerization”, *Polymer* **2000**, *41*, 445-452.

[51] X. X. Liu, X. H. Zhang, X. H. Zhang, G. G. Wu, J. W. Yang, L. X. Pang, Z. H. Zeng, Y. L. Chen, “Photoinduced controlled/living free-radical polymerization of 4-methacryloyl-1,2,2,6,6-pentamethyl-piperidenyl”, *Journal of Polymer Science Part a-Polymer Chemistry* **2004**, *42*, 2659-2665.

[52] G. Moad, J. Chiefari, Y. K. Chong, J. Krstina, R. T. A. Mayadunne, A. Postma, E. Rizzardo, S. H. Thang, “Living free radical polymerization with reversible addition-fragmentation chain transfer (the life of RAFT)”, *Polymer International* **2000**, *49*, 993-1001.

[53] G. Moad, E. Rizzardo, S. H. Thang, “Radical addition-fragmentation chemistry in polymer synthesis”, *Polymer* **2008**, *49*, 1079-1131.

[54] L. Lu, H. J. Zhang, N. F. Yang, Y. L. Cai, “Toward rapid and well-controlled ambient temperature RAFT polymerization under UV-Vis radiation: Effect of radiation wave range”, *Macromolecules* **2006**, *39*, 3770-3776.

[55] L. Li, B. Yu, T. You, “Nitrogen and sulfur co-doped carbon dots for highly selective and sensitive detection of Hg (II) ions”, *Biosensors and Bioelectronics* **2015**, *74*, 263-269.

[56] G. Moad, C. Barner-Kowollik, in *Handbook of RAFT polymerization* (Ed.: C. Barner-Kowollik), Wiley, Germany, **2008**, pp. 51-104.

[57] G. Moad, R. T. A. Mayadunne, E. Rizzardo, M. Skidmore, S. H. Thang, “Kinetics and mechanism of RAFT polymerization”, *Advances in Controlled/Living Radical Polymerization* **2003**, *854*, 520-535.

[58] A. Postma, T. P. Davis, R. A. Evans, G. X. Li, G. Moad, M. S. O'Shea, “Synthesis of well-defined polystyrene with primary amine end groups through the use of phthalimido-functional RAFT agents”, *Macromolecules* **2006**, *39*, 5293-5306.

[59] Y. K. Chong, G. Moad, E. Rizzardo, S. H. Thang, “Thiocarbonylthio end group removal from RAFT-synthesized polymers by radical-induced reduction”, *Macromolecules* **2007**, *40*, 4446-4455.

[60] C. J. Hawker, “Molecular-Weight Control by a Living Free-Radical Polymerization Process”, *Journal of the American Chemical Society* **1994**, *116*, 11185-11186.

[61] P. G. Griffiths, E. Rizzardo, D. H. Solomon, “Initiation Pathways in the Polymerization of Alkyl Methacrylates with tert-Butoxy Radicals”, *Journal of Macromolecular Science: Part A - Chemistry* **1982**, *17*, 45-50.

[62] G. Moad, E. Rizzardo, D. H. Solomon, “Selectivity of the reaction of free radicals with styrene”, *Macromolecules* **1982**, *15*, 909-914.

[63] V. Yadav, N. Hashmi, W. Ding, T.-H. Li, M. K. Mahanthappa, J. C. Conrad, M. L. Robertson, “Dispersity control in atom transfer radical polymerizations through addition of phenylhydrazine”, *Polymer Chemistry* **2018**, *9*, 4332-4342.

[64] R. B. Grubbs, “Nitroxide-Mediated Radical Polymerization: Limitations and Versatility”, *Polymer Reviews* **2011**, *51*, 104-137.

[65] K. Matyjaszewski, N. V. Tsarevsky, “Nanostructured functional materials prepared by atom transfer radical polymerization”, *Nature Chemistry* **2009**, *1*, 276-288.

[66] M. S. Kharasch, G. Sosnovsky, “The reactions of t-butyl perbenzoate and olefins-A stereospecific reaction”, *Journal of the American Chemical Society* **1958**, *80*, 756-756.

[67] F. Minisci, “Free-radical additions to olefins in the presence of redox systems”, *Accounts of Chemical Research* **1975**, *8*, 165-171.

[68] F. di Lena, K. Matyjaszewski, “Transition metal catalysts for controlled radical polymerization”, *Progress in Polymer Science* **2010**, *35*, 959-1021.

[69] M. Kamigaito, T. Ando, M. Sawamoto, “Metal-catalyzed living radical polymerization”, *Chemical Reviews* **2001**, *101*, 3689-3745.

[70] T. E. Patten, J. H. Xia, T. Abernathy, K. Matyjaszewski, “Polymers with very low polydispersities from atom transfer radical polymerization”, *Science* **1996**, *272*, 866-868.

[71] K. Matyjaszewski, S. Coca, S. G. Gaynor, M. Wei, B. E. Woodworth, “Zerovalent Metals in Controlled/“Living” Radical Polymerization”, *Macromolecules* **1997**, *30*, 7348-7350.

[72] J. Gromada, K. Matyjaszewski, “Simultaneous Reverse and Normal Initiation in Atom Transfer Radical Polymerization”, *Macromolecules* **2001**, *34*, 7664-7671.

[73] W. Jakubowski, K. Matyjaszewski, “Activator Generated by Electron Transfer for Atom Transfer Radical Polymerization”, *Macromolecules* **2005**, *38*, 4139-4146.

[74] K. Min, W. Jakubowski, K. Matyjaszewski, “AGET ATRP in the Presence of Air in Miniemulsion and in Bulk”, *Macromolecular Rapid Communications* **2006**, *27*, 594-598.

[75] R. Nicolaÿ, Y. Kwak, K. Matyjaszewski, “A Green Route to Well-Defined High-Molecular-Weight (Co)polymers Using ARGET ATRP with Alkyl Pseudohalides and Copper Catalysis”, *Angewandte Chemie International Edition* **2010**, *49*, 541-544.

[76] K. Min, H. Gao, K. Matyjaszewski, “Use of Ascorbic Acid as Reducing Agent for Synthesis of Well-Defined Polymers by ARGET ATRP”, *Macromolecules* **2007**, *40*, 1789-1791.

[77] W. Jakubowski, K. Matyjaszewski, “Activators Regenerated by Electron Transfer for Atom-Transfer Radical Polymerization of (Meth)acrylates and Related Block Copolymers”, *Angewandte Chemie International Edition* **2006**, *45*, 4482-4486.

[78] Y. Gnanou, G. Hizal, “Effect of phenol and derivatives on atom transfer radical polymerization in the presence of air”, *Journal of Polymer Science Part A: Polymer Chemistry* **2004**, *42*, 351-359.

[79] K. Matyjaszewski, W. Jakubowski, K. Min, W. Tang, J. Y. Huang, W. A. Braunecker, N. V. Tsarevsky, “Diminishing catalyst concentration in atom transfer radical polymerization with reducing agents”, *Proceedings of the National Academy of Sciences of the United States of America* **2006**, *103*, 15309-15314.

[80] W. Jakubowski, K. Min, K. Matyjaszewski, “Activators regenerated by electron transfer for atom transfer radical polymerization of styrene”, *Macromolecules* **2006**, *39*, 39-45.

[81] Y. Zhang, Y. Wang, K. Matyjaszewski, “ATRP of Methyl Acrylate with Metallic Zinc, Magnesium, and Iron as Reducing Agents and Supplemental Activators”, *Macromolecules* **2011**, *44*, 683-685.

[82] A. J. D. Magenau, N. Bortolamei, E. Frick, S. Park, A. Gennaro, K. Matyjaszewski, “Investigation of Electrochemically Mediated Atom Transfer Radical Polymerization”, *Macromolecules* **2013**, *46*, 4346-4353.

[83] Y. Kwak, K. Matyjaszewski, “Photoirradiated Atom Transfer Radical Polymerization with an Alkyl Dithiocarbamate at Ambient Temperature”, *Macromolecules* **2010**, *43*, 5180-5183.

[84] M. A. Tasdelen, M. Uygun, Y. Yagci, “Photoinduced Controlled Radical Polymerization”, *Macromolecular Rapid Communications* **2011**, *32*, 58-62.

[85] I. Y. Ma, E. J. Lobb, N. C. Billingham, S. P. Armes, A. L. Lewis, A. W. Lloyd, J. Salvage, “Synthesis of Biocompatible Polymers. 1. Homopolymerization of 2-Methacryloyloxyethyl Phosphorylcholine via ATRP in Protic Solvents: An Optimization Study”, *Macromolecules* **2002**, *35*, 9306-9314.

[86] K. Matyjaszewski, T. Pintauer, S. Gaynor, “Removal of Copper-Based Catalyst in Atom Transfer Radical Polymerization Using Ion Exchange Resins”, *Macromolecules* **2000**, *33*, 1476-1478.

[87] S. Munirasu, A. Deshpande, D. Baskaran, “Hydrated Clay for Catalyst Removal in Copper Mediated Atom Transfer Radical Polymerization”, *Macromolecular Rapid Communications* **2008**, *29*, 1538-1543.

[88] A. M. Kasko, A. M. Heintz, C. Pugh, “The Effect of Molecular Architecture on the Thermotropic Behavior of Poly[11-(4‘-cyanophenyl-4‘‘-phenoxy)undecyl acrylate] and Its Relation to Polydispersity”, *Macromolecules* **1998**, *31*, 256-271.

[89] C. Granel, P. Dubois, R. Jérôme, P. Teyssié, “Controlled Radical Polymerization of Methacrylic Monomers in the Presence of a Bis(ortho-chelated) Arylnickel(II) Complex and Different Activated Alkyl Halides”, *Macromolecules* **1996**, *29*, 8576-8582.

[90] N. J. Treat, H. Sprafke, J. W. Kramer, P. G. Clark, B. E. Barton, J. Read de Alaniz, B. P. Fors, C. J. Hawker, “Metal-Free Atom Transfer Radical Polymerization”, *Journal of the American Chemical Society* **2014**, *136*, 16096-16101.

[91] X. Pan, M. Lamson, J. Yan, K. Matyjaszewski, “Photoinduced Metal-Free Atom Transfer Radical Polymerization of Acrylonitrile”, *ACS Macro Letters* **2015**, *4*, 192-196.

[92] X. D. Liu, L. F. Zhang, Z. P. Cheng, X. L. Zhu, “Metal-free photoinduced electron transfer-atom transfer radical polymerization (PET-ATRP) via a visible light organic photocatalyst”, *Polymer Chemistry* **2016**, *7*, 689-700.

[93] C. Aydogan, G. Yilmaz, Y. Yagci, “Synthesis of Hyperbranched Polymers by Photoinduced Metal-Free ATRP”, *Macromolecules* **2017**, *50*, 9115-9120.

[94] K. Min, H. F. Gao, K. Matyjaszewski, “Preparation of homopolymers and block copolymers in miniemulsion by ATRP using activators generated by electron transfer (AGET)”, *Journal of the American Chemical Society* **2005**, *127*, 3825-3830.

[95] P. Krys, M. Fantin, P. V. Mendonca, C. M. R. Abreu, T. Guliashvili, J. Rosa, L. O. Santos, A. C. Serra, K. Matyjaszewski, J. F. J. Coelho, “Mechanism of supplemental activator and reducing agent atom transfer radical polymerization mediated by inorganic sulfites: experimental measurements and kinetic simulations”, *Polymer Chemistry* **2017**, *8*, 6506-6519.

[96] M. A. Tasdelen, M. Uygun, Y. Yagci, “Studies on Photoinduced ATRP in the Presence of Photoinitiator”, *Macromolecular Chemistry and Physics* **2011**, *212*, 2036-2042.

[97] G. M. Miyake, J. C. Theriot, “Perylene as an Organic Photocatalyst for the Radical Polymerization of Functionalized Vinyl Monomers through Oxidative Quenching with Alkyl Bromides and Visible Light”, *Macromolecules* **2014**, *47*, 8255-8261.

[98] J. C. Theriot, G. M. Miyake, C. A. Boyer, “N,N-Diaryl Dihydrophenazines as Photoredox Catalysts for PET-RAFT and Sequential PET-RAFT/O-ATRP”, *ACS Macro Letters* **2018**, *7*, 662-666.

[99] C. Decker, “Photoinitiated crosslinking polymerisation”, *Progress in Polymer Science* **1996**, *21*, 593-650.

[100] M. A. Tasdelen, M. Uygun, Y. Yagci, “Photoinduced Controlled Radical Polymerization in Methanol”, *Macromolecular Chemistry and Physics* **2010**, *211*, 2271-2275.

[101] F. Mauguiere-Guyonnet, D. Burget, J. P. Fouassier, “Photopolymerization of wood coatings under visible lights”, *Progress in Organic Coatings* **2006**, *57*, 23-32.

[102] K. Nakamura, Photopolymers: Photoresist Materials, Processes, and Applications, Taylor & Francis, **2014**.

[103] H. Wang, L. Ma, B. Yang, W. Zhang, B. Huang, X. Wei, in *Advances in Graphic Communication, Printing and Packaging* (Eds.: P. Zhao, Y. Ouyang, M. Xu, L. Yang, Y. Ren), Springer Singapore, Singapore, **2019**, pp. 769-777.

[104] K. Dean, W. D. Cook, "Effect of Curing Sequence on the Photopolymerization and Thermal Curing Kinetics of Dimethacrylate/Epoxy Interpenetrating Polymer Networks", *Macromolecules* **2002**, *35*, 7942-7954.

[105] L. Lu, N. Yang, Y. Cai, "Well-controlled reversible addition–fragmentation chain transfer radical polymerisation under ultraviolet radiation at ambient temperature", *Chemical Communications* **2005**, 5287-5288.

[106] C. Dietlin, S. Schweizer, P. Xiao, J. Zhang, F. Morlet-Savary, B. Graff, J.-P. Fouassier, J. Lalevée, "Photopolymerization upon LEDs: new photoinitiating systems and strategies", *Polymer Chemistry* **2015**, *6*, 3895-3912.

[107] J. Kindernay, A. Blažková, J. Rudá, V. Jančovičová, Z. Jakubíková, "Effect of UV light source intensity and spectral distribution on the photopolymerisation reactions of a multifunctional acrylated monomer", *Journal of Photochemistry and Photobiology A: Chemistry* **2002**, *151*, 229-236.

[108] T. Otsu, M. Yoshida, T. Tazaki, "A Model for Living Radical Polymerization", *Makromolekulare Chemie-Rapid Communications* **1982**, *3*, 133-140.

[109] K. Koumura, K. Satoh, M. Kamigaito, "Manganese-Based Controlled/Living Radical Polymerization of Vinyl Acetate, Methyl Acrylate, and Styrene: Highly Active, Versatile, and Photoresponsive Systems", *Macromolecules* **2008**, *41*, 7359-7367.

[110] Z. B. Guan, B. Smart, "A remarkable visible light effect on atom-transfer radical polymerization", *Macromolecules* **2000**, *33*, 6904-6906.

[111] S. Telitel, F. Dumur, S. Telitel, O. Soppera, M. Lepeltier, Y. Guillaneuf, J. Poly, F. Morlet-Savary, P. Fioux, J.-P. Fouassier, D. Gigmes, J. Lalevée, "Photoredox catalysis using a new iridium complex as an efficient toolbox for radical, cationic and controlled polymerizations under soft blue to green lights", *Polymer Chemistry* **2015**, *6*, 613-624.

[112] M. Ciftci, M. A. Tasdelen, Y. Yagci, "Sunlight induced atom transfer radical polymerization by using dimanganese decacarbonyl", *Polymer Chemistry* **2014**, *5*, 600-606.

[113] X. Pan, N. Malhotra, A. Simakova, Z. Wang, D. Konkolewicz, K. Matyjaszewski, "Photoinduced Atom Transfer Radical Polymerization with ppm-Level Cu Catalyst

by Visible Light in Aqueous Media", *Journal of the American Chemical Society* **2015**, *137*, 15430-15433.

[114] S. Dadashi-Silab, M. Atilla Tasdelen, Y. Yagci, "Photoinitiated atom transfer radical polymerization: Current status and future perspectives", *Journal of Polymer Science Part A: Polymer Chemistry* **2014**, *52*, 2878-2888.

[115] M. Uo, E. Kudo, A. Okada, K. Soga, Y. Jogo, "Preparation and Properties of Dental Composite Resin Cured under Near Infrared Irradiation", *Journal of Photopolymer Science and Technology* **2009**, *22*, 551-554.

[116] H. Zhang, D. Salo, D. M. Kim, S. Komarov, Y.-C. Tai, M. Y. Berezin, "Penetration depth of photons in biological tissues from hyperspectral imaging in shortwave infrared in transmission and reflection geometries", *Journal of biomedical optics* **2016**, *21*, 126006-126006.

[117] Q. Xiao, Y. Ji, Z. Xiao, Y. Zhang, H. Lin, Q. Wang, "Novel multifunctional NaYF4:Er3+,Yb3+/PEGDA hybrid microspheres: NIR-light-activated photopolymerization and drug delivery", *Chemical Communications* **2013**, *49*, 1527-1529.

[118] Z. Chen, X. Wang, S. Li, S. Liu, H. Miao, S. Wu, "Near-Infrared Light Driven Photopolymerization Based On Photon Upconversion", *ChemPhotoChem* **2019**, *3*, 1077-1083.

[119] C. Kütahya, C. Schmitz, V. Strehmel, Y. Yagci, B. Strehmel, "Near-Infrared Sensitized Photoinduced Atom-Transfer Radical Polymerization (ATRP) with a Copper(II) Catalyst Concentration in the ppm Range", *Angewandte Chemie International Edition* **2018**, *57*, 7898-7902.

[120] S. H. Qin, D. Q. Qin, K. Y. Qiu, "A novel photo atom transfer radical polymerization of methyl methacrylate", *New Journal of Chemistry* **2001**, *25*, 893-895.

[121] J. Mosnacek, M. Ilcikova, "Photochemically Mediated Atom Transfer Radical Polymerization of Methyl Methacrylate Using ppm Amounts of Catalyst", *Macromolecules* **2012**, *45*, 5859-5865.

[122] D. Konkolewicz, K. Schroder, J. Buback, S. Bernhard, K. Matyjaszewski, "Visible Light and Sunlight Photoinduced ATRP with ppm of Cu Catalyst", *ACS Macro Letters* **2012**, *1*, 1219-1223.

[123] J. K. Fink, Reactive Polymers: Fundamentals and Applications: A Concise Guide to Industrial Polymers, Elsevier Science, **2017**.

[124] N. Wu, Y. Zhang, Y. Wang, “Photo-polymerization efficiency of self-etch dental adhesives composed of camphorquinone or trimethylbenzoyl-diphenyl-phosphine oxide”, *International Journal of Adhesion and Adhesives* **2013**, *45*, 53-58.

[125] K. Kaeriyama, Y. Shimura, “Photopolymerization with the use of titanocene dichoride as sensitizer”, *Journal of Polymer Science Part A-1: Polymer Chemistry* **1972**, *10*, 2833-2840.

[126] S. Protti, M. Fagnoni, “The sunny side of chemistry: green synthesis by solar light”, *Photochemical & Photobiological Sciences* **2009**, *8*, 1499-1516.

[127] K. Hayase, R. G. Zepp, “Photolysis of copper(II)-amino acid complexes in water”, *Environmental Science & Technology* **1991**, *25*, 1273-1279.

[128] S. Giuffrida, G. G. Condorelli, L. L. Costanzo, I. L. Fragalà, G. Ventimiglia, G. Vecchio, “Photochemical Mechanism of the Formation of Nanometer-Sized Copper by UV Irradiation of Ethanol Bis(2,4-pentandionato)copper(II) Solutions”, *Chemistry of Materials* **2004**, *16*, 1260-1266.

[129] O. S. Taskin, G. Yilmaz, M. A. Tasdelen, Y. Yagci, “Photoinduced reverse atom transfer radical polymerization of methyl methacrylate using camphorquinone/ benzhydrol system”, *Polymer International* **2014**, *63*, 902-907.

[130] T. Gong, B. J. Adzima, C. N. Bowman, “A novel copper containing photoinitiator, copper(ii) acylphosphinate, and its application in both the photomediated CuAAC reaction and in atom transfer radical polymerization”, *Chemical Communications* **2013**, *49*, 7950-7952.

[131] J. F. Lutz, “Copper-free azide-alkyne cycloadditions: New insights and perspectives”, *Angewandte Chemie-International Edition* **2008**, *47*, 2182-2184.

[132] E. H. Discekici, A. Anastasaki, J. Read de Alaniz, C. J. Hawker, “Evolution and Future Directions of Metal-Free Atom Transfer Radical Polymerization”, *Macromolecules* **2018**, *51*, 7421-7434.

[133] N. J. Treat, H. Sprafke, J. W. Kramer, P. G. Clark, B. E. Barton, J. R. de Alaniz, B. P. Fors, C. J. Hawker, “Metal-Free Atom Transfer Radical Polymerization”, *Journal of the American Chemical Society* **2014**, *136*, 16096-16101.

[134] X. C. Pan, C. Fang, M. Fantin, N. Malhotra, W. Y. So, L. A. Peteanu, A. A. Isse, A. Gennaro, P. Liu, K. Matyjaszewskit, “Mechanism of Photoinduced Metal-Free Atom Transfer Radical Polymerization: Experimental and Computational Studies”, *Journal of the American Chemical Society* **2016**, *138*, 2411-2425.

[135] S. Dadashi-Silab, X. Pan, K. Matyjaszewski, “Phenyl Benzo[b]phenothiazine as a Visible Light Photoredox Catalyst for Metal-Free Atom Transfer Radical Polymerization”, *Chemistry – A European Journal* **2017**, *23*, 5972-5977.

[136] A. Allushi, S. Jockusch, G. Yilmaz, Y. Yagci, “Photoinitiated Metal-Free Controlled/ Living Radical Polymerization Using Polynuclear Aromatic Hydrocarbons”, *Macromolecules* **2016**, *49*, 7785-7792.

[137] C.-H. Lim, M. D. Ryan, B. G. McCarthy, J. C. Theriot, S. M. Sartor, N. H. Damrauer, C. B. Musgrave, G. M. Miyake, “Intramolecular Charge Transfer and Ion Pairing in N,N-Diaryl Dihydrophenazine Photoredox Catalysts for Efficient Organocatalyzed Atom Transfer Radical Polymerization”, *Journal of the American Chemical Society* **2017**, *139*, 348-355.

[138] R. M. Pearson, C.-H. Lim, B. G. McCarthy, C. B. Musgrave, G. M. Miyake, “Organocatalyzed Atom Transfer Radical Polymerization Using N-Aryl Phenoxazines as Photoredox Catalysts”, *Journal of the American Chemical Society* **2016**, *138*, 11399-11407.

[139] J. C. Theriot, C. H. Lim, H. Yang, M. D. Ryan, C. B. Musgrave, G. M. Miyake, “Organocatalyzed atom transfer radical polymerization driven by visible light”, *Science* **2016**, *352*, 1082-1086.

[140] C. Kutahya, A. Allushi, R. Isci, J. Kreutzer, T. Ozturk, G. Yilmaz, Y. Yagci, “Photoinduced Metal-Free Atom Transfer Radical Polymerization Using Highly Conjugated Thienothiophene Derivatives”, *Macromolecules* **2017**, *50*, 6903-6910.

[141] C. Kutahya, F. S. Aykac, G. Yilmaz, Y. Yagci, “LED and visible light-induced metal free ATRP using reducible dyes in the presence of amines”, *Polymer Chemistry* **2016**, *7*, 6094-6098.

[142] X. Liu, L. Zhang, Z. Cheng, X. Zhu, “Metal-free photoinduced electron transfer–atom transfer radical polymerization (PET–ATRP) via a visible light organic photocatalyst”, *Polymer Chemistry* **2016**, *7*, 689-700.

[143] G. Yilmaz, Y. Yagci, “Photoinduced metal-free atom transfer radical polymerizations: state-of-the-art, mechanistic aspects and applications”, *Polymer Chemistry* **2018**, *9*, 1757-1762.

[144] H. C. Kolb, M. G. Finn, K. B. Sharpless, “Click Chemistry: Diverse Chemical Function from a Few Good Reactions”, *Angewandte Chemie International Edition* **2001**, *40*, 2004-2021.

[145] H. C. Kolb, K. B. Sharpless, “The growing impact of click chemistry on drug discovery”, *Drug Discovery Today* **2003**, *8*, 1128-1137.

[146] W. H. Binder, R. Sachsenhofer, "'Click' Chemistry in Polymer and Materials Science", *Macromolecular Rapid Communications* **2007**, *28*, 15-54.

[147] in Click Reactions in Organic Synthesis, pp. 77-97.

[148] V. V. Rostovtsev, L. G. Green, V. V. Fokin, K. B. Sharpless, "A Stepwise Huisgen Cycloaddition Process: Copper(I)-Catalyzed Regioselective "Ligation" of Azides and Terminal Alkynes", *Angewandte Chemie International Edition* **2002**, *41*, 2596-2599.

[149] M. Meldal, C. W. Tornøe, "Cu-Catalyzed Azide−Alkyne Cycloaddition", *Chemical Reviews* **2008**, *108*, 2952-3015.

[150] G. Franc, A. K. Kakkar, "Diels–Alder "Click" Chemistry in Designing Dendritic Macromolecules", *Chemistry – A European Journal* **2009**, *15*, 5630-5639.

[151] A. Sanyal, "Diels–Alder Cycloaddition-Cycloreversion: A Powerful Combo in Materials Design", *Macromolecular Chemistry and Physics* **2010**, *211*, 1417-1425.

[152] G. Hizal, U. Tunca, A. Sanyal, "Discrete macromolecular constructs via the Diels–Alder "Click" reaction", *Journal of Polymer Science Part A: Polymer Chemistry* **2011**, *49*, 4103-4120.

[153] M. A. Tasdelen, "Diels–Alder "click" reactions: recent applications in polymer and material science", *Polymer Chemistry* **2011**, *2*, 2133-2145.

[154] N. B. Cramer, J. P. Scott, C. N. Bowman, "Photopolymerizations of Thiol−Ene Polymers without Photoinitiators", *Macromolecules* **2002**, *35*, 5361-5365.

[155] L. M. Campos, K. L. Killops, R. Sakai, J. M. J. Paulusse, D. Damiron, E. Drockenmuller, B. W. Messmore, C. J. Hawker, "Development of Thermal and Photochemical Strategies for Thiol−Ene Click Polymer Functionalization", *Macromolecules* **2008**, *41*, 7063-7070.

[156] K. L. Killops, L. M. Campos, C. J. Hawker, "Robust, Efficient, and Orthogonal Synthesis of Dendrimers via Thiol-ene "Click" Chemistry", *Journal of the American Chemical Society* **2008**, *130*, 5062-5064.

[157] C. Syldatk, S. Lang, F. Wagner, V. Wray, L. Witte, in *Zeitschrift für Naturforschung C, Vol. 40*, **1985**, p. 51.

[158] W. H. Binder, R. Sachsenhofer, "'Click' Chemistry in Polymer and Material Science: An Update", *Macromolecular Rapid Communications* **2008**, *29*, 952-981.

[159] J. Lahann, Click Chemistry for Biotechnology and Materials Science, Wiley, **2009**.

[160] Craig S. McKay, M. G. Finn, "Click Chemistry in Complex Mixtures: Bioorthogonal Bioconjugation", *Chemistry & Biology* **2014**, *21*, 1075-1101.

[161] O. Diels, K. Alder, “Synthesen in der hydroaromatischen Reihe”, *Justus Liebigs Annalen der Chemie* **1928**, *460*, 98-122.

[162] J. L. Ripoll, A. Rouessac, F. Rouessac, “Applications recentes de la reaction de retro-diels-alder en synthese organique”, *Tetrahedron* **1978**, *34*, 19-40.

[163] G. Mantovani, F. Lecolley, L. Tao, D. M. Haddleton, J. Clerx, J. J. L. M. Cornelissen, K. Velonia, “Design and Synthesis of N-Maleimido-Functionalized Hydrophilic Polymers via Copper-Mediated Living Radical Polymerization: A Suitable Alternative to PEGylation Chemistry”, *Journal of the American Chemical Society* **2005**, *127*, 2966-2973.

[164] W. H. Binder, C. Kluger, “Combining Ring-Opening Metathesis Polymerization (ROMP) with Sharpless-Type “Click” Reactions: An Easy Method for the Preparation of Side Chain Functionalized Poly(oxynorbornenes)”, *Macromolecules* **2004**, *37*, 9321-9330.

[165] H. Durmaz, A. Dag, A. Hizal, G. Hizal, U. Tunca, “One-pot synthesis of star-block copolymers using double click reactions”, *Journal of Polymer Science Part A: Polymer Chemistry* **2008**, *46*, 7091-7100.

[166] P. S. Omurtag, U. S. Gunay, A. Dag, H. Durmaz, G. Hizal, U. Tunca, “Diels-alder click reaction for the preparation of polycarbonate block copolymers”, *Journal of Polymer Science Part A: Polymer Chemistry* **2013**, *51*, 2252-2259.

[167] S. Sinnwell, C. V. Synatschke, T. Junkers, M. H. Stenzel, C. Barner-Kowollik, “A Study into the Stability of 3,6-Dihydro-2H-thiopyran Rings: Key Linkages in the RAFT Hetero-Diels−Alder Click Concept”, *Macromolecules* **2008**, *41*, 7904-7912.

[168] L. Nebhani, S. Sinnwell, C. Y. Lin, M. L. Coote, M. H. Stenzel, C. Barner-Kowollik, “Strongly electron deficient sulfonyldithioformate based RAFT agents for hetero Diels-Alder conjugation: Computational design and experimental evaluation”, *Journal of Polymer Science Part A: Polymer Chemistry* **2009**, *47*, 6053-6071.

[169] B. Gacal, H. Durmaz, M. A. Tasdelen, G. Hizal, U. Tunca, Y. Yagci, A. L. Demirel, “Anthracene−Maleimide-Based Diels−Alder “Click Chemistry” as a Novel Route to Graft Copolymers”, *Macromolecules* **2006**, *39*, 5330-5336.

[170] A. Dag, H. Durmaz, E. Demir, G. Hizal, U. Tunca, “Heterograft copolymers via double click reactions using one-pot technique”, *Journal of Polymer Science Part A: Polymer Chemistry* **2008**, *46*, 6969-6977.

[171] A. A. Kavitha, N. K. Singha, ““Click Chemistry” in Tailor-Made Polymethacrylates Bearing Reactive Furfuryl Functionality: A New Class of Self-Healing Polymeric Material”, *ACS Applied Materials & Interfaces* **2009**, *1*, 1427-1436.

[172] H.-L. Wei, Z. Yang, L.-M. Zheng, Y.-M. Shen, “Thermosensitive hydrogels synthesized by fast Diels–Alder reaction in water”, *Polymer* **2009**, *50*, 2836-2840.

[173] C. Goussé, A. Gandini, “Synthesis of 2-furfurylmaleimide and preliminary study of its Diels-Alder polycondensation”, *Polymer Bulletin* **1998**, *40*, 389-394.

[174] B. J. Adzima, H. A. Aguirre, C. J. Kloxin, T. F. Scott, C. N. Bowman, “Rheological and chemical analysis of reverse gelation in a covalently crosslinked Diels-Alder polymer network”, *Macromolecules* **2008**, *41*, 9112-9117.

[175] K. Inoue, M. Yamashiro, M. Iji, “Recyclable shape-memory polymer: Poly(lactic acid) crosslinked by a thermoreversible Diels–Alder reaction”, *Journal of Applied Polymer Science* **2009**, *112*, 876-885.

[176] S. Magana, A. Zerroukhi, C. Jegat, N. Mignard, “Thermally reversible crosslinked polyethylene using Diels–Alder reaction in molten state”, *Reactive and Functional Polymers* **2010**, *70*, 442-448.

[177] S. Huang, J. Luo, Z. Jin, X.-H. Zhou, Z. Shi, A. K. Y. Jen, “Enhanced temporal stability of a highly efficient guest–host electro-optic polymer through a barrier layer assisted poling process”, *Journal of Materials Chemistry* **2012**, *22*, 20353-20357.

[178] W. H. Heath, F. Palmieri, J. R. Adams, B. K. Long, J. Chute, T. W. Holcombe, S. Zieren, M. J. Truitt, J. L. White, C. G. Willson, “Degradable Cross-Linkers and Strippable Imaging Materials for Step-and-Flash Imprint Lithography”, *Macromolecules* **2008**, *41*, 719-726.

[179] J. A. Syrett, G. Mantovani, W. R. S. Barton, D. Price, D. M. Haddleton, “Self-healing polymers prepared via living radical polymerisation”, *Polymer Chemistry* **2010**, *1*, 102-106.

[180] A. M. Peterson, R. E. Jensen, G. R. Palmese, “Reversibly Cross-Linked Polymer Gels as Healing Agents for Epoxy−Amine Thermosets”, *ACS Applied Materials & Interfaces* **2009**, *1*, 992-995.

[181] C. Toncelli, D. C. De Reus, F. Picchioni, A. A. Broekhuis, “Properties of Reversible Diels–Alder Furan/Maleimide Polymer Networks as Function of Crosslink Density”, *Macromolecular Chemistry and Physics* **2012**, *213*, 157-165.

[182] J. W. Chan, C. E. Hoyle, A. B. Lowe, M. Bowman, “Nucleophile-Initiated Thiol-Michael Reactions: Effect of Organocatalyst, Thiol, and Ene”, *Macromolecules* **2010**, *43*, 6381-6388.

[183] M. J. Kade, D. J. Burke, C. J. Hawker, “The power of thiol-ene chemistry”, *Journal of Polymer Science Part A: Polymer Chemistry* **2010**, *48*, 743-750.

[184] A. B. Lowe, “Thiol-ene “click” reactions and recent applications in polymer and materials synthesis”, *Polymer Chemistry* **2010**, *1*, 17-36.

[185] A. B. Lowe, C. E. Hoyle, C. N. Bowman, “Thiol-yne click chemistry: A powerful and versatile methodology for materials synthesis”, *Journal of Materials Chemistry* **2010**, *20*, 4745-4750.

[186] R. M. Hensarling, S. B. Rahane, A. P. LeBlanc, B. J. Sparks, E. M. White, J. Locklin, D. L. Patton, “Thiol–isocyanate “click” reactions: rapid development of functional polymeric surfaces”, *Polymer Chemistry* **2011**, *2*, 88-90.

[187] J. Xu, L. Tao, C. Boyer, A. B. Lowe, T. P. Davis, “Combining Thio−Bromo “Click” Chemistry and RAFT Polymerization: A Powerful Tool for Preparing Functionalized Multiblock and Hyperbranched Polymers”, *Macromolecules* **2010**, *43*, 20-24.

[188] C. R. Morgan, F. Magnotta, A. D. Ketley, “Thiol/ene photocurable polymers”, *Journal of Polymer Science: Polymer Chemistry Edition* **1977**, *15*, 627-645.

[189] A. B. Lowe, “Thiol–ene “click” reactions and recent applications in polymer and materials synthesis: a first update”, *Polymer Chemistry* **2014**, *5*, 4820-4870.

[190] A. F. Senyurt, H. Wei, C. E. Hoyle, S. G. Piland, T. E. Gould, “Ternary Thiol−Ene/ Acrylate Photopolymers: Effect of Acrylate Structure on Mechanical Properties”, *Macromolecules* **2007**, *40*, 4901-4909.

[191] L. M. Campos, I. Meinel, R. G. Guino, M. Schierhorn, N. Gupta, G. D. Stucky, C. J. Hawker, “Highly Versatile and Robust Materials for Soft Imprint Lithography Based on Thiol-ene Click Chemistry”, *Advanced Materials* **2008**, *20*, 3728-3733.

[192] F. Jivan, R. Yegappan, H. Pearce, J. K. Carrow, M. McShane, A. K. Gaharwar, D. L. Alge, “Sequential Thiol–Ene and Tetrazine Click Reactions for the Polymerization and Functionalization of Hydrogel Microparticles”, *Biomacromolecules* **2016**, *17*, 3516-3523.

[193] A. Dondoni, “The Emergence of Thiol–Ene Coupling as a Click Process for Materials and Bioorganic Chemistry”, *Angewandte Chemie International Edition* **2008**, *47*, 8995-8997.

[194] C. E. Hoyle, C. N. Bowman, “Thiol–Ene Click Chemistry”, *Angewandte Chemie International Edition* **2010**, *49*, 1540-1573.

[195] P. Wu, V. V. Fokin, “Catalytic azide-alkyne cycloaddition: Reactivity and applications”, *Aldrichimica Acta* **2007**, *40*, 7-17.

[196] C. W. Tornøe, C. Christensen, M. Meldal, “Peptidotriazoles on Solid Phase: [1,2,3]-Triazoles by Regiospecific Copper(I)-Catalyzed 1,3-Dipolar Cycloadditions

of Terminal Alkynes to Azides", *The Journal of Organic Chemistry* **2002**, *67*, 3057-3064.

[197] J.-F. Lutz, "1,3-Dipolar Cycloadditions of Azides and Alkynes: A Universal Ligation Tool in Polymer and Materials Science", *Angewandte Chemie International Edition* **2007**, *46*, 1018-1025.

[198] V. D. Bock, H. Hiemstra, J. H. van Maarseveen, "CuI-Catalyzed Alkyne–Azide "Click" Cycloadditions from a Mechanistic and Synthetic Perspective", *European Journal of Organic Chemistry* **2006**, *2006*, 51-68.

[199] M. H. B. Stowell, T. M. McPhillips, D. C. Rees, S. M. Soltis, E. Abresch, G. Feher, "Light-Induced Structural Changes in Photosynthetic Reaction Center: Implications for Mechanism of Electron-Proton Transfer", *Science* **1997**, *276*, 812.

[200] N. K. Devaraj, P. H. Dinolfo, C. E. D. Chidsey, J. P. Collman, "Selective Functionalization of Independently Addressed Microelectrodes by Electrochemical Activation and Deactivation of a Coupling Catalyst", *Journal of the American Chemical Society* **2006**, *128*, 1794-1795.

[201] V. Hong, A. K. Udit, R. A. Evans, M. G. Finn, "Electrochemically Protected Copper(I)-Catalyzed Azide–Alkyne Cycloaddition", *ChemBioChem* **2008**, *9*, 1481-1486.

[202] Y. Wang, W. Song, W. J. Hu, Q. Lin, "Fast Alkene Functionalization In Vivo by Photoclick Chemistry: HOMO Lifting of Nitrile Imine Dipoles", *Angewandte Chemie International Edition* **2009**, *48*, 5330-5333.

[203] S. V. Orski, A. A. Poloukhtine, S. Arumugam, L. Mao, V. V. Popik, J. Locklin, "High Density Orthogonal Surface Immobilization via Photoactivated Copper-Free Click Chemistry", *Journal of the American Chemical Society* **2010**, *132*, 11024-11026.

[204] A. Kuzmin, A. Poloukhtine, M. A. Wolfert, V. V. Popik, "Surface Functionalization Using Catalyst-Free Azide−Alkyne Cycloaddition", *Bioconjugate Chemistry* **2010**, *21*, 2076-2085.

[205] Y. Y. Durmaz, V. Kumbaraci, A. L. Demirel, N. Talinli, Y. Yagci, "Graft Copolymers by the Combination of ATRP and Photochemical Acylation Process by Using Benzodioxinones", *Macromolecules* **2009**, *42*, 3743-3749.

[206] S. Arumugam, V. V. Popik, "Light-Induced Hetero-Diels−Alder Cycloaddition: A Facile and Selective Photoclick Reaction", *Journal of the American Chemical Society* **2011**, *133*, 5573-5579.

[207] B. J. Adzima, Y. Tao, C. J. Kloxin, C. A. DeForest, K. S. Anseth, C. N. Bowman, “Spatial and temporal control of the alkyne–azide cycloaddition by photoinitiated Cu(II) reduction”, *Nature Chemistry* **2011**, *3*, 256-259.

[208] S. Dadashi-Silab, B. Kiskan, M. Antonietti, Y. Yagci, “Mesoporous graphitic carbon nitride as a heterogeneous catalyst for photoinduced copper(i)-catalyzed azide–alkyne cycloaddition”, *RSC Advances* **2014**, *4*, 52170-52173.

[209] Y. Yagci, M. A. Tasdelen, S. Jockusch, “Reduction of Cu(II) by photochemically generated phosphonyl radicals to generate Cu(I) as catalyst for atom transfer radical polymerization and azide-alkyne cycloaddition click reactions”, *Polymer* **2014**, *55*, 3468-3474.

[210] G. Yilmaz, B. Iskin, Y. Yagci, “Photoinduced Copper(I)-Catalyzed Click Chemistry by the Electron Transfer Process Using Polynuclear Aromatic Compounds”, *Macromolecular Chemistry and Physics* **2014**, *215*, 662-668.

[211] M. Arslan, G. Yilmaz, Y. Yagci, “Dibenzoyldiethylgermane as a visible light photo-reducing agent for CuAAC click reactions”, *Polymer Chemistry* **2015**, *6*, 8168-8175.

[212] M. A. Tasdelen, Y. Yagci, “Light-Induced Click Reactions”, *Angewandte Chemie International Edition* **2013**, *52*, 5930-5938.

[213] S. Shanmugam, J. Xu, C. Boyer, “Light-Regulated Polymerization under Near-Infrared/Far-Red Irradiation Catalyzed by Bacteriochlorophyll a”, *Angewandte Chemie International Edition* **2016**, *55*, 1036-1040.

[214] S. Wu, H.-J. Butt, “Near-Infrared-Sensitive Materials Based on Upconverting Nanoparticles”, *Advanced Materials* **2016**, *28*, 1208-1226.

[215] X. Meng, H. Lu, Z. Li, C. Wang, R. Liu, X. Guan, Y. Yagci, “Near-infrared light induced cationic polymerization based on upconversion and ferrocenium photochemistry”, *Polymer Chemistry* **2019**, *10*, 5574-5577.

[216] J. S. Katz, J. A. Burdick, “Light-Responsive Biomaterials: Development and Applications”, *Macromolecular Bioscience* **2010**, *10*, 339-348.

[217] C. Wang, H. Tao, L. Cheng, Z. Liu, “Near-infrared light induced in vivo photodynamic therapy of cancer based on upconversion nanoparticles”, *Biomaterials* **2011**, *32*, 6145-6154.

[218] W. Wu, L. Yao, T. Yang, R. Yin, F. Li, Y. Yu, “NIR-Light-Induced Deformation of Cross-Linked Liquid-Crystal Polymers Using Upconversion Nanophosphors”, *Journal of the American Chemical Society* **2011**, *133*, 15810-15813.

[219] S. Zhang, B. Li, L. Tang, X. Wang, D. Liu, Q. Zhou, “Studies on the near infrared laser induced photopolymerization employing a cyanine dye–borate complex as the photoinitiator”, *Polymer* **2001**, *42*, 7575-7582.

[220] T. Brömme, D. Oprych, J. Horst, P. S. Pinto, B. Strehmel, “New iodonium salts in NIR sensitized radical photopolymerization of multifunctional monomers”, *RSC Advances* **2015**, *5*, 69915-69924.

[221] A. Shiraishi, H. Kimura, D. Oprych, C. Schmitz, B. Strehmel, “Comparison between NIR and UV-Sensitized Radical and Cationic Reactivity of Iodonium Salts Comprising Anions with Different Coordination Behavior”, *Journal of Photopolymer Science and Technology* **2017**, *30*, 633-638.

[222] A. H. Bonardi, F. Dumur, T. M. Grant, G. Noirbent, D. Gigmes, B. H. Lessard, J. P. Fouassier, J. Lalevée, “High Performance Near-Infrared (NIR) Photoinitiating Systems Operating under Low Light Intensity and in the Presence of Oxygen”, *Macromolecules* **2018**, *51*, 1314-1324.

[223] M. Haase, H. Schäfer, “Upconverting Nanoparticles”, *Angewandte Chemie International Edition* **2011**, *50*, 5808-5829.

[224] J. Zhou, Q. Liu, W. Feng, Y. Sun, F. Li, “Upconversion Luminescent Materials: Advances and Applications”, *Chemical Reviews* **2015**, *115*, 395-465.

[225] R. Liu, H. Chen, Z. Li, F. Shi, X. Liu, “Extremely deep photopolymerization using upconversion particles as internal lamps”, *Polymer Chemistry* **2016**, *7*, 2457-2463.

[226] Z. Chen, D. Oprych, C. Xie, C. Kutahya, S. Wu, B. Strehmel, “Upconversion-Nanoparticle-Assisted Radical Polymerization at λ=974 nm and the Generation of Acidic Cations”, *ChemPhotoChem* **2017**, *1*, 499-503.

[227] Z. Li, H. Chen, C. Wang, L. Chen, J. Liu, R. Liu, “Efficient photopolymerization of thick pigmented systems using upconversion nanoparticles-assisted photochemistry”, *Journal of Polymer Science Part A: Polymer Chemistry* **2018**, *56*, 994-1002.

[228] V. V. Rocheva, A. V. Koroleva, A. G. Savelyev, K. V. Khaydukov, A. N. Generalova, A. V. Nechaev, A. E. Guller, V. A. Semchishen, B. N. Chichkov, E. V. Khaydukov, “High-resolution 3D photopolymerization assisted by upconversion nanoparticles for rapid prototyping applications”, *Scientific Reports* **2018**, *8*, 3663.

[229] Z. Li, X. Zou, R. Liu, Z. Li, R. Liu, Y. Yagci, F. Shi, Y. Yagci, “Highly efficient dandelion-like near-infrared light photoinitiator for free radical and thiol-ene photopolymerizations”, *Nat Commun* **2019**, *10*, 3560.

[230] D. Oprych, C. Schmitz, C. Ley, X. Allonas, E. Ermilov, R. Erdmann, B. Strehmel, “Photophysics of Up-Conversion Nanoparticles: Radical Photopolymerization of Multifunctional Methacrylates Comprising Blue- and UV-Sensitive Photoinitiators”, *ChemPhotoChem* **2019**, *3*, 1119-1126.

[231] D. Yang, P. a. Ma, Z. Hou, Z. Cheng, C. Li, J. Lin, “Current advances in lanthanide ion (Ln3+)-based upconversion nanomaterials for drug delivery”, *Chemical Society Reviews* **2015**, *44*, 1416-1448.

[232] Z. Chen, S. He, H.-J. Butt, S. Wu, “Photon Upconversion Lithography: Patterning of Biomaterials Using Near-Infrared Light”, *Advanced Materials* **2015**, *27*, 2203-2206.

[233] Z. Chen, L. Zhou, W. Bing, Z. Zhang, Z. Li, J. Ren, X. Qu, “Light Controlled Reversible Inversion of Nanophosphor-Stabilized Pickering Emulsions for Biphasic Enantioselective Biocatalysis”, *Journal of the American Chemical Society* **2014**, *136*, 7498-7504.

[234] R. Liu, X. Zou, Y. Xu, X. Liu, Z. Li, “Deep Thiol-ene Photopolymerization Using Upconversion Nanoparticle-assisted Photochemistry”, *Chemistry Letters* **2016**, *45*, 1054-1056.

[235] C. Ding, J. Wang, W. Zhang, X. Pan, Z. Zhang, W. Zhang, J. Zhu, X. Zhu, “Platform of near-infrared light-induced reversible deactivation radical polymerization: upconversion nanoparticles as internal light sources”, *Polymer Chemistry* **2016**, *7*, 7370-7374.

[236] A. Kocaarslan, S. Tabanli, G. Eryurek, Y. Yagci, “Near-Infrared Free-Radical and Free-Radical-Promoted Cationic Photopolymerizations by In-Source Lighting Using Upconverting Glass”, *Angewandte Chemie International Edition* **2017**, *56*, 14507-14510.

[237] Z. Li, J. Zhu, X. Guan, R. Liu, Y. Yagci, “Near-Infrared-Induced Cationic Polymerization Initiated by Using Upconverting Nanoparticles and Titanocene”, *Macromolecular Rapid Communications* **2019**, *40*, 1900047.

[238] S. Beyazit, S. Ambrosini, N. Marchyk, E. Palo, V. Kale, T. Soukka, B. Tse Sum Bui, K. Haupt, “Versatile Synthetic Strategy for Coating Upconverting Nanoparticles with Polymer Shells through Localized Photopolymerization by Using the Particles as Internal Light Sources”, *Angewandte Chemie International Edition* **2014**, *53*, 8919-8923.

[239] A. Bagheri, Z. Sadrearhami, N. N. M. Adnan, C. Boyer, M. Lim, “Surface functionalization of upconversion nanoparticles using visible light-mediated polymerization”, *Polymer* **2018**, *151*, 6-14.

[240] C. J. Shearer, A. Cherevan, D. Eder, “Application and Future Challenges of Functional Nanocarbon Hybrids”, *Advanced Materials* **2014**, *26*, 2295-2318.

[241] X. Li, M. Rui, J. Song, Z. Shen, H. Zeng, “Carbon and Graphene Quantum Dots for Optoelectronic and Energy Devices: A Review”, *Advanced Functional Materials* **2015**, *25*, 4929-4947.

[242] S. Y. Lim, W. Shen, Z. Gao, “Carbon quantum dots and their applications”, *Chemical Society Reviews* **2015**, *44*, 362-381.

[243] J. Jiang, G. Ye, Z. Wang, Y. Lu, J. Chen, K. Matyjaszewski, “Heteroatom-Doped Carbon Dots (CDs) as a Class of Metal-Free Photocatalysts for PET-RAFT Polymerization under Visible Light and Sunlight”, *Angewandte Chemie International Edition* **2018**, *57*, 12037-12042.

[244] C. Kütahya, Y. Yagci, B. Strehmel, “Near-Infrared Photoinduced Copper-Catalyzed Azide-Alkyne Click Chemistry with a Cyanine Comprising a Barbiturate Group”, *ChemPhotoChem* **2019**, *3*, 1180-1186.

[245] C. Kütahya, P. Wang, S. Li, S. Liu, J. Li, Z. Chen, B. Strehmel, “Carbon Dots as a Promising Green Photocatalyst for Free Radical and ATRP-Based Radical Photopolymerization with Blue LEDs”, *Angewandte Chemie International Edition* **2020**, *59*, 3166-3171.

[246] A. Kocaarslan, C. Kütahya, D. Keil, Y. Yagci, B. Strehmel, “Near-IR and UV-LED Sensitized Photopolymerization with Onium Salts Comprising Anions of Different Nucleophilicities”, *ChemPhotoChem* **2019**, *3*, 1127-1132.

[247] A. Allushi, C. Kutahya, C. Aydogan, J. Kreutzer, G. Yilmaz, Y. Yagci, “Conventional Type II photoinitiators as activators for photoinduced metal-free atom transfer radical polymerization”, *Polymer Chemistry* **2017**, *8*, 1972-1977.

[248] B. Strehmel, C. Schmitz, T. Brömme, A. Halbhuber, D. Oprych, J. S. Gutmann, “Advances of Near Infrared Sensitized Radical and Cationic Photopolymerization: from Graphic Industry to Traditional Coatings”, *Journal of Photopolymer Science and Technology* **2016**, *29*, 111-121.

[249] J. J. L. Zwikker, “Detection of saccharin and the composition of its complexes with copper and pyridine”, *Pharm. Weekbl.* **1933**, *70*, 551-559.

[250] C. Kütahya, N. Meckbach, V. Strehmel, J. S. Gutmann, B. Strehmel, “NIR Light-induced ATRP of Block Copolymers comprising UV-Absorbing Moieties”, *Chem. Eur. J.* **2020**, *submitted*.

[251] C. Kütahya, P. Wang, S. Li, S. Liu, J. Li, Z. Chen, B. Strehmel, “Carbon Dots as a Promising Green Photocatalyst for Free Radical and ATRP-Based Radical Photopolymerization with Blue LEDs”, *Angewandte Chemie International Edition* **2019**, *n/a*.

[252] J. G. Huddleston, A. E. Visser, W. M. Reichert, H. D. Willauer, G. A. Broker, R. D. Rogers, “Characterization and comparison of hydrophilic and hydrophobic room temperature ionic liquids incorporating the imidazolium cation”, *Green Chemistry* **2001**, *3*, 156-164.

[253] M. K. McBride, T. Gong, D. P. Nair, C. N. Bowman, “Photo-mediated copper(I)-catalyzed azide-alkyne cycloaddition (CuAAC) “click” reactions for forming polymer networks as shape memory materials”, *Polymer* **2014**, *55*, 5880-5884.

[254] W. Xi, T. F. Scott, C. J. Kloxin, C. N. Bowman, “Click Chemistry in Materials Science”, *Advanced Functional Materials* **2014**, *24*, 2572-2590.

Acknowledgements

I would like to thank Niederrhein University of Applied Sciences giving me the opportunity to pursue this thesis in cooperation with the University of Duisburg-Essen. This was a great opportunity where I took to chance to extend my background in both fundamental and applied sciences. Therefore, I am thankful for the Vize President for Research, Prof. Dr. Dr. Dr. A. Prange, who has managed the Promotionskolleg at Niederrhein University of Applied Sciences, which received the founding of the County of North-Rhine Westphalia. I worked here in a research program and was additionally involved in teaching duties.

Furthermore, we acknowledge the federal ministry for economy within the ZIM program for additional funding. This project helped to extend my viewpoint to receive more experience in cooperative projects with industrial partners. My thanks go particular to FEW Chemicals GmbH with who we published one nice article together. In addition, I thank also partial financial support to the county of North Rhine Westfalia for funding of the project REFUBELAS and the Project D−NL−HIT carried out in the framework of the INTERREG−Program Deutschland−Nederland. These additional fundings facilitated nice research surrounding, which I liked to transfer into nice publications.

Finally, my thank goes to my supervisors, Prof. Dr. Strehmel and Prof. Dr. J. S. Gutmann, who always had an open ear to my questions and enough patience during the time of the thesis.

Curriculum Vitae

The curriculum vitae is not included in the online version for data protection reasons.

The curriculum vitae is not included in the online version for data protection reasons.